STUDIES ON THE COMPLEXATION OF TRANS-CINNAMIC ACID AND SOME RELATED COMPOUNDS WITH ALPHA-CYCLODEXTRIN

Thomas Walter Rosanske

Under the supervision of Professor Kenneth A. Connors

The complex formation of trans-cinnamic acid and some related compounds (substrates, S) with α-cyclodextrin (ligand, L) was studied over a wide range of ligand concentrations. Cinnamic acid derivatives in which the aromatic ring is unsubstituted (trans-cinnamic acid, trans-cinnamate ion, methyl trans-cinnamate, and benzalacetone) can be quantitatively described in terms of the 1:1 (SL) and 1:2 (SL_2) complexes, whereas 3,5-dimethoxycinnamic acid apparently forms only a 1:1 complex. The cinnamic acid:cyclodextrin system was studied by the solubility, spectral, and potentiometric methods, which yielded consistent estimates for the complex formation constants, namely, K_{11} = 2260 M^{-1} and K_{12} = 60 M^{-1} at 25°. Thermodynamic parameters for the cinnamic acid:cyclodextrin system obtained from spectral data were ΔH°_{11} = -9.3 kcal/mol, ΔS°_{11} = -8 e.u.; ΔH°_{12} = -12 kcal/mol, ΔS°_{12} = -26 e.u. Two experimental methods were used to study each of the other substrates. For the cinnamate ion, the potentiometric and spectral data gave consistent formation constants at 25° of K_{11} = 110 M^{-1} and K_{12} = 15 M^{-1}, and the spectral data gave ΔH°_{11} = -1.9 kcal/mol,

ΔS°_{11} = +11 e.u.; ΔH°_{12} = -9 kcal/mol, ΔS°_{12} = -15 e.u. (all entropy changes are unitary quantities). The methyl cinnamate:cyclodextrin system was studied by the solubility and kinetic methods; the stability constants were K_{11} = 1200 $\underline{M}^{-1}$ and K_{12} = 50 $\underline{M}^{-1}$. The solubility and spectral methods were used to study the benzalacetone:cyclodextrin and 3,5-dimethoxycinnamic acid:cyclodextrin systems. For benzalacetone, K_{11} = 105 $\underline{M}^{-1}$ and K_{12} = 15 $\underline{M}^{-1}$, and for 3,5-dimethoxycinnamic acid, K_{11} = 1970 $\underline{M}^{-1}$.

Thermodynamic cycles for the cinnamic acid:cyclodextrin and cinnamate ion:cyclodextrin systems, using solubility data, reveal that complex formation in the solid phase is thermodynamically favorable, but that complex stability is greater in aqueous solution than in the solid phase.

A proposed stoichiometric model of cyclodextrin complexation allows for two possible 1:1 isomeric complexes having different ends of the substrate molecule included in the cyclodextrin cavity, and a single 1:2 complex with each end of the substrate molecule included in the cavity of a cyclodextrin molecule. The 3,5-dimethoxycinnamic acid:cyclodextrin system is consistent with this model, showing a strong 1:1 complexation but no 1:2 complexation, the aromatic group being too bulky to be included. A good correlation between substrate dipole moment and log K_{11} was observed for cinnamic acid, methyl cinnamate, and

benzalacetone, with the more polar substrates forming less stable complexes. This is consistent with the relatively non-polar nature of the cavity.

All evidence favors a strong cyclodextrin complexation with the cinnamate side-chain of cinnamic acid and related substrates and weaker complexation with the aromatic moiety.

APPROVED: _____
Kenneth A. Connors

DATE: _____

STUDIES ON THE COMPLEXATION OF TRANS-CINNAMIC ACID AND SOME RELATED COMPOUNDS WITH ALPHA-CYCLODEXTRIN

BY

THOMAS WALTER ROSANSKE

A thesis submitted in partial fulfillment of the requirements for the degree of

DOCTOR OF PHILOSOPHY

(Pharmacy)

at the

UNIVERSITY OF WISCONSIN-MADISON

1979

To my wife, Pat

my son, Matthew

and my daughter Rebecca

ACKNOWLEDGEMENT

I wish to express my sincere thanks to Dr. Kenneth A. Connors for his guidance and suggestions throughout the course of this investigation.

I also wish to thank my lab mates who helped make my graduate career more enjoyable.

I wish to thank the National Science Foundation, the American Foundation for Pharmaceutical Education, and The Upjohn Company whose financial support helped make this investigation possible.

TABLE OF CONTENTS

Page

CHAPTER ONE: INTRODUCTION

The cyclodextrins are homologous macrocyclic oligosaccharides produced by the action of Bacillus macerans on starch. They are sometimes called cycloamyloses, cycloglucans, or Schardinger dextrins, the latter in honor of Schardinger, who first isolated and identified Bacillus macerans and described the preparation and properties of cyclodextrins in reliable detail. Greek letters are used in the designation of the cyclodextrins, with α- denoting the lowest homolog, β- the next higher, etc. Cyclodextrins containing as few as six and as many as twelve glucose units have been identified.

The cyclodextrins have gained the attention of many investigators over the past several years because they possess interesting complexation properties. This thesis describes a study of complex formation between one of the cyclodextrins and some cinnamic acid derivatives. This introductory chapter is devoted primarily to a general discussion of the cyclodextrins. A brief historical section is followed by sections on the physical properties, catalytic properties, and complexing properties of the cyclodextrins.

A. History of Cyclodextrins

The history of cyclodextrins has been divided roughly into three periods by French (1). The earliest period ranges from the initial discovery by Villiers in 1891 (2) to the mid-1930's. This was a relatively unproductive period, dominated by the work of Schardinger and Pringsheim (1), and highlighted by Schardinger's isolation and identification of the bacteria Bacillus macerans. Schardinger's interest in cyclodextrins arose during a study on food spoilage in which he was investigating isolated strains of bacteria that had survived a rigorous cooking process. He noted that when Bacillus macerans (then identified as strain II) was subcultured on starch, the degradation products were an alcohol-insoluble "soluble starch" and two types of crystalline materials. The crystalline products were described primarily in terms of their lack of reducing power and their high resistance to hydrolysis; these were the cyclodextrins. Pringsheim followed Schardinger's work with fruitless efforts to characterize the cyclodextrins (4).

French designated the second period in cyclodextrin history as the maturation period. It spans the time from around 1935 to 1950. Freudenberg is credited with the principal contributions to cyclodextrin chemistry during this period (5). Citing the work of Pringsheim as essentially worthless because it was based on mixtures of the

cyclodextrins, Freudenberg and Jacobi described a straightforward means of separating them, which then made possible studies on the properties of the pure compounds (4). Scheme I shows the Freudenberg and Jacobi fractionation scheme, as modified by French (6), for the separation of α-, β-, and γ-cyclodextrins. It was during the maturation period that the cyclodextrins were determined to be cyclic compounds.

The third period in cyclodextrin history covers from the early 1950's to the present. With the preparation and isolation procedures, structures, and physical properties having been described during the maturation period, the focus of attention during the third period has been on the complexes formed between the cyclodextrins and various "substrate" molecules. Much of the work done in this period is described in the sections on the catalytic properties and complexing properties of cyclodextrins.

B. Physical Properties of Cyclodextrins

The cyclodextrins are conical-doughnut shaped molecules as shown schematically below (I). They consist of α-D-glucopyranose units linked at the 1 and 4 positions by bridging acetal oxygens (see Figures 1 and 2). Structural studies of the crystalline α-cyclodextrin-potassium acetate complex by x-ray diffraction indicated that the glucose units are in the C1 chair conformation (7). Conformational studies of

SCHEME I. Fractionation of cyclodextrins (from ref. 5).

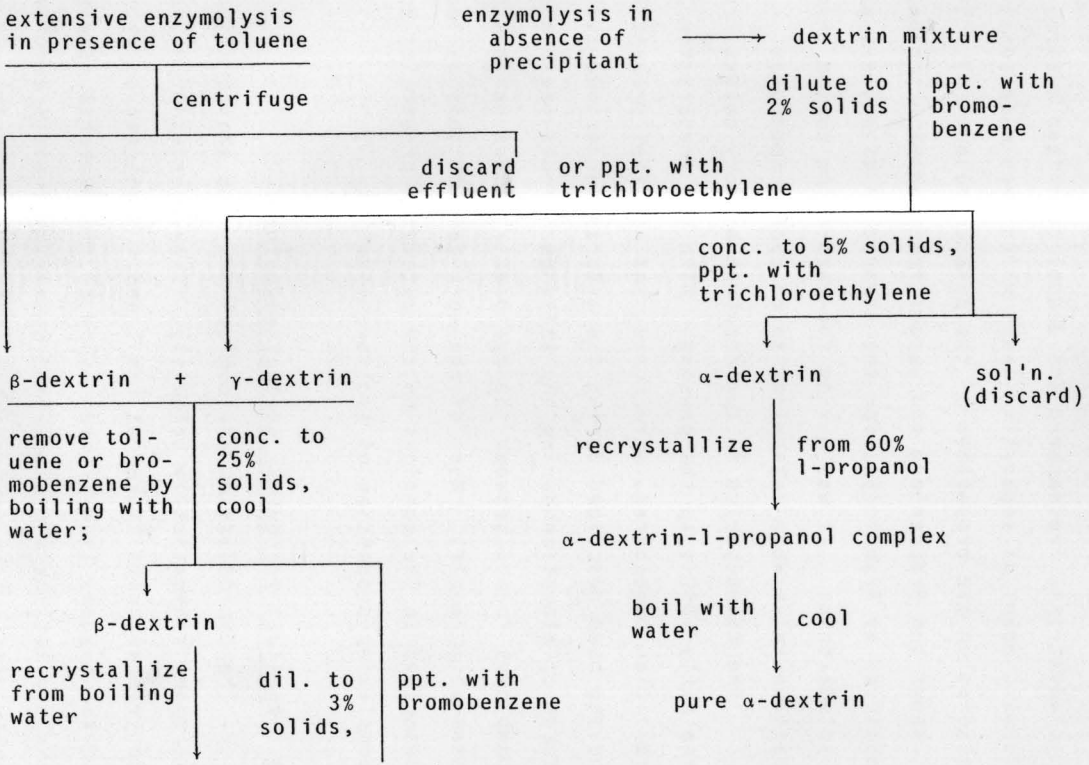

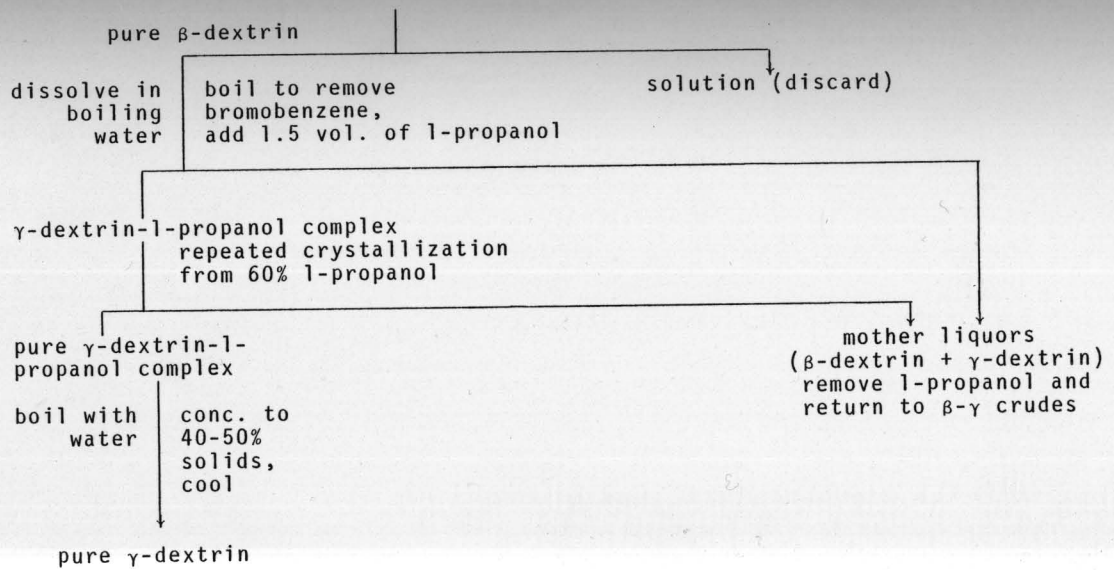
pure β-dextrin
dissolve in boiling water
boil to remove bromobenzene, add 1.5 vol. of 1-propanol
solution (discard)
γ-dextrin-1-propanol complex
repeated crystallization from 60% 1-propanol
pure γ-dextrin-1-propanol complex
mother liquors (β-dextrin + γ-dextrin) remove 1-propanol and return to β-γ crudes
boil with water
conc. to 40-50% solids, cool
pure γ-dextrin

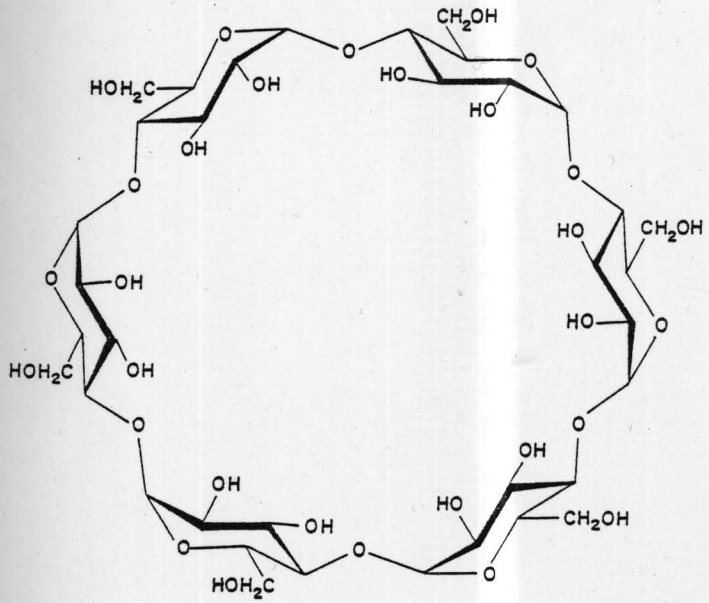

FIGURE 1. Structure of α-cyclodextrin.

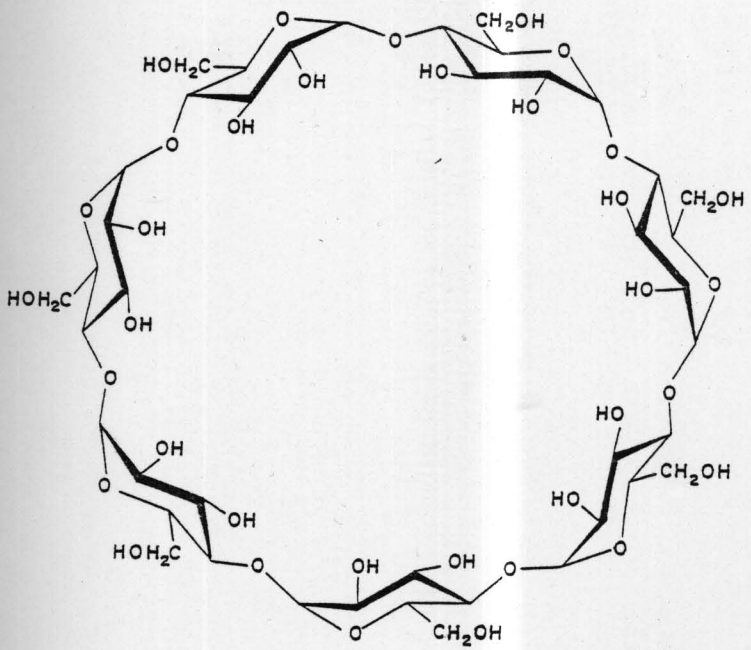

FIGURE 2. Structure of β-cyclodextrin.

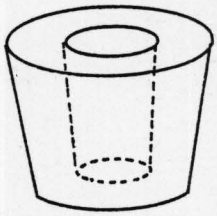

I

cyclodextrins by nuclear magnetic resonance (8-13), optical rotatory dispersion (13,14), and infrared spectroscopy (9, 14) techniques indicate that the solution conformation of the glucose units is also C1.

The rim of larger diameter of a cyclodextrin molecule is lined with the secondary hydroxyls on the number 2 and 3 carbons (C-2 and C-3, respectively) of the glucose units. The smaller rim is lined with the primary hydroxyls of the number 6 carbons. The secondary hydroxyls lining the large rim interact by hydrogen bonds between the C-3 hydroxyl group of one glucose unit and the C-2 hydroxyl group of an adjacent glucose residue, as shown in Figure 3 (9,15,16). This hydrogen bonding may explain in part the relatively high acidity of cyclodextrins. A pK_a of 12.1-12.5 has been reported for the ionization of one of the secondary hydroxyl groups (15,17-19).

A space filling Corey-Pauling-Koltun model of

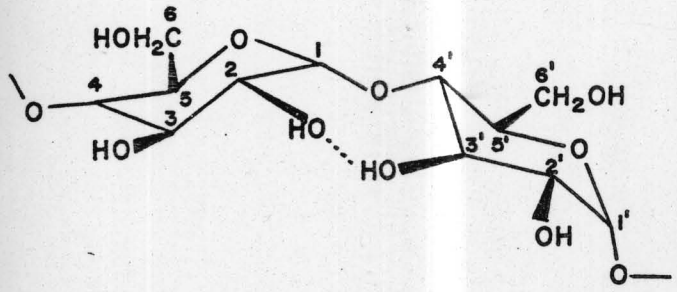

FIGURE 3. Two adjacent glucose units of cyclodextrin.

α-cyclodextrin shows the interior of the molecule containing the bridging acetal oxygens symmetrically distributed with their lone π orbitals orthogonal to the cylindrical axis of the molecule (14), suggesting that the cavity is a region of high electron density and may behave like a Lewis base (20,22). Each acetal oxygen is surrounded by four hydrogen atoms (attached to the C-3 and C-5 of neighboring glucose residues) in a square array.

Of the seven cyclodextrins that have been identified, only three, the α-, β-, and γ- cyclodextrins, have been well-characterized. Some of their properties are shown in Table I.

A peculiar property of the cyclodextrins is their ability to form complexes with many organic and inorganic substances by means of inclusion within the cavity. The cyclodextrin plays the role of "host" and the "guest" substrate is found in the cyclodextrin cavity. The ability of cyclodextrins to form complexes was first noted by Villiers (2) and Schardinger (3). These authors observed the formation of insoluble crystalline materials when cyclodextrins were mixed with relatively simple alcohols. Many studies have since been made of the complexing properties of cyclodextrins. Cyclodextrins have been shown to complex with such polar compounds as organic acids and bases, inorganic ions like ClO_4^- (23), NO_3^- (23), SCN^- (15), and halogens

TABLE I. Some properties of cyclodextrins.

Cyclodextrin	No. of glucose units	Mol. wt.	Water solubility (g/100 ml)	Cavity size (Å)	
				Dia.	Depth
α	6	972	14.5[a] 12.1[b]	4.5[c]	6.7[c]
β	7	1136	1.85[a]	7.0[d]	7.0[d]
γ	8	1297	23.2[a]	8.5[d]	7.0[d]

[a]Ref. 6.

[b]Determined in this work.

[c]Ref. 21.

[d]Ref. 23

(24), and with highly apolar substances such as aliphatic and aromatic hydrocarbons. Complexes have been observed in solution as well as in the solid state.

Though it was assumed for many years that complexes formed with cyclodextrins were of the inclusion type, no direct proof for the fixation of the guest molecules in the cyclodextrin cavity was given until 1967. Cramer and coworkers, in a classic study on the formation of cyclodextrin complexes, reported spectral, thermodynamic, and kinetic data on complex formation between α-cyclodextrin and p-nitrophenol, p-nitrophenolate, and several azo dyes, that supported the inclusion mechanism (23). More direct evidence for inclusion has since been given by several investigators using x-ray and nuclear magnetic resonance (NMR) techniques. For example, Thakkar and Demarco used proton NMR to study the interaction of β-cyclodextrin and a number of aromatic substrates (25) and barbiturates (26); they observed large upfield shifts of the protons located in the interior of the cavity and small or no shifts of the exterior protons.

Several potential uses have been suggested for cyclodextrins based on their ability to form inclusion complexes. Studies by Lach (27-30,34) and others (31-33) have shown that cyclodextrins can markedly increase the solubility of water-insoluble drugs. Cyclodextrins can alter the stability of drugs; Schlenk and coworkers reported a decrease

in the rate of autoxidation of vitamin A palmitate in the presence of β-cyclodextrin (33). Lach and Chin reported that α- and β-cyclodextrin may completely inhibit the hydrolysis of certain aromatic esters; presumably the labile group is "protected" by being included in the cavity (34, 35). Cyclodextrins have been shown to improve absorption characteristics of some drugs (36) as well as facilitate peritoneal dialysis (37). A prostaglandin-β-cyclodextrin formulation has recently been introduced on the Japanese market for oral use (38). One investigator found α-cyclodextrin to be an effective ^{1}H NMR shift reagent for hydrocarbons, for which lanthanide shift reagents are not effective (39). Connors and Lipari recently reported changes in the pK_a values of some organic acids in the presence of α-cyclodextrin; they showed that it is possible to differentiate titrimetrically in cyclodextrin solutions some organic acids that cannot be titrimetrically differentiated in water (80).

C. Catalytic Properties of Cyclodextrins

Many reported studies of cyclodextrin chemistry concern the catalytic properties of these molecules. The catalytic effect of cyclodextrins was not studied in the present investigation, but because of the considerable work that has been reported in this area, a brief review will be given.

Cramer and Dietsche (40,41) first noted the catalytic ability of the cyclodextrins. They observed a 1.38 fold increase in the rate of hydrolysis of ethyl p-chloromandelate upon the addition of 1.32×10^{-3} M β-cyclodextrin, and an acceleration of the cleavage of diphenylpyrophosphate with a concomitant phosphorylation of the cyclodextrin. Cyclodextrins have since been shown to catalyze such reactions as the hydrolysis of phenyl esters (17,43-45,55), acylimidazoles (56), acetanilides (54), and penicillins (49). A valuable advance in this area was made by Bender in his study of the cyclodextrin-accelerated hydrolysis of phenyl esters (17,43-45). Table II shows some of Bender's results (45). Of particular note in Table II is the apparent meta-para selectivity exhibited by α-cyclodextrin, the catalytic effect of α-cyclodextrin being much more pronounced with meta-substituted phenyl esters than with para-substituted ones. Similar meta-para selectivity was observed in the cyclodextrin-catalyzed hydrolysis of diaryl methylphosphonates (46); Van Hooidonk observed a D-L specificity in the α-cyclodextrin-catalyzed hydrolysis of isopropyl methylphosphonofluridate (47) and isopropyl p-nitrophenyl methylphosphonate (19), the L form being more reactive. In addition to catalytic selectivity, Bender observed competitive inhibition and saturation; he thus suggested that the catalytic properties of cyclodextrins make them very good models for

TABLE II. Hydrolysis rates of some phenyl acetates in the presence and absence of α-cyclodextrin.[a,b]

Acetate ester	[α - CD] = 0 10^4 k_{un} x sec	[α - CD] = 0.01 M 10^2 k_{obs} x sec	k_{obs}/k_{un}
Phenyl	8.04	0.779	9.7
m-t-Butylphenyl	4.90	11.1	226
p-t-Butylphenyl	6.07	0.102	1.7
p-Methoxyphenyl	7.49	0.174	2.3
p-Bromophenyl	16.4	0.347	2.1
m-Chlorophenyl	19.1	21.5	113
p-Chlorophenyl	15.2	0.453	3.0
o-Nitrophenyl	53.2	5.37	10.1
m-Nitrophenyl	46.4	47.9	103
p-Nitrophenyl	69.4	1.79	2.6

[a] Ref. 45.

[b] Conditions: 25.0 ± 0.2°; pH = 10.60 carbonate buffer; I = 0.2; 0.5% acetonitrile.

enzymes readily interpretable in terms of Fisher's lock-and-key theory of enzymatic catalysis (45). In later studies on the effects of cyclodextrins on the hydrolysis of several phenyl benzoates, Bender and coworkers observed that the rate of phenol release was dependent on the phenyl substituents, but a subsequent, much slower, reaction associated with the benzoate ion was observed, the rate of which was independent of the substrate (17). They suggested that the ester hydrolysis proceeded through an acylated cyclodextrin intermediate, benzoyl cyclodextrin, the deacylation of which was the slow reaction. Scheme II shows the reaction scheme for a cyclodextrin-catalyzed ester hydrolysis that proceeds through an acylated cyclodextrin intermediate.

SCHEME II

$$\text{CD-OH} + \text{RCOOR}' \underset{\longleftarrow}{\overset{\text{complexation}}{\longrightarrow}} \text{CD-OH}\cdot\text{RCOOR}'$$

$$\text{CD-OH}\cdot\text{RCOOR}' \underset{\longleftarrow}{\overset{\text{acylation}}{\longrightarrow}} \text{CD-OCOR} + \text{R}'\text{OH}$$

$$\text{CD-OCOR} + \text{H}_2\text{O} \xrightarrow{\text{deacylation}} \text{CD-OH} + \text{RCOOH}$$

The reaction mechanism for cyclodextrin-catalyzed hydrolysis is characterized by complex formation, followed by acylation of the cyclodextrin and then its deacylation; this is the

same general mechanism operative in the enzymatic action of serine proteases.

The use of cyclodextrins as enzyme models has two serious deficiencies. First, its maximum catalytic effects are observed at pH 13, whereas enzymatic reactions exhibit maximal rates near neutral pH. Second, the deacylation rate of acylated cyclodextrins - regeneration of the catalyst - is very slow, slower, in fact, than the alkaline hydrolysis of the esters. Some investigators have attempted to overcome these problems by introducing either an internal catalyst that could facilitate the deacylation step, or a more reactive nucleophile that would speed the acylation or deacylation reactions. Cramer initiated these efforts by covalently attaching imidazole to one of the rims of β-cyclodextrin (57); imidazoyl groups are present at the active sites of serine proteases. The acceleration rate of p-nitrophenyl acetate hydrolysis at pH 7.5 and 23° was only two- to three-fold greater than that observed with imidazole alone. The large acceleration that was expected was not observed presumably because the imidazole groups were attached to the primary hydroxyl sites, whereas it is the secondary hydroxyl groups that are active in cyclodextrin-accelerated reactions. Improvements in synthetic procedures allowed Iwakura (58) to selectively modify one of the secondary hydroxyl groups of α-cyclodextrin with a histamine

group (II). This histamine-cyclodextrin compound has a

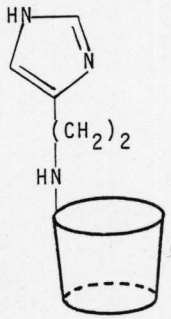

(II)

catalytic site containing both imidazoyl and hydroxyl groups together with a binding site (the cyclodextrin cavity) that merit a comparison with such enzymes as α-chymotrypsin, trypsin, and elastase (15). The hydrolysis of p-nitrophenyl acetate near neutral pH in the presence of II proceeded 80- and 6.3-times faster than in the presence of α-cyclodextrin and a 1:1 mixture of α-cyclodextrin and histamine, respectively (58). Introduction of acetohydroxamic derivatives on the secondary hydroxyl rim of α-cyclodextrin (III) resulted in $\sim 10^3$-fold accelerations, relative to α-cyclodextrin, of some phenyl acetate hydrolyses (59,60). Other studies showed that addition of nucleophiles such as 1,4-diazobicyclo(2.2.2)octane, triethylamine, quinuclidine, piperidine,

IIIa) X = $-CH_2\overset{\overset{O}{\|}}{C}-\overset{\overset{OH}{|}}{N}-CH_2CH_2N(CH_3)_2$

IIIb) X = $-CH_2\overset{\overset{O}{\|}}{C}-\overset{\overset{OH}{|}}{N}-CH_2$ 

IIIc) X = 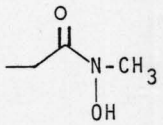

(III)

n-butylamine (61), 6-nitrobenzimidazole, and 5-nitrobenzimidazole (62) substantially accelerate the rates of hydrolysis of α- and β-cyclodextrin trans-cinnamates and α-cyclodextrin acetate. Kitano (63) observed acceleration of both the acylation and deacylation steps in the β-cyclodextrin-catalyzed hydrolysis of p-nitrophenyl indol-3-yl acetate.

Interest in finding better models for metalloenzymes resulted in a study in which Breslow prepared the α-cyclodextrin ester of pyridine-2,5-dicarboxylic acid (IV) and, from that, the nickel chelate (V). The chelate (V) is four

times more reactive in the hydrolysis of p-nitrophenyl acetate than the nickel chelate of pyridine-2,5-dicarboxylic acid without cyclodextrin. Furthermore, the acceleration was observed near neutral pH. Breslow observed a competitive inhibition of the reaction upon the addition of cyclohexanol,

IV: X = 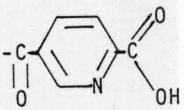

V: X = 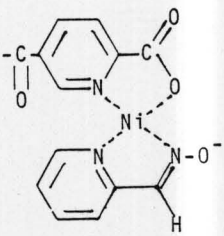

prompting the postulation that the acceleration is due both to binding of the substrate in the cyclodextrin cavity and to reaction within the nickel-cyclodextrin chelate.

In 1975, Breslow proposed "capping" of the cyclodextrins to make the cavity more hydrophobic (65). He attached

several N-formyl groups to the primary alcohol rim of β-cyclodextrin (VI) in expectation that the formyl groups would cluster and form a hydrophobic "floor" on the cyclodextrin, leading to stronger complexation. The observed catalytic rates for the hydrolysis of phenyl esters with VI were 10-20 greater than those with native β-cyclodextrin,

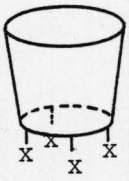

VIa: X = -N(CH$_3$)-CH=O

VIb: X = -N(CH$_2$CH$_3$)-CH=O

but the overall binding to cyclodextrin was either unaffected or slightly weakened as reflected in the observed formation constants, K_f, defined below for a 1:1 interaction between substrate (S) and cyclodextrin (L).

$$S + L \rightleftarrows SL \qquad K_f = \frac{[SL]}{[S][L]} \qquad (1)$$

The weaker binding is possibly due to the cavity being made

shallower by capping. The enhanced catalytic rates are probably due to a greater rigidity of the bound substrates. Other reports (66-69) of capped cyclodextrin include one in which β-cyclodextrin was flexibly capped with the divalent metal ions Cu^{++}, Zn^{++}, and Mg^{++}, enabling them to bind anions with hydrophobic moieties more strongly than the parent cyclodextrin or the functionalized cyclodextrin without the metal coordination (68).

Though few studies used cyclodextrin as a synthetic tool, Breslow reported that α-cyclodextrin catalyzes the chlorination of anisole, with the chlorination occurring exclusively at the para position (70,71). Tabushi indicated the possibility of using cyclodextrins to synthesize bioactive compounds with specific inclusion catalysis, by using β-cyclodextrin to simplify the synthesis of vitamin K_1 or K_2 analogues (72,73).

D. Complexing Properties of Cyclodextrins

Many investigations using several experimental techniques have been made of the complexing or binding properties of cyclodextrins. Cramer, using spectrophotometric and kinetic methods, studied the complexing of α-cyclodextrin with p-nitrophenol, p-nitrophenolate anion, and several azo dyes (23). Using spectrophotometric, induced circular dichroism, and nuclear magnetic resonance techniques (74-78)

and high performance liquid chromatography (79), Uekama investigated the binding of several drugs, including fenamates, phenothiazines, sulfonamides, and barbiturates, to α- and β-cyclodextrins. Lach used solubility methods to study the complexation between several drugs and α- and β-cyclodextrin (27-30). Connors and Lipari (80), Uekama (81), and Gelb (82) used potentiometric methods to study the interaction between cyclodextrins and some organic acids and bases.

Table III gives formation constants for complexes of some typical organic substrates with α- and β-cyclodextrins as determined by various methods. It is evident that cyclodextrins have a high affinity for many types of substrates. The strong complexing ability of cyclodextrins has resulted in efforts to determine the forces controlling the inclusion of substrates into the cavity. Studies of complexes both in solution and in the solid state have resulted in many proposals for these driving forces.

Using x-ray diffraction methods, Saenger showed that one of the glucose residues in α-cyclodextrin hexahydrate is considerably distorted, with its 6-hydroxyl group pointing into the cavity, thus serving as a hydrogen bond acceptor for cavity water. Structural studies of α-cyclodextrin complexes of methanol (86), iodine (87), polyiodide (88), krypton (89), p-iodoaniline (90,91), and potassium acetate

TABLE III. Formation constants for some organic molecules with cyclodextrins.

Substrate	Cyclodextrin	K_f/M^{-1} [a]	Method of data	Ref.
Phenol	α	18.9	S[b]	45
3,5-Dimethylphenol	α	62.5	S	45
p-Nitrophenol	α	38.5	S	23
p-Nitrophenolate	α	3700	S	23
m-Chlorophenyl acetate	α	179	K[c]	45
	β	212	K	45
p-Chlorocinnamate	α	200	S, K	45
Benzoylacetic acid	β	100	K	52
Methyl orange	α	4545	K	45
Benzoic acid	α	1400	P[d]	80
Promazine	β	5600	S	75
Promethazine	β	2100	S	75
Flufenamic acid	β	1330	S	74
Diphenylamine	β	800	S	74
Sulfanilamide	β	350	S	78

Sulfathiazole	β	1650	S	78

[a]Formation constants, defined by Eq. 1, were obtained assuming 1:1 stoichiometry.

[b]Spectrophotometric.

[c]Kinetic.

[d]Potentiometric.

showed the α-cyclodextrin to be isostructural and symmetrical with the substrates located in the center of the cavity. This indicates a conformational change from a high energy strained configuration (92) to a more relaxed symmetrical configuration upon inclusion. However, Bergeron and Meeley studied the complexing of dodecakis-2,6-O-methyl-α-cyclodextrin, tetradecakis-2,6-O-methyl-β-cyclodextrin, and heptakis-3-O-methyl-β-cyclodextrin - molecules in which no distortion is present - with p-nitrophenolate (93). They observed only small changes in the formation constants from those of the parent cyclodextrins, indicating that strain energy plays at most only a minor role in the complexing.

Bergeron and Rowan observed that p-nitrophenolate complexed more strongly with α- and β-cyclodextrin than p-nitrophenol or p-nitrophenyl acetate and interpreted this in terms of an increase in the dipole-induced dipole (van der Waals) interaction caused by an increase in dipole moment as charge increases (94). This, however, could not explain the fact that p-nitrophenyl acetate complexes more strongly with β-cyclodextrin than with α-cyclodextrin, whereas the reverse is true for p-nitrophenolate. Bergeron and Rowan (94) indicated that Griffiths and Bender's (95) suggestion of expulsion of high energy water may, in part, be responsible for this observation, though no substantial evidence to support this was given. The latter contribution, if indeed it is

important, implies that water necessarily be present for complexation to occur. The necessity of water was reported by Cramer (23), but Breslow recently reported significant formation constants for complexes between β-cyclodextrin and some organic substances in dimethyl sulfoxide (96), suggesting that the "lyophobic" force involved in complexation is similar to that in aqueous solution - a lowering of the system energy by increasing solvent-solvent interactions when solvent-substrate and solvent cavity interfaces are diminished.

Hydrogen bonding has been proposed as a contributor to complexing. Lach, in his studies of drug-cyclodextrin interactions, observed that substrates with shapes and structures such that inclusion allowed hydrogen bonding with the hydroxyl groups of the cyclodextrin were more strongly bound than substrates that could not hydrogen bond (27-30). Matsui (97) reported that t-butyl hydroperoxide, which can form hydrogen bonds more easily than t-butyl alcohol, forms an inclusion complex with α-cyclodextrin, whereas the latter does not.

Spectral shifts are often observed when chromophores interact with cyclodextrins. Van Etten et al. observed that the ultraviolet spectrum of p-t-butyl phenol in an aqueous cyclodextrin solution is nearly identical with the spectrum in dioxane (45). This suggests that the cavity is

relatively hydrophobic, leading to a possible role of hydrophobic binding in the complexation process (98,101). However, thermodynamic studies on the complexation of several substrates with cyclodextrins indicate that the inclusion process is primarily enthalpy driven (99,100). Hydrophobic interactions are generally characterized by large favorable entropies (due to the breaking of water structures) and unfavorable enthalpies (15).

The controversy over the forces governing inclusion in a cyclodextrin cavity remains unresolved. Tabushi recently made a theoretical attempt to quantitatively sort out these binding forces using the hypothesis of a thermodynamic process together with semiempirical potential functions of van der Waals interactions and conformational energy (102). The only forces considered in Tabushi's model are those due to van der Waals interactions, water structuring, and conformational changes. Each was shown to contribute significantly to overall stabilization of complexes, but calculated free energies for the interaction between α-cyclodextrin and p-iodoaniline and methyl orange were not in good agreement with observed values.

The process of inclusion depends, in part, on the ability of a substrate to fit into the cavity. Hence, it is a common practice of many investigators to assume a simple 1:1 stoichiometry for complexation systems. Stoichiometries

other than 1:1 have been reported for cinnamic acid (30) and salicylic acid (27) with β-cyclodextrin and also for some normal aliphatic acids with α- and β-cyclodextrins. More recently, Laufer and coworkers (104-106) studied some anions, finding 1:2 substrate:cyclodextrin complexes with 4-biphenyl carboxylate and p-methyl cinnamate. In many studies, usually by spectrophotometric methods, stoichiometries were determined to be simple 1:1, but experimental conditions were such that the presence of other complexes may have been overlooked.

E. Plan of Research

Attempts to explain complex stability or to explicate complex structures and the forcesinvolved cannot be successful unless the stoichiometries and stabilities of all complexes in a system are known. Very few rigorous studies to determine stoichiometries have been reported. The present study primarily concerns a determination of the stoichiometries and stabilities in the trans-cinnamic acid:α-cyclodextrin system. The chemical and physical properties of trans-cinnamic acid and its derivatives make these compounds useful substrates in molecular complex studies (107-113). Preliminary studies on the aqueous trans-cinnamic acid:α-cyclodextrin system indicated that the system could not be adequately described by a simple 1:1 stoichiometry, though

cinnamic acid has been reported to form a 1:1 complex with α-cyclodextrin (76). Cinnamic acid does not seem to be an atypical substrate for cyclodextrin complexation studies; it contains a relatively apolar aromatic moiety together with a polar carboxyl group, two features common to many substrates used in such studies.

Our approach to sorting out stoichiometric relationships is to use more than one experimental technique, each of which can provide estimates of stability constants (114). Disagreement of apparent 1:1 stability constants by several methods is definitive evidence for the presence of at least one complex with a stoichiometry other than 1:1; quantitative agreement of stability constants among several methods strengthens the argument for a model leading to such consistency. Three techniques were used in this study of the trans-cinnamic acid:α-cyclodextrin system: solubility (115), spectral (110), and potentiometric (80). Cinnamic acid is well suited for study by these three techniques. It has a low solubility (3.01×10^{-3} M), changes in which can easily be measured titrimetrically; it has good ultraviolet absorption characteristics (λ_{max} = 279 nm, $\varepsilon_{279} = 1.98 \times 10^4$, for unionized acid) that change considerably on complexation with α-cyclodextrin. Being a weak acid (pK_a = 4.35), cinnamic acid is also suitable for study by a potentiometric method (80), in which complexation is followed by observing

changes in the pK_a of the acid.

Having characterized the trans-cinnamic acid:α-cyclodextrin system, the research plan is focused on other substrates, selected on the basis ofthe findings for the cinnamic acid system and ideas to be described in the Discussion section, in attempts to determine the structural nature of the complexes and to lend some predictability to the complex stability of similar substrates.

CHAPTER TWO: EXPERIMENTAL

A. Materials

Trans-cinnamic acid (Aldrich) was recrystallized from water: m.p. 133.5-133.7° (lit. (117) 133-134°). Methyl trans-cinnamate (Eastman) was distilled under reduced pressure: b.p. 95-97° (10-12 mm); m.p. 32.9-33.9° (lit. (118) 33.5-34.5°). Benzalacetone (trans-4-phenyl-3-butene-2-one) (Aldrich) was recrystallized twice from n-hexane: m.p. 39.7-40.7° (lit. (119) 41-42°). 3,5-Dimethoxy trans-cinnamic acid (Aldrich) was recrystallized twice from water: m.p. 174.6-175°. Benzoic acid (Mallinkrodt) was recrystallized from water: m.p. 122-122.2° (lit. (120) 122°). p-Nitrophenol was recrystallized from dilute HCl: m.p. 112.5-113.5° (lit. (23) 113°).

α-Cyclodextrin (Sigma Lot 106C-0046-1) was used without further purification. Repeated drying to constant weight at 90° indicated 9.77% water content, corresponding closely to the hexahydrate (9.99%): $[\alpha]_D^{25}$ = +150.4 ± 2.2° (10 measurements) (lit. (6) +150.5°).

α-Methyl glucoside (Aldrich) was recrystallized from 80% ethanol: m.p. 166.7-167.3° (lit. (121) 165-166°). Tris(hydroxymethyl)aminomethane (TRIS) base and hydrochloride (Sigma) were used directly in making buffers. All other chemicals were analytical reagent grade. Water was deionized

and distilled from alkaline permanganate.

Sodium trans-cinnamate was prepared by dissolving trans-cinnamic acid in hot 0.5 N NaOH. Hydrochloric acid was added to the solution until a precipitate appeared (pH about 9). The solution was allowed to cool and the precipitate was filtered. The precipitate was slightly yellow and repeated recrystallization from dilute NaOH could not remove the color. A solubility study of the sodium cinnamate indicated about 4.1% impurity.

B. Apparatus

Solubility studies were carried out in a constant temperature water bath equipped to rotate samples end-over-end at 32 rpm. Spectrophotometric measurements were made on either a Cary 14 or a Cary 16 UV-visible spectrophotometer fitted with jacketted cell compartments for temperature control. pH measurements were made with a combination glass electrode (Sargent) on an Orion model 801 Ionalyzer digital pH meter.

C. Solubility Studies

Equal amounts of substrate were accurately weighed into each of several 10-ml glass ampuls. To each ampul was added 0.50 ml of 0.10 N HCl to ensure that acidic substrates remain in the unionized form and to maintain the ionic

strength at 0.01 M. Graded measured volumes of a concentrated, freshly prepared stock α-cyclodextrin solution were added, followed by distilled water to make the total solution phase volume 5.0 ml. The ampuls were sealed and rotated end-over-end in a 25.0 ± 0.05° water bath until solubility equilibrium was reached; equilibration times ranged from 10 days to 1 month. These equilibration times are relatively long (122), but were necessary to achieve solubility equilibrium of the complexes.

After equilibration, the ampuls were stood upright and motionless, at 25°, overnight, to allow the precipitates to settle. A portion of the clear supernatant was carefully withdrawn using either a 1-ml syringe equipped with a 1.5-inch, 20-gauge needle, or a 9-inch disposable pipet. The supernatants were analyzed for total substrate in two ways. For trans-cinnamic acid, a 2.0-ml aliquot was titrated to a phenolphthalein endpoint with standard 0.05 N NaOH. A correction was applied to account for the HCl present in the sample solution. For methyl trans-cinnamate, benzalacetone, benzoic acid, and 3,5-dimethoxy trans-cinnamic acid, portions of the supernatants were appropriately diluted and analyzed for spectrophotometrically. Solutions of the latter two were made basic prior to measuring to minimize errors due to spectral perturbations caused by complexing, since acid anions have generally been observed to complex to

a lesser extent than their unionized counterparts.

The precipitates were carefully removed from the ampuls, filtered, dried, and thoroughly mixed. Accurately weighed portions of the precipitates were analyzed for substrates (titrimetrically for trans-cinnamic acid and spectrophotometrically for the others). The α-cyclodextrin content of the precipitates was found by difference.

D. Spectral Studies

Increasing amounts of α-cyclodextrin were weighed into a series of 10-ml volumetric flasks. For studies of benzalacetone and unionized acids, 1.0-ml of 0.10 N HCl was added to each flask, followed by equal volumes of a stock substrate solution. Water was added to volume. Reference solutions were prepared for each sample solution having an identical α-cyclodextrin and HCl concentration, but no substrate. Sample spectra of complexed and uncomplexed substrate were obtained in order to select a wavelength at which the substrate absorptivity changes substantially upon complexing. Absorbance measurements were made at the selected wavelengths using a 1.0-cm quartz cell. For studies at temperatures other than 25°, the solutions were prepared at 35° and concentrations at other temperatures were corrected using the density of water.

Cinnamate, p-nitrophenolate, and benzoate anions were

studied in a similar manner, except that the pH was brought to 9 with a TRIS buffer. This pH ensured that the substrates were in the anion form and that the α-cyclodextrin was not appreciably ionized. A separate potentiometric experiment showed that TRIS does not significantly complex with α-cyclodextrin (123). The ionic strength in all spectral studies was constant at 0.01 M.

E. Potentiometric Study

This method was used for the trans-cinnamic acid:α-cyclodextrin system only. A stock solution containing equal concentrations of cinnamic acid and sodium cinnamate was prepared by exactly half-neutralizing a weighed sample of trans-cinnamic acid with standard NaOH. Increasing amounts of α-cyclodextrin were accurately weighed into a series of 5-ml volumetric flasks. Equal volumes of the cinnamic acid-cinnamate stock solution were added to the flasks. Sodium chloride was added to bring the ionic strength to 0.01 M and the flasks were diluted to volume with distilled water. The pH of each solution was measured at 25°, with this pH being interpreted as the apparent pK_a of trans-cinnamic acid in that solution.

F. Kinetic Study

This method was used to study the methyl cinnamate:α-

cyclodextrin system. Increasing amounts of α-cyclodextrin were accurately weighed into a series of 10-ml volumetric flasks. The α-cyclodextrin in each flask was dissolved in a pH 10.36 carbonate buffer. To each flask, 0.2 ml of a saturated aqueous solution of methyl cinnamate was added. The flasks were quickly brought to volume with the carbonate buffer; the ionic strength was 0.01 M. The samples were maintained at 25.0 ± 0.1°. At recorded times, samples were withdrawn from the flasks and analyzed spectrophotometrically at 295 nm.

CHAPTER THREE: RESULTS

A. Trans-Cinnamic Acid[1]

1. Solubility Study

The results of the solubility study of the cinnamic acid:α-cyclodextrin[2] system are given in Tables IV and V and shown graphically in Figure 4. These data were obtained using 50.0 mg samples of solid cinnamic acid. On the abscissa of Figure 4 is specified L_t, the total molar concentration of ligand (cyclodextrin) added to the solution. The left-hand ordinate of this figure gives S_t, the total molar concentration of substrate (cinnamic acid) found in the solution phase; the open circles refer to this ordinate. The right-hand ordinate of Figure 4 gives X_L, the mole fraction of ligand in the solid phase; the solid circles refer to this ordinate.

Figure 4 is extremely informative. The appearance of the solution phase diagram is evidence for the presence of at least two complexes with differing stoichiometries. A complex system of this nature containing only a 1:1[3] complex would exhibit what Higuchi and Connors label a Type B_S

---

[1] Hereafter referred to as cinnamic acid.

[2] Hereafter referred to as cyclodextrin.

[3] All reported stoichiometries will be of the form substrate: ligand.

TABLE IV. Solubility of cinnamic acid as a function of cyclodextrin concentration at 25.0 ± 0.05°.[a]

10^3 L_t/M	10^3 S_t/M
0.00	3.01 ± 0.05[b]
5.11	7.19
10.2	11.7
15.3	15.4
20.4	19.4
25.5	22.5
30.6	22.4
35.7	22.3
40.8	22.5
46.0	22.5
51.1	22.4
56.2	22.4
61.3	22.4
66.4	22.5
71.5	23.6
76.6	23.9
81.7	23.9
86.8	23.9
91.9	23.9

[a]Cinnamic acid sample size = 50.0 mg; equilibration time = 10 days; I = 0.01 M; pH = 2.2

[b]Average of 11 samples ± std dev.

TABLE V. Solid phase composition as a function of cyclodextrin concentration for solubility study of cinnamic acid:cyclodextrin system.

10^3 L_t/M	X_L
0.00	0
5.11	0
10.2	0
15.3	0
20.4	0
25.5	0.017
30.6	0.111
35.7	0.214
40.8	0.272
46.0	0.339
51.1	0.384
56.2	0.423
61.3	0.445
66.4	0.474
71.5	0.505
76.6	0.525
81.7	0.546
86.8	0.566
91.9	0.579

FIGURE 4. Solubility study of the cinnamic acid:cyclodextrin system at 25.0°. Open circles (left vertical axis): total solution phase concentration of substrate; solid circles (right vertical axis): mole fraction of cyclodextrin in the solid phase. The total added concentration of ligand (cyclodextrin) is given on the horizontal axis. The smooth lines were calculated as described in the text.

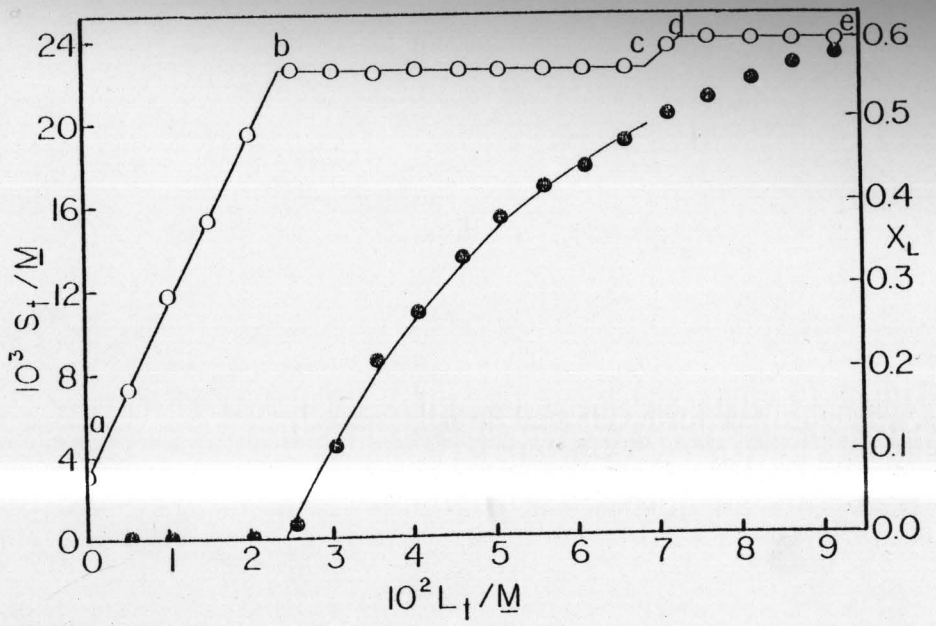
24
20
16
12
8
4
0
10^3 S_t / M
0
1
2
3
4
5
6
7
8
9
$10^2 L_t$ / M
0.6
0.5
0.4
0.3
0.2
0.1
0.0
X_L
a
b
c
d
e

diagram (Fig. 5) (124). In this type of system, a soluble complex is formed upon adding ligand, this being reflected in a linear increase in the total solubility of the substrate. When the solubility limit of the complex is reached (point a, Fig. 5), S_t becomes invariant, and a plateau is observed in the diagram, since adding more ligand results in the formation of more complex, which must precipitate; the concentration of free substrate is maintained constant by dissolution of solid substrate. At point b (Fig. 5), all of the solid substrate has been dissolved. Addition of more ligand results in precipitation of more complex; the free substrate concentration cannot be maintained by dissolution of solid substrate, since there is none left. Hence, the total concentration of substrate must decrease, leveling off at approximately the solubility of the complex.

The solution phase solubility diagram for the cinnamic acid:cyclodextrin system (Fig. 4) shows an initial rising segment (a-b) that appears linear, followed by a plateau region (b-c), as would be expected for a Type B_S, 1:1 system. At point c, however, a rising segment (c-d) is observed, followed by a second plateau (d-e), indicating the presence of another complex. Analysis of the solid phase (solid circles, Fig. 4) indicatesthat a complex is present with a ligand/substrate ratio greater than unity. These observations therefore suggest that the simplest description

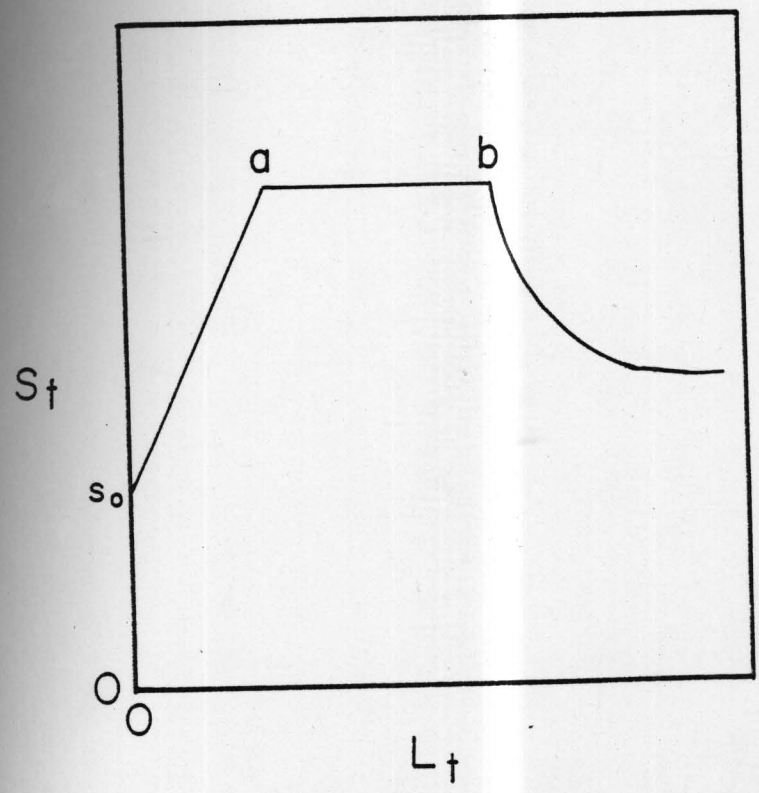

FIGURE 5. Type B_S solubility diagram for a 1:1 complexation system (124).

of the system will invoke complexes with 1:1 and 1:2 stoichiometries (SL and SL_2). This conclusion may seem inconsistent with the linear nature of the initial rising portion of the diagram, since Higuchi and Connors reported that the presence of complexes of higher order than one in L should result in an initial rising portion that is concave upward; this will be shown not to be a problem here.

A quantitative description is required in order to extract numerical estimates from Figure 4. The complex formation equilibria and stability constants are defined

$$S + L \rightleftarrows SL \tag{1}$$

$$K_{11} = \frac{[SL]}{[S][L]} \tag{2}$$

$$SL + L \rightleftarrows SL_2 \tag{3}$$

$$K_{12} = \frac{[SL_2]}{[SL][L]} \tag{4}$$

where K_{11} and K_{12} are concentration constants referred to the experimental condition of 0.01 M ionic strength. Equation (5) gives the theoretical relationship between S_t and L_t for the initial rising portion of the solution phase solubility diagram before the solubility limit of either complex has been reached. A complete derivation of Equation

(5) is given in the Appendix.

$$S_t = s_o + \frac{L_t}{2} + \frac{ab}{c} - \frac{b}{c}(a^2 + 8K_{11}K_{12}s_oL_t)^{1/2} \qquad (5)$$

where s_o = molar solubility of free S

$$a = 1 + K_{11}s_o$$

$$b = \frac{a}{2K_{11}s_o} - 1$$

$$c = 4K_{12}$$

Equation (5) shows that S_t is a non-linear function of L_t in this region. The slope is given by

$$\frac{dS_t}{dL_t} = \frac{1}{2}\left[1 - \frac{8bK_{11}K_{12}s_o}{c(a^2 + 8K_{11}K_{12}s_oL_t)^{1/2}}\right] \qquad (6)$$

Since a and c must be positive quantities, the curvature in the slope depends on the sign of b. If b = 0, the slope is constant with a value of 0.5; this implies that $K_{11} = 1/s_o$. A negative value of b - meaning $K_{11} > 1/s_o$ - gives a decreasing slope as L_t increases, whereas if b is positive ($K_{11} < 1/s_o$), the slope increases as L_t increases. Whether or not any curvature will be experimentally observed depends on the magnitude of b and the range of L_t over which S_t is observable. The slope at $L_t = 0$ is given by Equation (7).

$$\left(\frac{dS_t}{dL_t}\right)_{L_t=0} = \frac{1}{2} - \frac{1}{2}\left[\frac{1 - K_{11}s_o}{1 + K_{11}s_o}\right] \qquad (7)$$

Now consider the discontinuity giving rise to segment b-c of Figure 4 (the "first plateau"). Ultimately, the solubility limit of one or both of the complexes will be reached (as long as the solid S is not exhausted first and the solubility limit of L is not reached). Three cases are possible: (i) the solubility limit of SL is reached before that of SL_2, (ii) the solubility limit of SL_2 is reached before that of SL, and (iii) the solubility limits of SL and SL_2 are reached simultaneously. We consider here only case (i). Equation (8) gives the resulting equation for the total substrate concentration in the plateau region (see Appendix)

$$S_t = s_o + s_{11} + \frac{K_{12}s_{11}^2}{K_{11}s_o} \qquad (8)$$

where s_{11} is the molar solubility of SL.
Equation (8) shows that S_t becomes invariant as soon as one of the complexes, in this case SL, reaches its solubility limit. The complexation equilibria ensure that the concentration of the second complex also remains fixed. This conclusion is general for any number of complexes no matter which complex reaches its solubility limit first. Thus the

first plateau in Figure 4 is accounted for. The reason for choosing the case of SL reaching its solubility limit first is found in the solid phase data. As L_t increases along the first plateau, SL is being formed and precipitating, with the concentration of pure S being held constant by dissolution of solid S. When all of the solid S is depleted - point c in Figure 4 - the mole fraction of L is close to 0.5, consistent with the precipitate being pure SL.

At the point where solid S disappears, the constraint on S_t is lost (although the condition [SL] = s_{11} still holds). An equation for the dependence of S_t on L_t is given in the Appendix, but since it plays no role in the quantitative interpretation of the present data it is not discussed here except to say that at sufficiently high L_t concentrations, or over limited L_t intervals, the dependence may be considered to be essentially linear. S_t will rise until the concentration of the second complex, SL_2, reaches its solubility limit (point d, Fig. 4). At this point S_t is given by Equation (9) (see Appendix for details), where s_{12} is the molar solubility of SL_2

$$S_t = \frac{K_{12}s_{11}^2}{K_{11}s_{12}} + s_{11} + s_{12} \qquad (9)$$

From Equation (9), it is seen that again S_t becomes invariant. Thus a "second plateau" is observed. If L_t could be

made sufficiently large, eventually all solid SL would disappear and S_t would decrease to a final value of s_{12}.

Consider now the composition of the solid phase. From $L_t = 0$ to $L_t = a$, it is postulated that the complex species are soluble so that only pure S is present in the solid phase; thus X_L, the mole fraction of cyclodextrin in the solid phase, should be zero, as is found experimentally (Fig. 4). From $L_t = a$ to $L_t = b$, the essential feature is that solid S is being replaced by solid SL. Therefore it is expected that at $L_t = a$, $X_L = 0$ and at $L_t = b$, $X_L = 0.5$, as is observed. The theoretical equation for X_L in this region is

$$X_L = \frac{V(L_t K_{11} s_o - d s_{11})}{V(L_t K_{11} s_o - d s_{11}) + m_s^t K_{11} s_o - V K_{11} s_o S_t} \qquad (10)$$

where $d = 1 + K_{11} s_o + 2K_{11} s_{11}$

V is the total volume (this is somewhat ambiguous but will be taken as the solution volume added in calculations)

m_s^t is the total moles of substrate added.

From Equation (10), it is seen that X_L increases non-linearly with L_t.

From $L_t = c$ to $L_t = d$ (Fig. 4), X_L should remain at 0.5 since SL_2 has not yet begun to precipitate, but X_L should begin to rise again at $L_t = d$ as solid SL is replaced by

solid SL_2. The eventual value of X_L should be 0.667 (if L_t can be made large enough). An equation for this rise in X_L above 0.5 is given in the Appendix, but because of the ambiguity in the volumes, it is difficult to apply. Experimentally, Figure 4 shows that X_L does increase in this region, reaching a value of 0.58 at the highest cyclodextrin concentration studied.

The solubility data were not quantitatively interpreted independently of the spectral and potentiometric data; rather, for unionized cinnamic acid, the solubility and spectral data were analyzed to give K_{11} and K_{12} values that best fit both sets of results. These values were then imposed as constraints on the potentiometric data. Uncertainties attached to these values represent limits outside which the quantitative consistency among the independent sets of data is seriously degraded. The results obtained at 25° are $K_{11} = 2260 \pm 50\ \underline{M}^{-1}$ and $K_{12} = 60 \pm 5\ \underline{M}$. The solubility of free cinnamic acid, s_o, is $3.01 \pm 0.05 \times 10^{-3}\ \underline{M}$ (the uncertainty here is the standard deviation of 11 determinations). The line drawn in Figure 4 from $L_t = 0$ to $L_t =$ a is a calculated line using Equation (5) and the values of K_{11}, K_{12}, and s_o given above. Table VI gives some calculated values of S_t for selected L_t values in this region.

The solubility of SL can be calculated from Equation (8) and the value of S_t on the first plateau, providing K_{11},

TABLE VI. Calculated S_t values for various selected L_t values assuming a 1:1 + 1:2 complexation system where both complexes are soluble.[a]

10^2 $L_t/\underline{M}$	10^3 $S_t/\underline{M}$
0.000	3.01
0.500	7.25
1.00	11.3
1.50	15.3
2.00	19.1

[a]Calculated with Eqn. (5) and the values K_{11} = 2260 $\underline{M}^{-1}$, K_{12} = 60 $\underline{M}^{-1}$, and s_0 = 3.01 x 10^{-3}.

K_{12}, and s_o are known. Equation (8) is quadratic in s_{11}, and thus two values are possible. However, in the present case, only one value, $s_{11} = 1.7 \pm 0.2 \times 10^{-2}$ M, has any physical meaning. Similarly, Equation (9) can be used to calculate the solubility of SL_2. Equation (9) is quadratic in s_{12} and both values calculated, $5.5 \pm 0.5 \times 10^{-3}$ M and $1.4 \pm 0.6 \times 10^{-3}$ M, have physical meaning, so a choice between them could not be made.

Further evidence in support of the proposed model is given in the calculation of the expected value of L_t where the second rise begins. For the data in Figure 4, 50.0 mg samples of solid cinnamic acid were taken per ampul. This is equivalent to 3.38×10^{-4} mol. The total number of moles of S in solution at point b is S_t x volume per ampul, or $(2.25 \times 10^{-2}$ mol/l$)(5.0 \times 10^{-3}$ l$) = 1.13 \times 10^{-4}$ mol. Thus the number of moles of S left as solid is $3.38 \times 10^{-4} - 1.13 \times 10^{-4} = 2.25 \times 10^{-4}$ mol. This much cyclodextrin must be added to transform the 2.25×10^{-4} mol of solid S into solid SL. This is equivalent to 2.25×10^{-4} mol$/5.0 \times 10^{-3}$ l $= 4.5 \times 10^{-2}$ M cyclodextrin. Since the first plateau begins at $L_t = 2.41 \times 10^{-2}$ M, we therefore calculate that all solid S will be depleted at $L_t = 2.41 \times 10^{-2} + 4.5 \times 10^{-2} = 6.91 \times 10^{-2}$ M. This was found experimentally (Fig. 4). Results consistent with this were also obtained using 40.0 mg samples of cinnamic acid.

The slope of the line drawn from L_t = c to L_t = d in Figure 4 was calculated as follows (see Appendix for details):

$$\text{slope} = \frac{K_{12}s_{11}}{1 + 2K_{12}s_{11}} = \frac{(60)(1.7 \times 10^{-2})}{1 + (2)(60)(1.7 \times 10^{-2})} = 0.34$$

The smooth curve drawn for the solid phase composition in the first plateau region of Figure 4 was calculated using Equation (10). Calculated values are given in Table VII.

2. Spectral Study

One of the first indications that the stoichiometry of the cinnamic acid:cyclodextrin system was not just 1:1 came from examination of the ultraviolet spectra of cinnamic acid in the presence and absence of cyclodextrin. The spectrum of cinnamic acid is altered in the presence of cyclodextrin, as shown in Figure 6. At low cyclodextrin concentrations, isosbestic points are observed at 231 nm and 296 nm. However, these isosbestic points are lost at moderate cyclodextrin concentrations.[4] This is evidence for the presence of at least two complexes.

---

[4]The moderate concentrations are low enough ($\sim$0.003 M in this study) so that a general medium effect on the spectra cannot account for the departure from the isosbestic behavior, as demonstrated by incorporation of α-methylglucoside.

TABLE VII. Calculated values of X_L at various L_t values for a solubility study assuming a 1:1 + 1:2 complexation system.[a]

10^2 $L_t/\underline{M}$	X_L
2.75	0.061
3.00	0.107
3.50	0.188
4.00	0.255
4.50	0.312
5.00	0.361
5.50	0.403
6.00	0.440
6.50	0.473
6.75	0.488

[a]With Eqn. (10) and the values $K_{11} = 2260\ \underline{M}^{-1}$, $K_{12} = 60\ \underline{M}^{-1}$, $v = 5.0 \times 10^{-3}$ l, $S_t = 2.25 \times 10^{-2}\ \underline{M}$, $s_0 = 3.01 \times 10^{-3}\ \underline{M}$, $s_{11} = 1.7 \times 10^{-2}\ \underline{M}$, and $m_s^t = 3.38 \times 10^{-4}$ mol.

FIGURE 6. Ultraviolet spectra of cinnamic acid at various cyclodextrin concentrations; $S_t = 4.61 \times 10^{-5}$ M; pH $\approx$ 2; I = 0.01 M. Cyclodextrin concentrations: 1, 0.00 M; 2, 2.0×10^{-4} M; 3, 5.0×10^{-4} M; 4, 2.0×10^{-2} M; 5, 3.0×10^{-3} M.

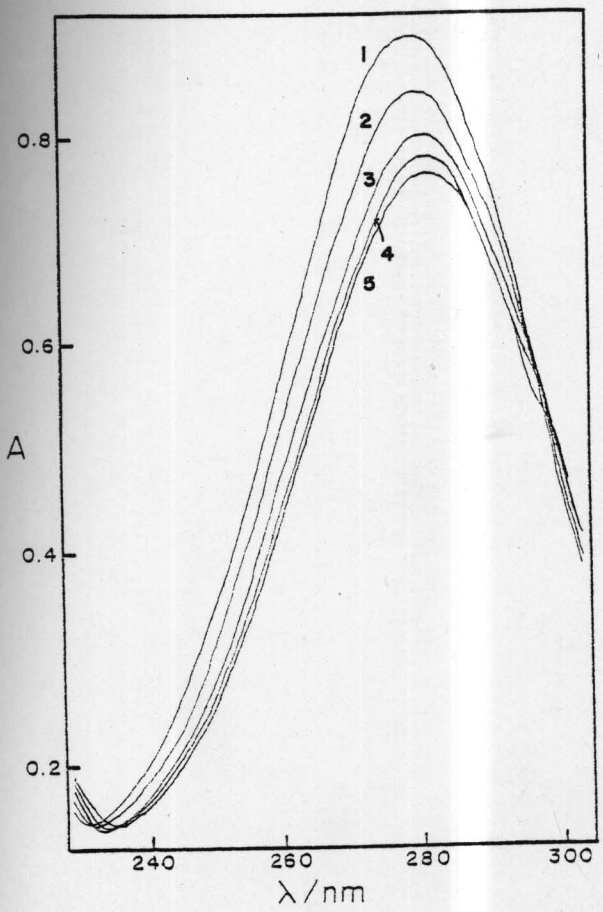
1
2
3
4
5
0.8
0.6
A
0.4
0.2
240
260
280
300
λ/nm

The spectral method makes use of changes in absorbance at a single wavelength as a function of ligand concentration. Table VIII gives the spectral data obtained at 279 nm for the cinnamic acid:cyclodextrin system at 25°. The conventional way to analyze spectral data is to construct a "double reciprocal" plot based on the Benesi-Hildebrand relationship, Equation (11) (114,116,125), which is readily derived for a 1:1 complex system (see Ref. 122, p. 107 ff.).

$$b/\Delta A = 1/K_{11}S_t\Delta a[L] + 1/S_t\Delta a \qquad (11)$$

From Equation (11), a plot of $1/\Delta A$ vs. $1/[L]$ is linear with K_{11} = intercept/slope. However, since [L] is an unknown quantity, the assumption $[L] = L_t$ is generally made. The error introduced by this assumption depends on the magnitude of K_{11}, the total substrate concentration, and L_t. For the present system and for systems discussed later, significant errors would be introduced only at very low cyclodextrin concentrations. The maximum error (lowest cyclodextrin concentrations used) introduced by this assumption in any of the systems studied is about 4%. A plot of $1/\Delta A$ vs. $1/L_t$ for the cinnamic acid:cyclodextrin system is shown in Figure 7. The non-linear appearance of this plot is further evidence of a complex or complexes wth stoichiometries other than 1:1. Hence, Equation (11) cannot be used to analyze

TABLE VIII. Spectral data for the cinnamic acid:cyclodextrin system at 25.0 ± 0.2°.[a]

$10^2 L_t/M$	$-\log L_t$	ΔA[b]	$(1/L_t)$ M	$1/\Delta A$
0.0245	3.61	0.155	4080	6.45
0.0324	3.49	0.168	3080	5.95
0.0597	3.22	0.233	1670	4.48
0.0978	3.01	0.263	1020	3.80
0.158	2.80	0.300	631	3.33
0.309	2.51	0.317	324	3.15
0.479	2.32	0.322	209	3.11
1.00	2.00	0.307	99.9	3.26
2.00	1.70	0.275[c]	49.9	3.70
10.0	1.00	0.203[c]	10.0	4.93

[a] $S_t = 8.48 \times 10^{-5}$; pH = 2.2; I = 0.01 M.

[b] λ = 279 nm; 1-cm pathlength.

[c] These ΔA values are corrected for a general medium effect as determined by using α-methylglucoside. The ΔA caused by an equivalent weight/volume concentration of α-methylglucoside at the highest L_t was +0.009.

FIGURE 7. Benesi-Hildebrand plot for the cinnamic acid: cyclodextrin system at 25.0°. Cinnamic acid concentration = 8.475×10^{-5} M.

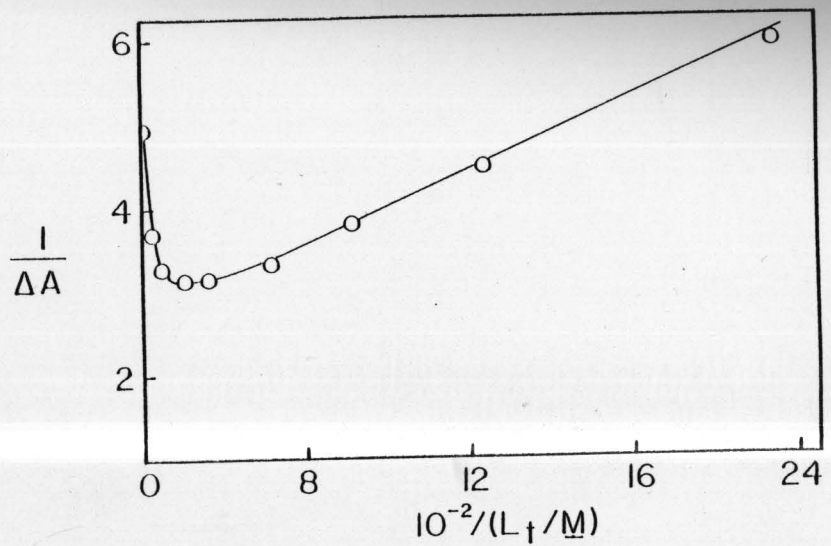
6
4
2
1/ΔA
0
8
12
16
24
10⁻²/(Lt/M)

this system. A more useful way to present the data is to plot directly the absorbance change as a function of the ligand concentration. This plot is shown in Figure 8.

The analysis of this system assumes SL + SL_2 complexes for consistency with the solubility results. This system has been treated before (114,126), but primarily in terms of the conventional double reciprocal graphical analysis, which, as we have seen, is not effective for extracting the stability constants. Equation (12) gives the relationship between the change in absorbance, ΔA, and the free ligand concentration, [L], and Equation (13) gives the relationship between the free ligand concentration and total ligand concentration, L_t (see Appendix for details).

$$\Delta A = \frac{S_t K_{11}[L](\Delta a_{11} + \Delta a_{12} K_{12}[L])}{1 + K_{11}[L] + K_{11}K_{12}[L]^2} \qquad (12)$$

$$L_t = [L] + \frac{S_t K_{11}[L](1 + 2K_{12}[L])}{1 + K_{11}[L] + K_{11}K_{12}[L]^2} \qquad (13)$$

where Δa_{11} and Δa_{12} are the differences between the molar absorptivities of the substrate and the 1:1 and 1:2 complexes, respectively. It is not practical to express ΔA as an explicit function of L_t, but a numerical curve-fitting procedure is straight-forward. Estimates of K_{11}, K_{12}, Δa_{11}, and Δa_{12} are obtained from preliminary trials and from the supplementary solubility data. An arbitrary but realistic

FIGURE 8. Change in absorbance (1-cm cell), at 279 nm, of cinnamic acid as a function of cyclodextrin concentration at 25.0°. The smooth curve was calculated from Eqns. (12) and (13). The total substrate concentration is 8.48×10^{-5} M. See Table IX for the calculated values.

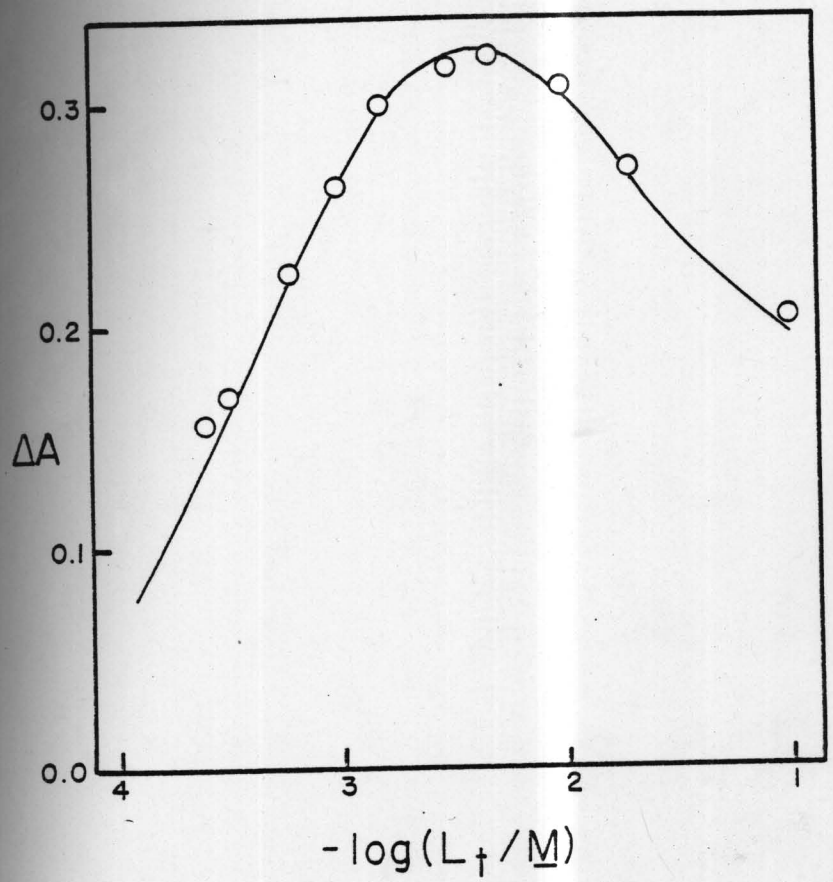
0.3
0.2
ΔA
0.1
0.0
4
3
2
1
-log(L_t/M)

value of [L] is selected, and with Equations (12) and (13) the corresponding quantities ΔA and L_t are calculated. These are compared with the experimental values, and the parameters are adjusted until a satisfactory agreement is achieved. As noted earlier, K_{11} and K_{12} were not permitted to vary freely, but were constrained by the condition that the final values must account for both the spectral and solubility data. The smooth curve in Figure 8 was calculated in this way; the calculated values are given in Table IX. The results at 25° are K_{11} = 2260 $\underline{M}^{-1}$, K_{12} = 60 $\underline{M}^{-1}$, Δa_{11} = 4700, Δa_{12} = 1900 (at 279 nm, $a_s = 1.98 \times 10^4$).

Table X gives the spectral data for the cinnamate ion: cyclodextrin system at 24.7°. Figure 9 shows a ΔA (269 nm) *vs.* log L_t plot for this system. The curve in Figure 9 has a sigmoid shape characteristic of simple 1:1 complexing, and a plot of $1/\Delta A$ *vs.* $1/L_t$ is linear; evidently the system can be described in terms of simply a 1:1 complex. The potentiometric data (discussed later), however, appear to require the presence of both SL and SL_2 in the cinnamate ion system, hence both complexes are considered to be present in the spectral study. The curve-fitting procedure described earlier was used for the cinnamate ion system, with the K_{11} and K_{12} values required to give consistent fits to both the spectral and potentiometric data. The smooth curve in Figure 9 was drawn with Equations (12) and (13) and the

TABLE IX. Calculated L_t and ΔA values for various [L] assuming a 1:1 + 1:2 complexation system.[a] The calculated ΔA *vs.* $-\log L_t$ curve is shown in Figure 8.

10^2 [L]/M	10^2 L_t/M	$-\log L_t$	ΔA
0.0100	0.0116	3.94	0.074
0.0500	0.0547	3.26	0.210
0.100	0.106	2.97	0.271
0.300	0.309	2.51	0.322
0.500	0.510	2.29	0.322
1.00	1.01	2.00	0.301
2.00	2.01	1.70	0.266
3.00	3.01	1.52	0.244
5.00	5.02	1.30	0.220
10.0	10.0	1.00	0.195

[a]Calculated with Eqns. (12) and (13) and the values K_{11} = 2260 M^{-1}, K_{12} = 60 M^{-1}, Δa_{11} = 4700, Δa_{12} = 1900, S_t = 8.48×10^{-5} M.

TABLE X. Spectral data for the cinnamate ion:cyclodextrin system at 24.7 ± 0.2°.[a]

10^2 L_t/M	-log L_t	ΔA[b]
0.0390	3.41	0.025
0.0992	3.00	0.036
0.178	2.75	0.062
0.704	2.15	0.158
1.78	1.75	0.243
5.02	1.30	0.299[c]
10.0	1.00	0.301[c]

[a] S_t = 8.56 x 10^{-5} M; pH = 9.0 (TRIS buffer; I = 0.01 M.

[b] λ = 269 nm; 1-cm pathlength.

[c] These values are corrected for a general medium effect as determined by using α-methylglucoside. The ΔA caused by an equivalent weight/volume concentration of α-methylglucoside at the highest L_t was +0.012.

FIGURE 9. Change in absorbance at 269 of cinnamate ion as a function of cyclodextrin concentration at 24.7°. The smooth curve was calculated using Eqns. (12) and (13). The total substrate concentration is 8.56×10^{-5} M.

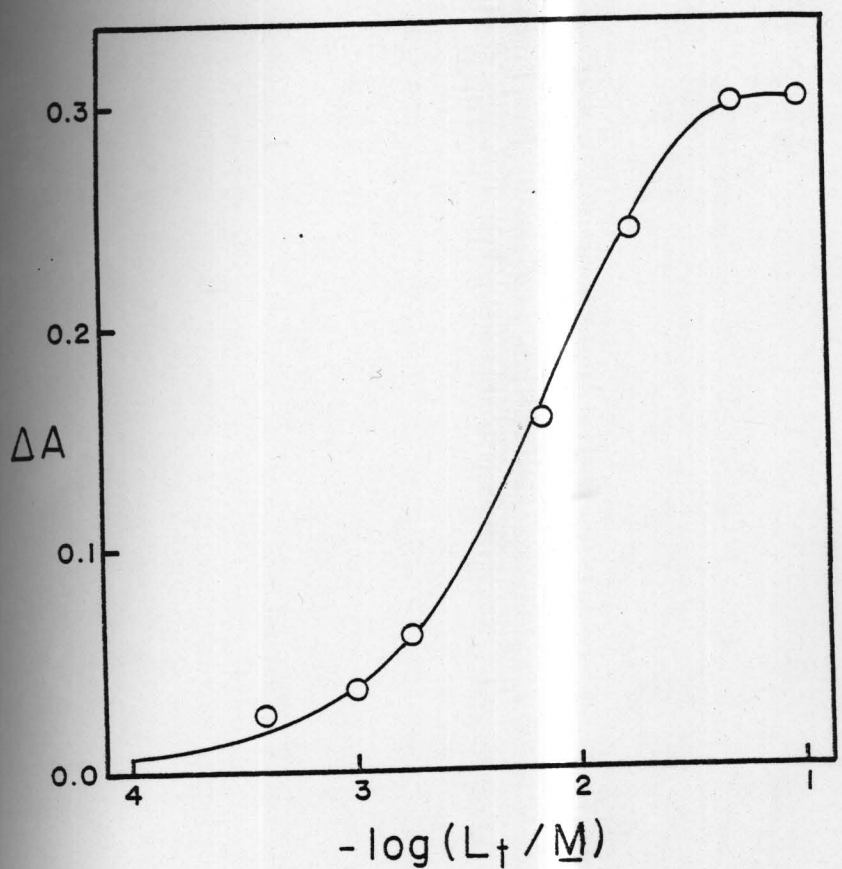
0.3
0.2
ΔA
0.1
0.0
4
3
2
1
- log (Lt / M)

values K_{11} = 110 $\underline{M}^{-1}$, K_{12} = 15 $\underline{M}^{-1}$, Δa_{11} = 4300, Δa_{12} = 3300 (at 269 nm, $a_s = 2.04 \times 10^4$).

3. Potentiometric Study

The potentiometric method for studying the cinnamic acid:cyclodextrin system is based on the change in substrate (cinnamic acid) acidity caused by complex formation. Let pK_a represent the negative logarithm of the dissociation constant of cinnamic acid in the absence of cyclodextrin (pK_a refers to the experimental conditions, and is not the thermodynamic constant), and let pK_a' be the corresponding quantity in the presence of cyclodextrin. ΔpK_a is then defined $\Delta pK_a = pK_a' - pK_a$. Table XI gives the potentiometric data obtained in this study, and Figure 10 illustrates the data graphically. The curve in Figure 10 cannot be satisfactorily accounted for in terms of only 1:1 complexes between cyclodextrin and the unionized and ionized forms of cinnamic acid. The theoretical equations relating $\Delta pK_a'$ to ligand concentration for a 1:1 + 1:2 system are developed in detail in the Appendix, resulting in Equations (14) and (15) (see the Appendix for an explanation of the symbols).

TABLE XI. Potentiometric data for the cinnamic acid cyclodextrin system at 25.0 ± 0.1°.[a]

$10^2 L_t/M$	ΔpK_a',[b]
0.00	0.000
0.251	0.369
0.499	0.663
1.00	0.999
1.50	1.21
2.01	1.32
3.00	1.47
4.01	1.55
5.00	1.61
6.01	1.65
7.02	1.69
8.01	1.72

[a] $A_t = 4.83 \times 10^{-3}$ M.

[b] $pK_a = 4.35$.

FIGURE 10. Change in apparent pK_a of cinnamic acid as a function of cyclodextrin concentration at 25.0°. The smooth curve was calculated with Eqns. (14) and (15). The total substrate concentration, A_t, is 4.83×10^{-3} M.

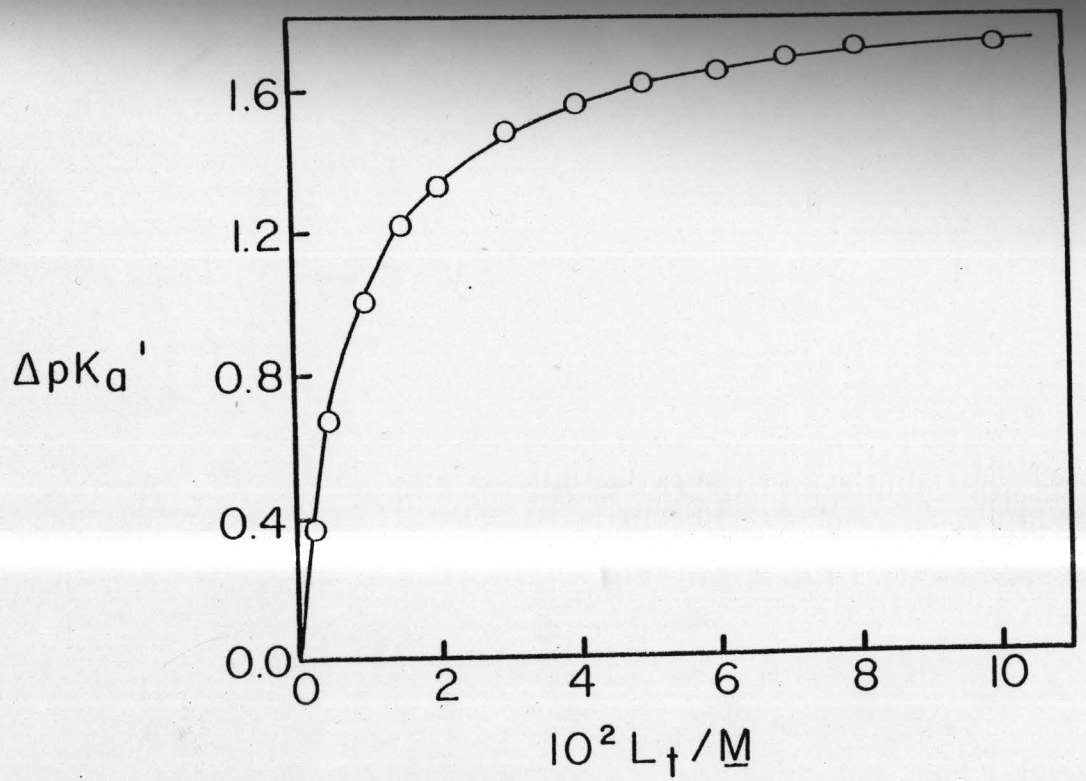
ΔpKa'
1.6
1.2
0.8
0.4
0.0
0
2
4
6
8
10
10² Lt / M

$$pK_a' = \log\left[\frac{1 + K_{11a}[L] + K_{11a}K_{12a}[L]^2}{1 + K_{11b}[L] + K_{11b}K_{12b}[L]^2}\right] \qquad (14)$$

$$L_t = [L]\left[1 + \frac{K_{11}'A_t + 2K_{12}'A_t[L]}{1 + C + K_{11}'[L] + K_{11}'[L]^2}\right] \qquad (15)$$

As in the spectral study, it is impractical to obtain a direct relation between $\Delta pK_a'$ and L_t, so a similar curve-fitting procedure was used; values were assigned to [L], and with Equations (14) and (15), corresponding values of L_t and $\Delta pK_a'$ were calculated. The smooth curve in Figure 10 was calculated in this manner. In the calculation, K_{11a} and K_{12a} were fixed at 2260 $\underline{M}^{-1}$ and 60 $\underline{M}^{-1}$, respectively, as determined from the solubility and spectral studies; thus only K_{11b} and K_{12b} were treated as adjustable parameters. Even these, however, were not completely free, since they had to account both for the potentiometric data and the spectral study on the cinnamate ion. The final values were K_{11b} = 110 $\underline{M}^{-1}$ and K_{12b} = 15 $\underline{M}^{-1}$. It was necessary to incorporate a finite value for K_{12b} in order to achieve a satisfactory fit at the higher L_t range in Figure 10. The calculated curve is given in Table XII. From the values of the stability constants, it is possible to calculate the pK_a's of SL and SL_2 (see Appendix). The values from this study are pK_{a11} = 5.66 and pK_{a12} = 6.27.

TABLE XII. Calculated potentiometric curve for a 1:1 + 1:2 complexation system.[a]

10^2 [L]/M	10^2 L_t/M	$\Delta pK_a'$
0.200	0.470	0.690
0.500	0.874	0.993
1.00	1.48	1.22
2.00	2.59	1.42
3.00	3.66	1.51
4.00	4.70	1.59
5.00	5.73	1.63
6.00	6.76	1.67
7.00	7.78	1.70
8.00	8.75	1.72

[a]Calculated with Eqns. (15) and (16) and the values K_{11a} = 2260 $\underline{M}^{-1}$, K_{12a} = 60 $\underline{M}^{-1}$, K_{11b} = 110 $\underline{M}^{-1}$, K_{12b} = 15 $\underline{M}^{-1}$, and A_t = 4.83 x 10^{-3} $\underline{M}$.

4. Thermodynamic Study

Since all of the methods used in the study of the cinnamic acid:cyclodextrin system give consistent results with the proposed model, only one method need be used to extract thermodynamic parameters; the spectral method was used for this purpose. The spectral data for the cinnamic acid:cyclodextrin system at 16.3°, 35.0°, and 45.0° are given in Tables XIII, XIV, and XV, respectively and are shown graphically in Figures 11, 12, and 13, respectively. The smooth curves drawn in these figures were calculated by methods previously described. The resulting stability constants are given in Table XVIII. Figures 14 and 15 are van't Hoff plots for K_{11} and K_{12} of the cinnamic acid:cyclodextrin system, from which the enthalpy and entropy changes for 1:1 and 1:2 complex formation were obtained. These thermodynamic parameters are given in Table XVIII.[5] Entropy changes on a mole fraction basis (unitary entropy changes) are obtained with Equation (17) (129).

---

[5]The errors given are standard deviations (s) calculated as follows (127,128): let the function sought be Q, so $Q = f(\bar{x}, \bar{y}, \ldots)$ where $\bar{x}$, $\bar{y}$ are the best estimates. Then the general expression for the variance in Q is

$$V_Q = \left(\frac{\partial f}{\partial x}\right)^2 V_{\bar{x}} + \left(\frac{\partial f}{\partial x}\right)^2 V_{\bar{y}} + \ldots$$

where v_i is the variance of $i = S_i^2$. For $Q = \ln X$, this gives $V_Q = \frac{V_{\bar{x}}}{\bar{x}^2}$.

TABLE XIII. Spectral data for the cinnamic acid:cyclodextrin system at 16.3 ± 0.2°.[a]

$10^2 L_t/M$	$-\log L_t$	ΔA[b]
0.0186	3.73	0.196
0.0505	3.30	0.303
0.0991	3.01	0.324
0.168	2.77	0.366
0.343	2.47	0.358
0.505	2.30	0.356
1.01	2.00	0.323
2.01	1.70	0.304
5.03	1.30	0.245[c]
10.0	1.00	0.218[c]

[a] $S_t = 8.51 \times 10^{-5}$ M; pH = 2.3; I = 0.01 M.

[b] λ = 279 nm; 1-cm pathlength.

[c] These ΔA values are corrected for a general medium effect as determined by using α-methylglucoside. The ΔA caused by an equivalent weight/volume concentration of α-methylglucoside at the highest L_t was +0.013.

FIGURE 11. Change in absorbance (1-cm cell) of cinnamic acid at 279 nm as a function of cyclodextrin concentration at 16.3°. The smooth curve was calculated with Eqns. (12) and (13). The total substrate concentration is 8.51×10^{-5} M.

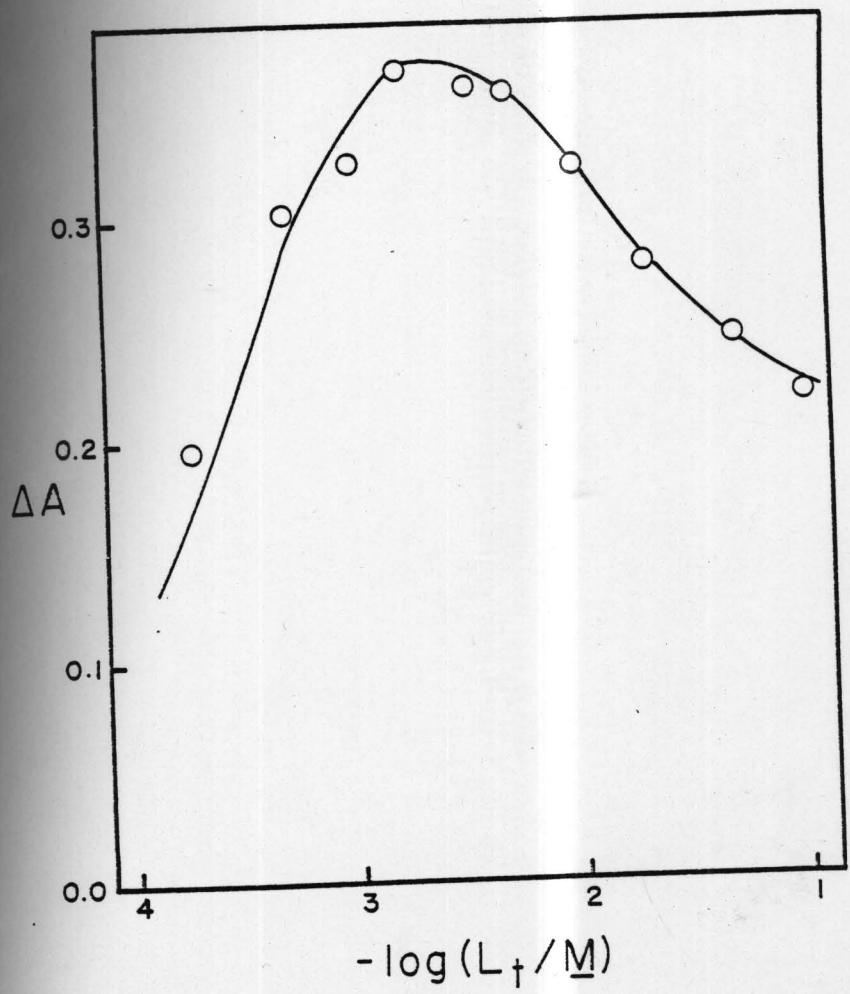
0.3
0.2
ΔA
0.1
0.0
1/4
1/3
1/2
1
-log (L_t / M)

TABLE XIV. Spectral data for the cinnamic acid:cyclodextrin system at 35.0 ± 0.2°.[a]

10^2 L_t/M	-log L_t	ΔA[b]
0.0185	3.73	0.080
0.0503	3.30	0.143
0.0986	3.01	0.178
0.167	2.78	0.228
0.341	2.47	0.269
0.503	2.30	0.275
1.00	2.00	0.282
2.00	1.70	0.272
5.00	1.30	0.234[c]
10.0	1.00	0.217[c]

[a] $S_t = 8.47 \times 10^{-5}$ M; pH = 2.3; I = 0.01 M.

[b] λ = 279 nm; 1-cm pathlength.

[c] These ΔA values are corrected for a general medium effect as determined by using α-methylglucoside. The ΔA caused by an equivalent weight/volume concentration of α-methylglucoside at the highest L_t was +0.011.

FIGURE 12. Change in absorbance (1-cm cell) of cinnamic acid at 279 nm as a function of cyclodextrin concentration at 35.0°. The smooth curve was calculated with Eqns. (12) and (13). The total substrate concentration is 8.47×10^{-5} M.

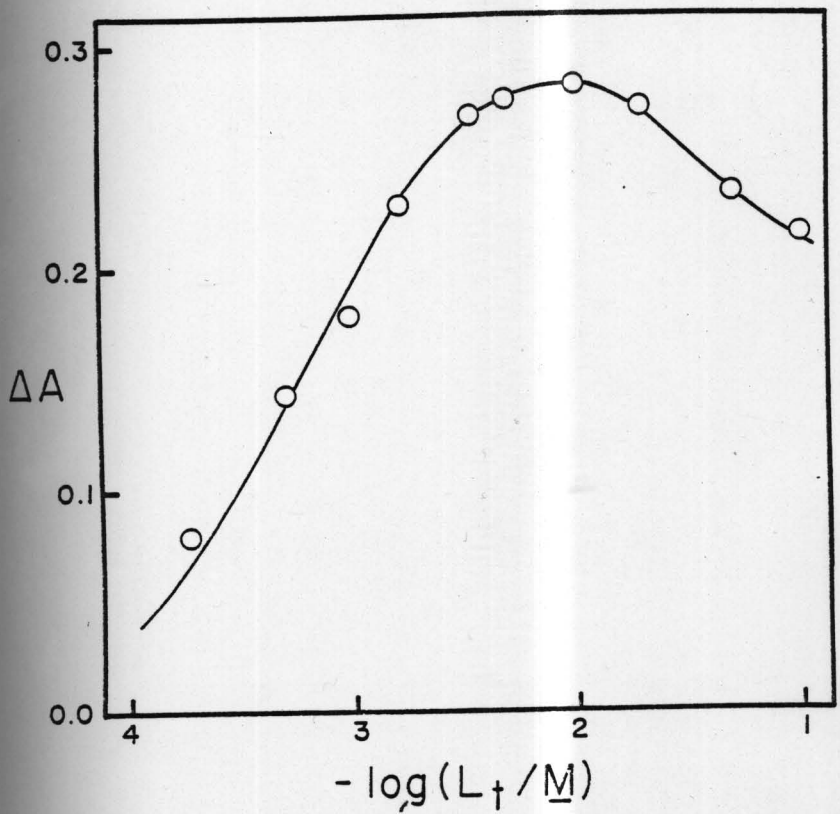
0.3
0.2
0.1
0.0
ΔA
4
3
2
1
- log (L_t / M)

TABLE XV. Spectral data for the cinnamic acid:cyclodextrin system at 45.0 ± 0.2°.[a]

10^2 L_t/M	-log L_t	ΔA[b]
0.0184	3.74	0.028
0.0501	3.30	0.081
0.0982	3.01	0.121
0.167	2.78	0.158
0.339	2.47	0.210
0.501	2.30	0.224
0.998	2.00	0.229
1.99	1.70	0.231
4.99	1.30	0.201[c]
10.0	1.00	0.182[c]

[a] $S_t = 8.44 \times 10^{-5}$ M; pH = 2.3; I = 0.01 M.

[b] λ = 279 nm.

[c] These ΔA values are corrected for a general medium effect as determined by using α-methylglucoside. The ΔA caused by an equivalent weight/volume concentration of α-methylglucoside at the highest L_t was +0.012.

FIGURE 13. Change in absorbance (1-cm cell) of cinnamic acid at 279 nm as a function of cyclodextrin concentration at 45.0°. The smooth curve was calculated with Eqns. (12) and (13). Total substrate concentration is 8.44×10^{-5} M.

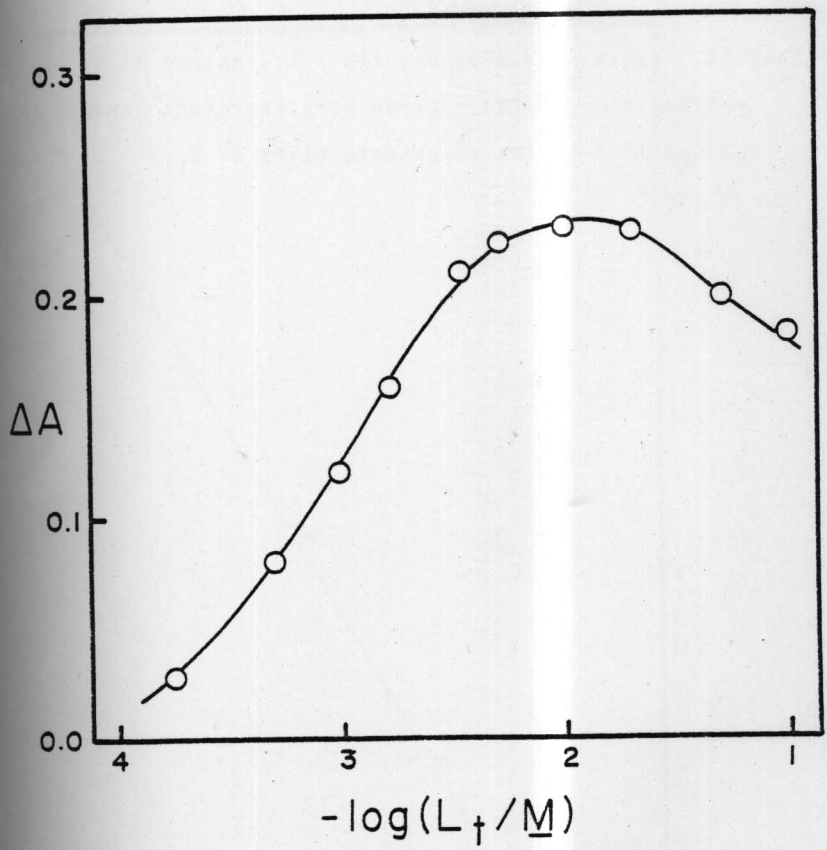
0.3
0.2
ΔA
0.1
0.0
4
3
2
1
-log(L_t/M)

FIGURE 14. van't Hoff plot for the 1:1 cinnamic acid: cyclodextrin complex. Error bars represent ranges derived from estimated uncertainties of K_{11}.

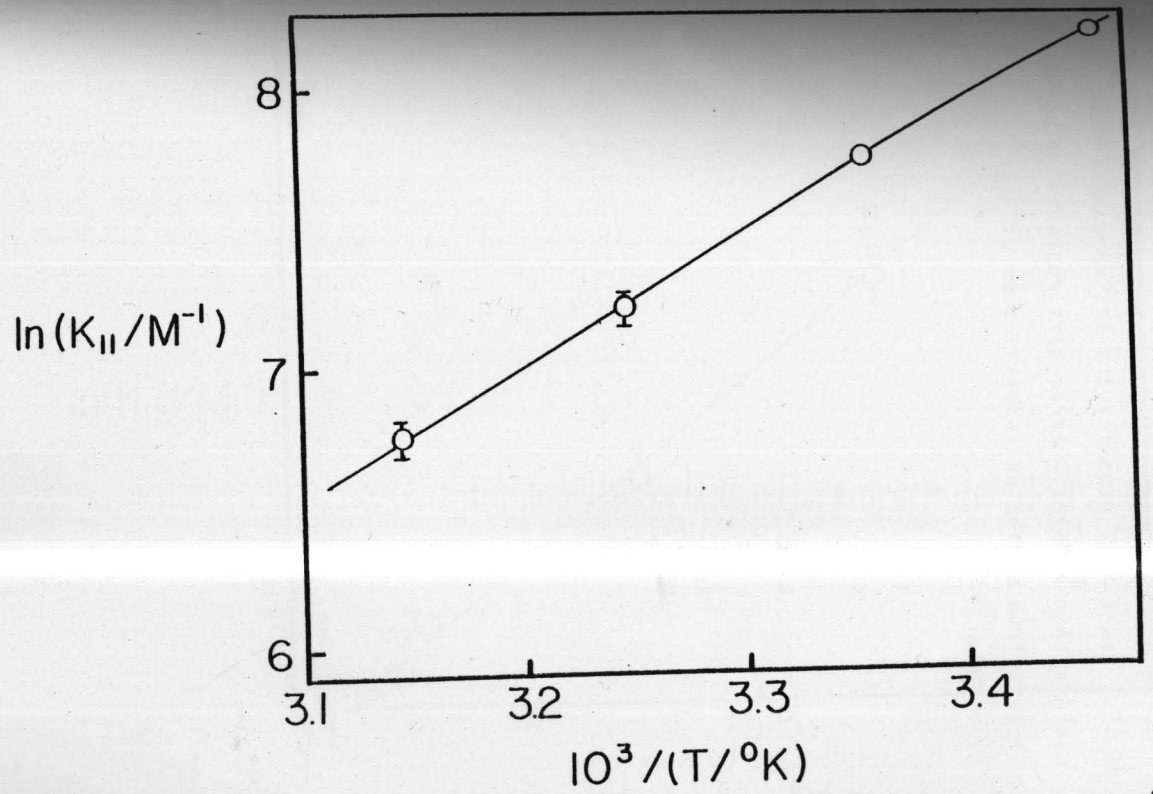
8
7
6
ln (K11 / M-1)
3.1
3.2
3.3
3.4
10³ / (T / °K)

FIGURE 15. van't Hoff plot for the 1:2 cinnamic acid: cyclodextrin complex. Error bars represent ranges derived from estimated uncertainties of K_{12}.

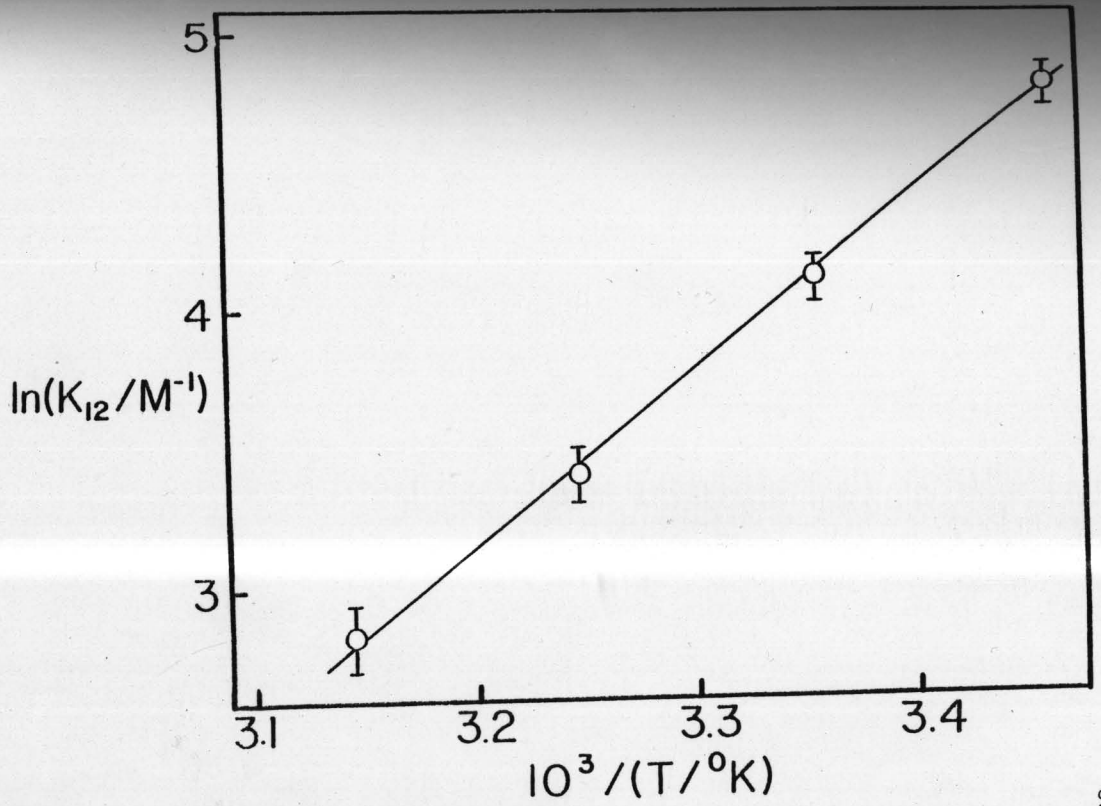
5
4
3
ln(K12/M-1)
3.1
3.2
3.3
3.4
10³/(T/°K)

$$\Delta S^\circ \text{ (unitary)} = \Delta S^\circ \text{ (molar)} + 8.0 \text{ e.u.} \qquad (17)$$

The spectral data for the cinnamate ion:cyclodextrin system at 34.8° and 45.1° are given in Tables XVI and XVII, respectively, and shown graphically in Figures 16 and 17. The smooth curves are theoretical curves with the K_{11} and K_{12} values given in Table XVIII. Figures 18 and 19 are van't Hoff plots for this system from which the thermodynamic parameters given in Table XVIII are obtained.

B. Benzoic Acid

The benzoic acid:cyclodextrin system has been studied by several authors. Reported formation constants obtained using several techniques are given in Table XIX. All of the formation constants in Table XIX were calculated assuming 1:1 stoichiometry. The wide range of K_{11} values reported renders questionable the assumed stoichiometry. This system was studied to check for the possible presence of other complexes. Examination of ultraviolet spectra of benzoic acid in the presence of varying concentrations shows behavior similar to that of the cinnamic acid:cyclodextrin system. Isosbestic points at 209 nm and 259 nm were observed at low cyclodextrin concentrations, but were lost at ligand concentrations greater than about 0.01 M, thus indicating the possibility of more than one complex. This system was studied

TABLE XVI. Spectral data for the cinnamate ion:cyclodextrin system at 34.8 ± 0.2°.[a]

10^2 L_t/M	-log L_t	ΔA[b]
0.0388	3.41	0.021
0.0989	3.01	0.032
0.177	2.75	0.059
0.709	2.15	0.136
1.78	1.75	0.228
5.01	1.30	0.292[c]
9.97	1.00	0.304[c]

[a] $S_t = 8.53 \times 10^{-5}$ M; pH = 9.0 (TRIS buffer; I = 0.01 M.

[b] λ = 269 nm; 1-cm pathlength.

[c] These ΔA values are corrected for a general medium effect as determined by using α-methylglucoside. The ΔA caused by an equivalent weight/volume concentration of α-methylglucoside at the highest L_t was +0.010.

FIGURE 16. Change in absorbance (1-cm cell) of cinnamate ion at 269 nm as a function of cyclodextrin concentration at 34.8°. The smooth curve was calculated with Eqns. (12) and (13). Total substrate concentration is 8.53×10^{-5} M.

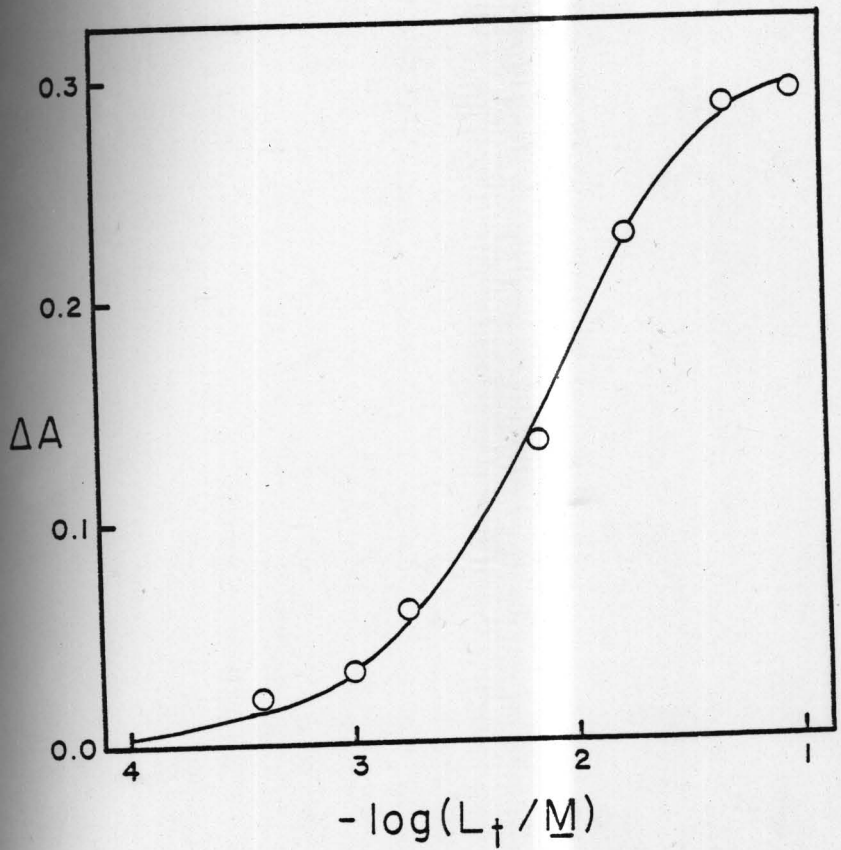
0.3
0.2
ΔA
0.1
0.0
4
3
2
1
- log(L_t / M)

TABLE XVII. Spectral data for the cinnamate ion:cyclodextrin 45.1 ± 0.2°.[a]

$10^2 L_t/M$	-Log L_t	ΔA[b]
0.0387	3.41	0.014
0.0986	3.01	0.025
0.176	2.75	0.037
0.699	2.16	0.103
1.77	1.75	0.177
4.99	1.30	0.262[c]
9.94	1.00	0.284[c]

[a] $S_t = 8.50 \times 10^{-5}$ M; pH = 9.0 (TRIS buffer); I = 0.01 M.

[b] λ = 269 nm; 1-cm pathlength.

[c] These ΔA values are corrected for a general medium effect as determined by using α-methylglucoside. The ΔA caused by an equivalent weight/volume concentration of α-methylglucoside at the highest L_t was +0.009.

FIGURE 17. Change in absorbance (1-cm cell) of cinnamate ion at 269 nm as a function of cyclodextrin concentration at 45.1°. The smooth curve was calculated with Eqns. (12) and (13). Total substrate concentration is 8.50×10^{-5} M.

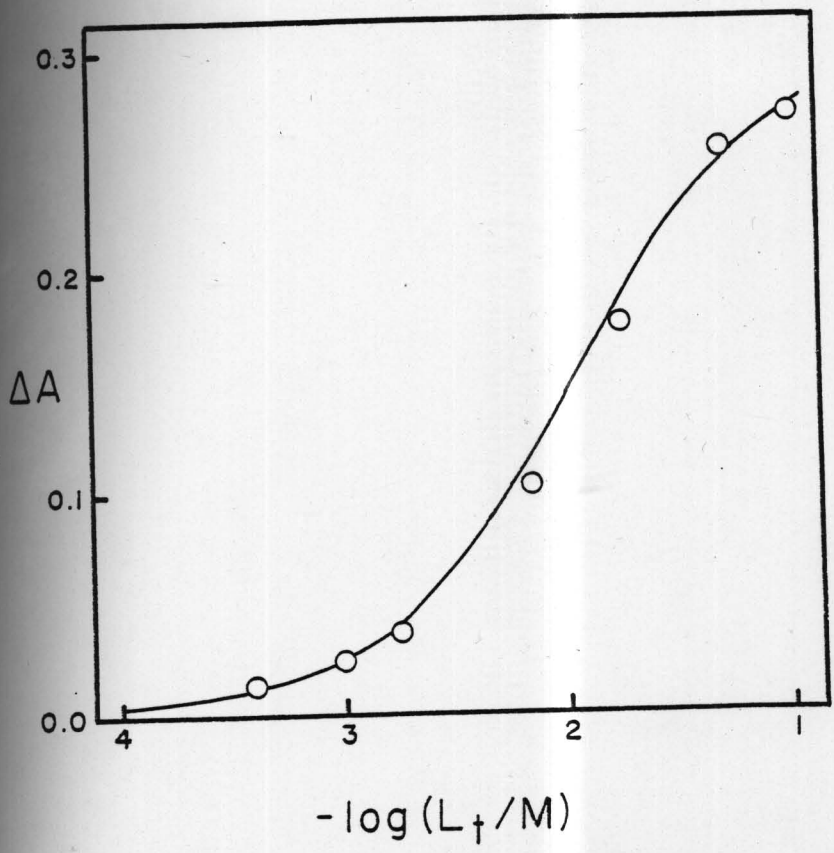
0.3
0.2
ΔA
0.1
0.0
4
3
2
1
-log (L_t/M)

FIGURE 18. van't Hoff plot for the 1:1 cinnamate ion: cyclodextrin complex. Error bars represent ranges derived from estimated uncertainties of K_{11}.

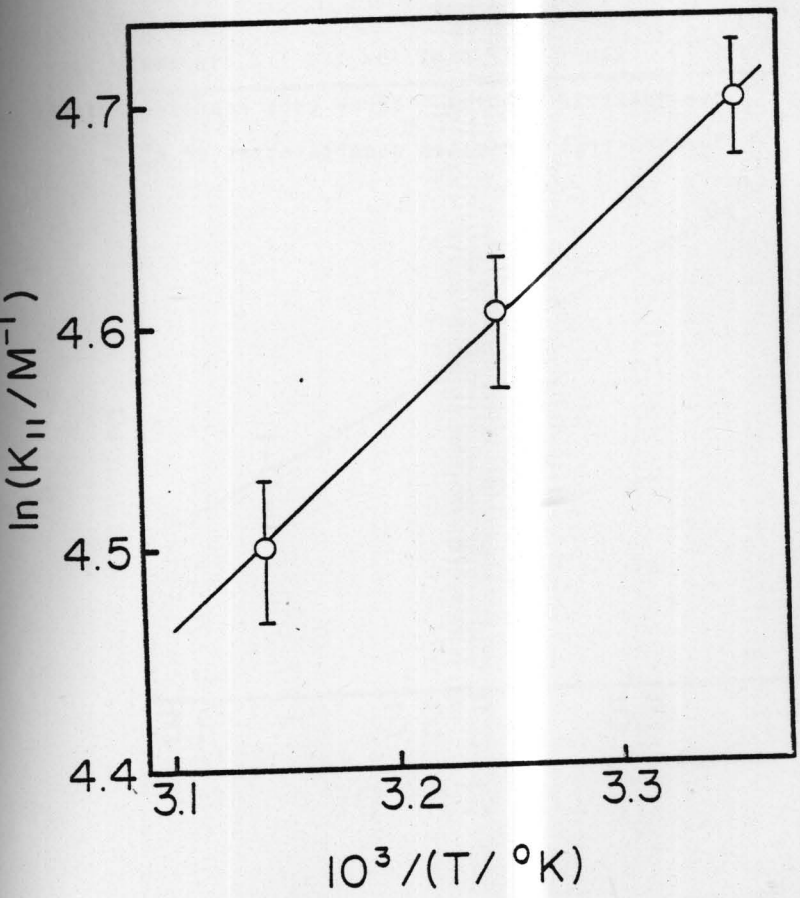
4.7
4.6
4.5
4.4
3.1
3.2
3.3
ln(K11/M-1)
10³/(T/°K)

FIGURE 19. van't Hoff plot for the 1:2 cinnamate ion: cyclodextrin complex. Error bars represent ranges derived from estimated uncertainties of K_{12}.

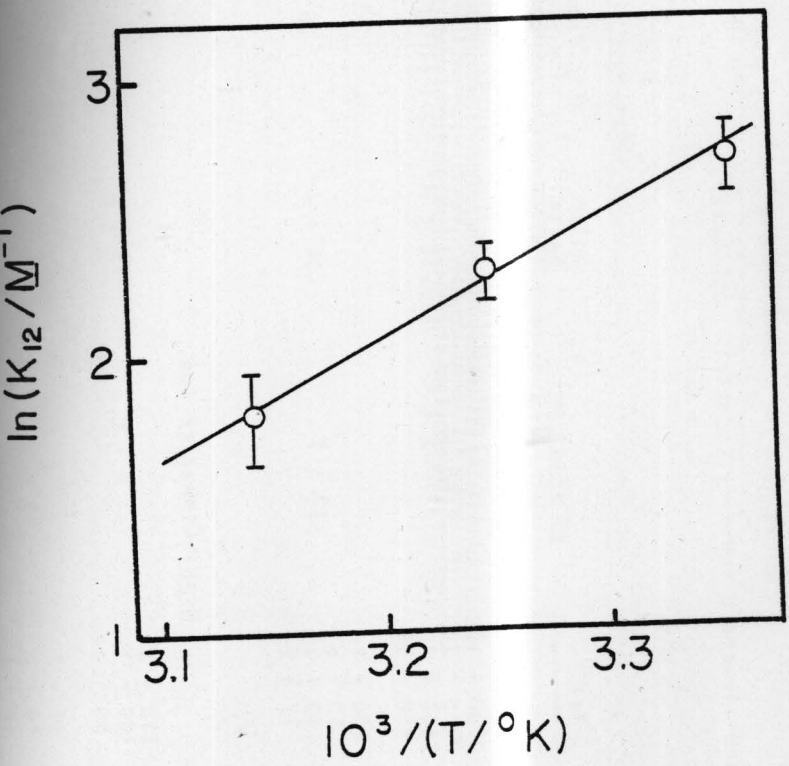
3
2
1
3.1
3.2
3.3
$\ln(K_{12}/M^{-1})$
$10^3/(T/^\circ K)$

TABLE XVIII. Thermodynamic quantities for cinnamic acid:α-cyclodextrin and cinnamate ion:α-cyclodextrin complexes.

T/°K	Complex[a]	K/M^{-1}	ΔH°/kcal-mol^{-1}	ΔS°/e.u. Molar basis	ΔS°/e.u. Mole fraction basis
		trans-Cinnamic Acid			
289	SL	3700 ± 100			
298	SL	2260 ± 50	-9.3 ± 0.6	-16 ± 2	-8
308	SL	1350 ± 80			
318	SL	850 ± 50			
289	SL_2	120 ± 10			
298	SL_2	60 ± 5	-12 ± 1	-34 ± 4	-26
308	SL_2	30 ± 3			
318	SL_2	17 ± 2			
		trans-Cinnamate Ion			
298	SL	110 ± 3			
308	SL	100 ± 3	-1.9 ± 0.6	+3 ± 2	+11
318	SL	90 ± 3			
298	SL_2	15 ± 2			
308	SL_2	10 ± 1	-9 ± 3	-23 ± 9	-15
318	SL_2	6 ± 1			

a_S = substrate (cinnamic acid or anion), L = ligand (cyclodextrin).

TABLE XIX. Formation constants for the benzoic acid:cyclodextrin system based on 1:1 stoichiometry.

K_{11}/M^{-1} [a]	Method	Ref.
1050	Competitive spectral	130
1300	Potentiometric	80
800	NMR-Chemical shifts of benzoic acid	131
230	NMR-Chemical shifts of cyclodextrin	131
751	Potentiometric	106
1000	Thermometric titration calorimetry	99
660	UV Spectral	This work
500	Solubility	This work

[a] All at 25°; ionic strengths vary.

using the spectral and solubility techniques. The spectral data are given in Table XX; a Benesi-Hildebrand plot for this system is shown in Figure 20 and a ΔA *vs.* log L_t plot is shown in Figure 21. The linear nature of the Benesi-Hildebrand plot and the sigmoid shape of Figure 21 support a 1:1 complexation system, as does the apparent linear appearance of the solubility diagram (Fig. 22). Assuming 1:1 stoichiometry, the apparent K_{11} values from the spectral and solubility studies were calculated (Table XIX). The system, however, can also be described in terms of 1:1 and 1:2 complexes. The smooth curves in Figures 21 and 22 are calculated with Equations (12) and (13) and (5), respectively, and the values: K_{11} = 750 $\underline{M}^{-1}$, K_{12} = 10 $\underline{M}^{-1}$, Δa_{11} = 1310, Δa_{12} = 1400. Since analysis of this system was not one of the primary goals in the study, it was not pursued further. A spectral study was attempted for the benzoate ion:cyclodextrin system, but spectral shifts were too small to be useful.

C. *p*-Nitrophenol

The *p*-nitrophenol:cyclodextrin and *p*-nitrophenolate:cyclodextrin systems are well documented (23,80,132). Both have been described in terms of 1:1 complexes. Spectral studies were carried out on these systems to determine whether or not other complexes were present. Results

TABLE XX. Spectral data for the benzoic acid:cyclodextrin system at 25.0 ± 0.2°.[a]

$10^2 L_t/M$	$-\log L_t$	ΔA^b	$(1/L_t) M$	$1/\Delta A$
0.00371	4.43	0.004	26900	250
0.0264	3.58	0.031	3780	32.3
0.0463	3.33	0.056	2160	17.9
0.0593	3.23	0.066	1690	15.2
0.102	2.99	0.095	986	10.5
0.170	2.77	0.126	589	7.94
0.345	2.46	0.165	290	6.06
0.503	2.30	0.176	199	5.68
1.01	2.00	0.201	99.0	4.98
2.00	1.70	0.219	50.0	4.57
10.0	1.00	0.229	10.0	4.37

[a] $S_t = 1.72 \times 10^{-4}$ M; pH = 2.1; I = 0.01 M.

[b] λ = 230 nm; 1-cm pathlength.

FIGURE 20. Benesi-Hildebrand plot for the benzoic acid: cyclodextrin system at 25.0°. The data are given in Table XX.

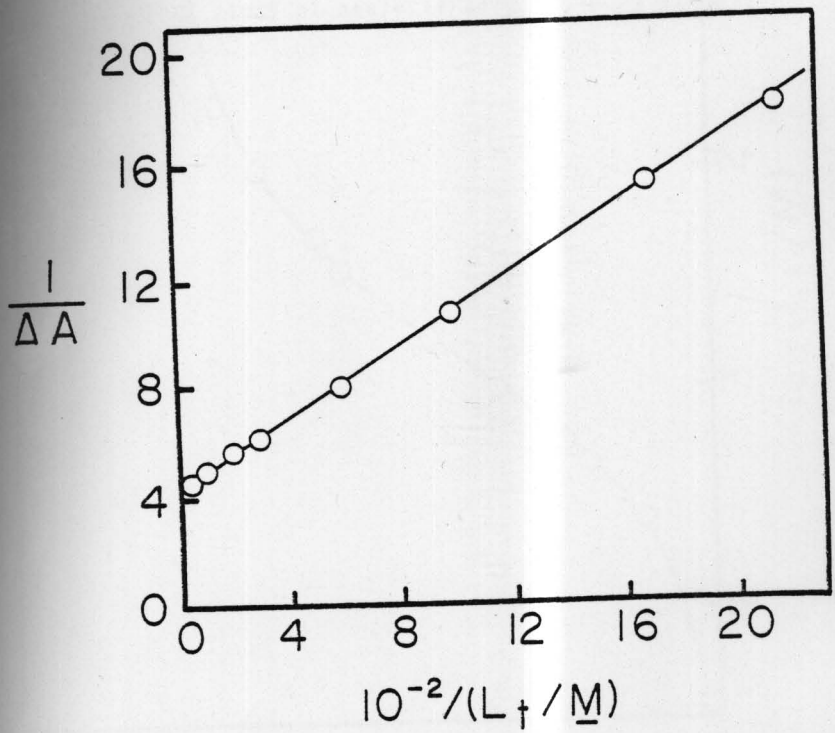
20
16
12
8
4
0
0
4
8
12
16
20
1/ΔA
10⁻²/(Lt/M)

FIGURE 21. Change in absorbance (1-cm cell) at 230 nm of benzoic acid as a function of cyclodextrin concentration at 25.0°. (Data is given in Table XX.)

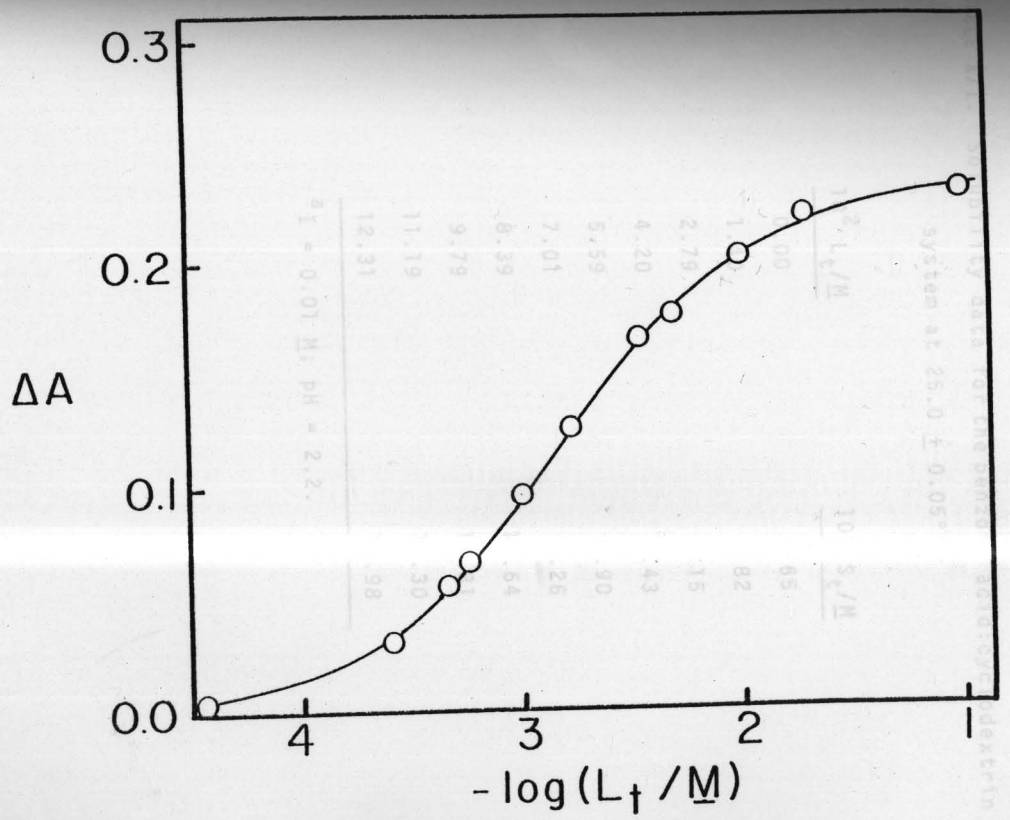
0.3
0.2
0.1
0.0
ΔA
4
3
2
1
- log (L_t / M)

TABLE XXI. Solubility data for the benzoic acid:cyclodextrin system at 25.0 ± 0.05°.[a]

$10^2 L_t/M$	$10^2 S_t/M$
0.00	2.65
1.40	3.82
2.79	5.15
4.20	6.43
5.59	7.90
7.01	9.26
8.39	10.64
9.79	11.81
11.19	13.30
12.31	13.98

[a] I = 0.01 M; pH = 2.2.

FIGURE 22. Solubility of benzoic acid as a function of cyclodextrin concentration at 25.0°. The data are given in Table XXI.

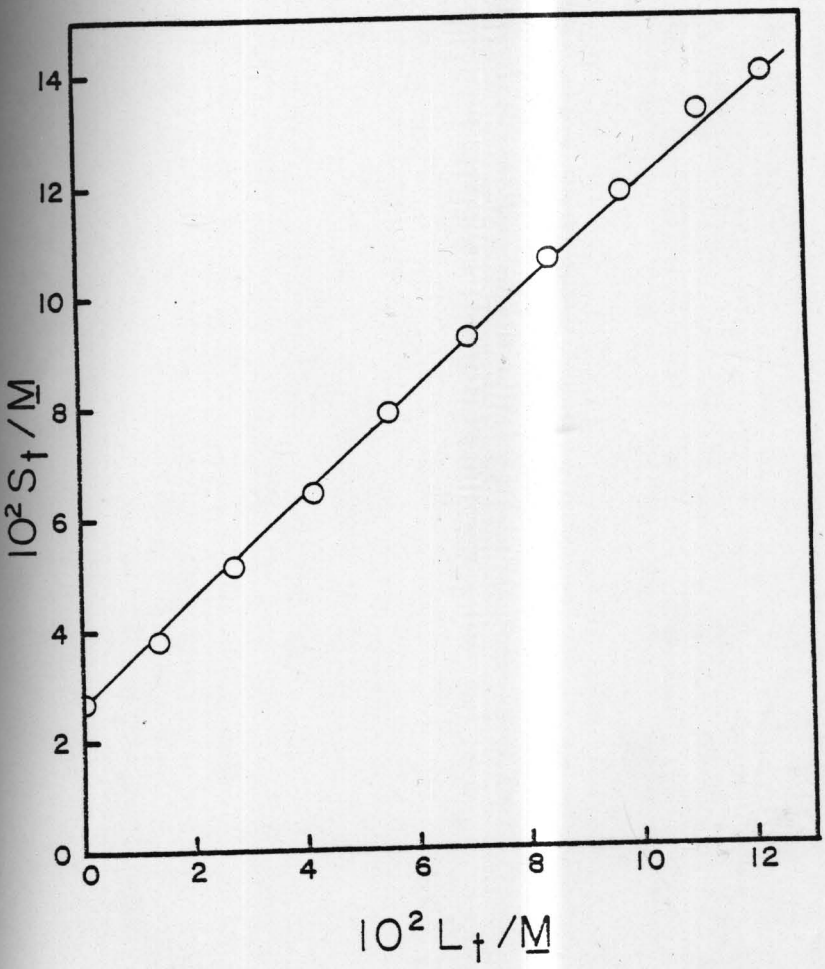
14
12
10
8
6
4
2
0
0
2
4
6
8
10
12
$10^2 S_t / \underline{M}$
$10^2 L_t / \underline{M}$

indicate that the stoichiometry of the p-nitrophenolate:cyclodextrin system is purely 1:1, with an apparent K_{11} of 2720 M^{-1} as obtained from a Benesi-Hildebrand plot. This apparent K_{11} agrees well with the value of 2820 M^{-1} reported by Cramer (23). For the p-nitrophenol:cyclodextrin system, a loss of isosbestic points was observed at high cyclodextrin concentrations (L_t > 0.03 M), possibly due to a general medium effect. An apparent K_{11} of 250 M^{-1} was obtained from a Benesi-Hildebrand plot. This compares well with Cramer's reported value of 280 M^{-1} (23). Because of the possibility that other complexes may exist in the p-nitrophenol:cyclodextrin system, a ΔA vs. log L_t plot was constructed and formation constants were obtained for the best fit assuming 1:1 and 1:2 complexes were present. These values are K_{11} = 175 M^{-1} and K_{12} = 16 M^{-1}, Δa_{11} = 1100 M^{-1} and Δa_{12} = 1825 M^{-1}. Since analysis of this system was not a primary goal in this study, it was not pursued further.

D. 3,5-Dimethoxycinnamic Acid

Two methods, solubility and spectral, were used to study the 3,5-dimethoxycinnamic acid:cyclodextrin system. Ultraviolet spectra of 3,5-dimethoxycinnamic acid with varying concentrations of cyclodextrin showed three isosbestic points at 231 nm, 240 nm and 300 nm. These isosbestic points were observed even at high ligand concentration.

Hence this system was analyzed in terms of simple 1:1 complex formation. The spectral data are given in Table XXII, and shown graphically in the form of a Benesi-Hildebrand plot in Figure 23. Least squares analysis of the data gives an apparent K_{11} (= intercept/slope) of 1970 $\underline{M}^{-1}$. Figure 24 shows a solubility diagram for the 3,5-dimethoxycinnamic acid:cyclodextrin system. The linear nature of this plot is consistent with a 1:1 complexation system. Least squares analysis (excluding the last three data points) and use of Equation (17) (114) gives an apparent K_{11} of 1960 $\underline{M}^{-1}$, in excellent agreement with the spectral results.

$$K_{11}^{app} = \frac{\text{slope}}{\text{intercept}(1 - \text{slope})} \qquad (17)$$

The points at high ligand concentration appear to deviate from the straight line. This is attributed to a small spectral perturbation caused by complexation in the analytical solution. The ligand concentrations after dilution are still large enough (1×10^{-4} $\underline{M}$ - 3×10^{-4} $\underline{M}$) to cause a shift in the spectrum of 3,5-dimethoxycinnamate ion by complexation.

E. Benzalacetone (trans-4-phenyl-3-butene-2-one)

Benzalacetone was studied by the solubility and spectral methods. Ultraviolet spectra of benzalacetone at varying

TABLE XXII. Spectral data for the 3,5-dimethoxycinnamic acid:cyclodextrin system at 25.0 ± 0.2°.[a]

10^2 L_t/M	ΔA^b	$(1/L_t)$ M	$1/\Delta A^b$
0.0174	0.050	5750	20.0
0.0355	0.071	2820	14.1
0.102	0.112	977	8.93
0.182	0.135	550	7.41
0.363	0.150	275	6.67
0.708	0.159	141	6.29
1.78	0.165	56.2	6.06
5.01	0.170	20.0	5.88
10.0	0.172	10.0	5.81

[a] $S_t = 4.54 \times 10^{-5}$ M; pH = 2.3; I = 0.01 M.

[b] λ = 291 nm; 1-cm pathlength.

FIGURE 23. Benesi-Hildebrand plot for the 3,5-dimethoxycinnamic acid:cyclodextrin system at 25.0°. The data are given in Table XXII.

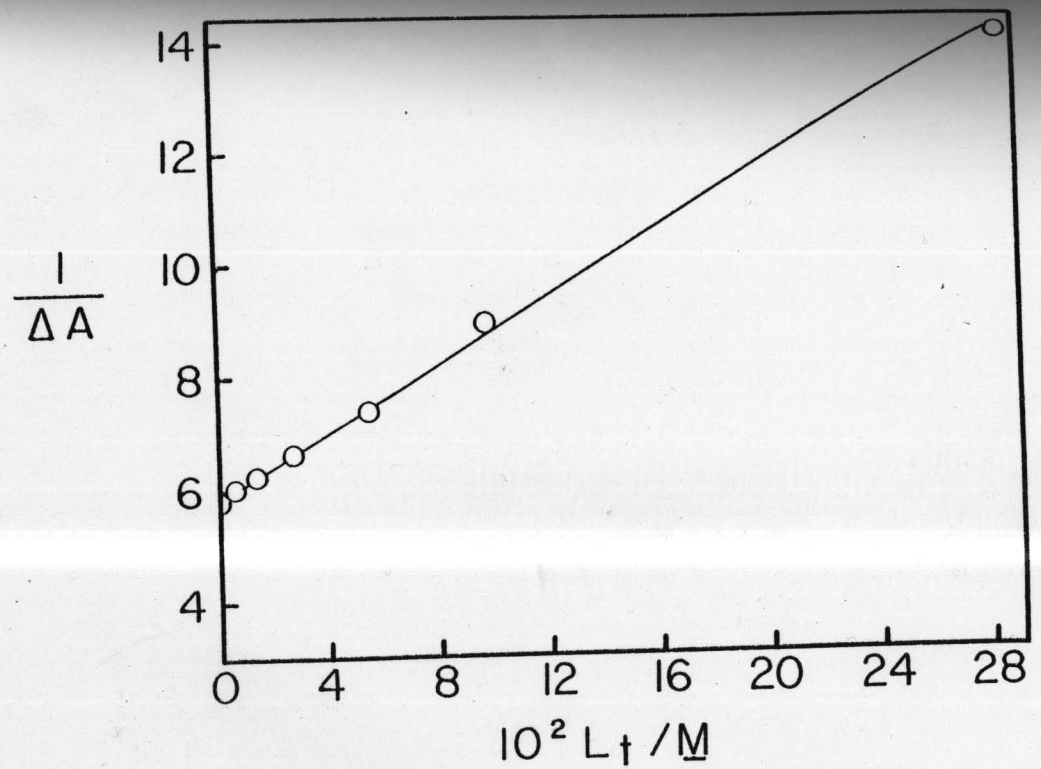
14
12
10
8
6
4
1/ΔA
0
4
8
12
16
20
24
28
10² Lt / M

TABLE XXIII. Solubility data for the 3,5-dimethoxycinnamic acid:cyclodextrin system at 25.0 ± 0.05°.[a]

10^2 L_t/M	10^3 S_t/M
0.00	0.151
0.400	1.01
1.00	2.64
1.60	3.81
2.00	5.06
3.00	7.41
4.00	9.64
5.00	12.0
5.60	13.6
6.00	14.0
7.00	17.0
8.00	19.0
9.00	21.2
10.0	23.2

[a] I = 0.01 M; pH = 2.2.

FIGURE 24. Solubility of 3,5-dimethoxycinnamic acid as a function of cyclodextrin concentration at 25.0°. (See Table XXIII for data.)

$10^3 S_t / \bar{M}$
$10^2 L_t / \bar{M}$
0
4
8
12
16
20
24
1
2
3
4
5
6
7
8
9
10

cyclodextrin concentrations show a loss of isosbestic points (241 nm and 304 nm) at cyclodextrin concentrations greater than about 0.007 M, similar to the behavior of the cinnamic acid:cyclodextrin system. A solubility diagram is shown in Figure 25. This diagram shows the familiar initial rising segment followed by a plateau. This first plateau is followed by a decrease in total solubility, then a "shoulder" and an apparent further decrease in total solubility. This apparent second decrease is explained, in part, by a spectral perturbation due to significant cyclodextrin concentrations in the measured samples, but it is doubtful that this alone can account for the decrease. Analysis of some of the solid phases from this study gave the results in Table XXIV. From these solid phase data, it is evident that complexes that are of higher ligand order than unity are present. It is not possible at this time to quantitatively account for the solution phase data. Analysis of the initial rising portion of the diagram in terms of a 1:1 and 1:2 system presents an interesting result. The slope of this line is 0.496 $\approx$ 0.50. From Equation (6), this indicates that $K_{11} \gg 1/s_o$. This gives $K_{11} = 105\ \underline{M}^{-1}$ and with this condition, the data will fit regardless of the value of K_{12}.

The spectral data are shown graphically in Figure 26. The curve-fitting procedure for calculating the smooth line in Figure 26 involved fixing K_{11} at 105 $\underline{M}^{-1}$ and varying the

TABLE XXIV. Solubility data for the benzalacetone:cyclodextrin system at 25.0 ± 0.05°.[a]

$10^2 L_t/M$	$10^2 S_t/M$	X_L
0.000	0.956	
0.450	1.19	
1.14	1.52	
1.56	1.72	
2.00	1.95	
2.90	2.28	0.26
3.00[b]	2.28[b]	
3.60[b]	2.29[b]	
4.01	2.33	
4.60[b]	2.31[b]	
4.90	2.31	0.60
5.20[b]	2.29[b]	
5.57	2.18	
6.01	2.00	0.61

6.60[b]	1.60[b]	
6.90	1.51	0.65
7.20[b]	1.47[b]	
7.80[b]	1.47[b]	
8.02	1.47	0.66
8.60[b]	1.45[b]	
9.00[b]	1.33[b]	
9.58	1.21	
9.80[b]	1.16[b]	
11.1	8.57	0.67

[a] pH = 2.2; I = 0.01 M.

[b] Equilibrated for 35 days; all others were equilibrated for 10 days.

FIGURE 25. Solubility of benzalacetone as a function of cyclodextrin concentration at 25.0°. The data are given in Table XXIV.

24
20
16
12
8
4
0
0
1
2
3
4
5
6
7
8
9
10
$10^3 S_t / \bar{M}$
$10^2 L t / \bar{M}$

TABLE XXV. Spectral data for the benzalacetone:cyclodextrin system at 25.0 ± 0.2°.[a]

$10^2 L_t/M$	$-\log L_t$	ΔA^b
0.0174	3.76	0.000
0.0355	3.45	0.001
0.102	2.99	0.023
0.182	2.74	0.032
0.363	2.44	0.062
0.708	2.15	0.091
1.78	1.75	0.169
5.01	1.30	0.213
10.0	1.00	0.236

[a] $S_t = 4.39 \times 10^{-5}$ M; pH = 2.3; I = 0.01 M.

[b] λ = 291 nm; 1-cm pathlength.

FIGURE 26. Change in absorbance (1-cm cell) of benzalacetone at 291 nm as a function of cyclodextrin concentration at 25.0°. (See Table XV for data.) The smooth curve was calculated with Eqns. (12) and (13).

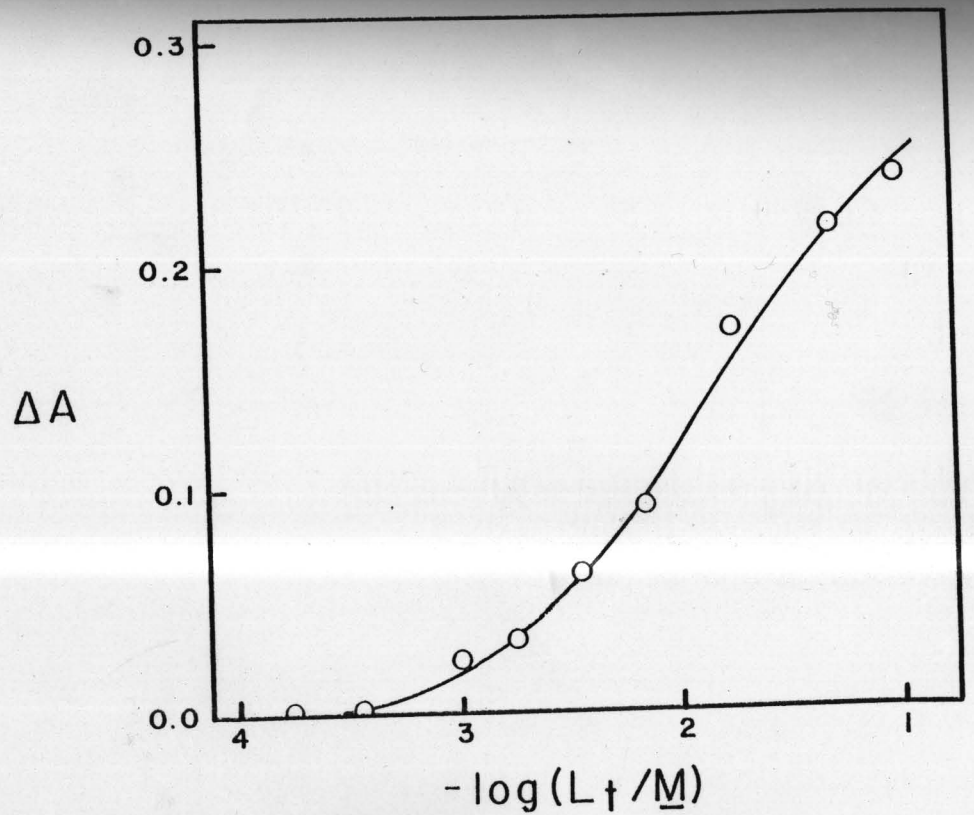
0.3
0.2
0.1
0.0
ΔA
4
3
2
1
-log(Lt/M)

other parameters. The best fit smooth line was calculated (Eqns. (12) and (13)) with $K_{11} = 105\ \underline{M}^{-1}$, $K_{12} = 15\ \underline{M}^{-1}$, $\Delta a_{11} = 4500$, and $\Delta a_{12} = 6600$.

F. Methyl Cinnamate

The methyl cinnamate:cyclodextrin system was studied by the solubility and kinetic methods. The solubility diagram for this system is shown in Figure 27, with the data given in Table XXVI. The appearance of the diagram is similar to that of the benzalacetone:cyclodextrin system, and as such, cannot be fully accounted for quantitatively at this time. As in the benzalacetone:cyclodextrin system, analysis of the solid phases (Table XXVI) indicate that a complex of higher order in L than unity is present. As before, we assume a 1:1 + 1:2 complexation system. From the initial rising portion of the solubility diagram and Equation (5) values of 1200 $\underline{M}^{-1}$ and 50 $\underline{M}^{-1}$ are obtained for K_{11} and K_{12}, respectively.

The kinetic method used to study this system is based on the effect of cyclodextrin on the rate of alkaline hydrolysis of methyl cinnamate. The reactions involved are

$$S + R \xrightarrow{k_s} P$$

$$SL + R \xrightarrow{k_{11}} P$$

TABLE XXVI. Solubility data for the methyl cinnamate:cyclodextrin system at 25.0 ± 0.05°.[a]

$10^2 L_t/M$	$10^2 S_t/M$	X_L
0.000	0.250	
0.450	0.576	
1.14	1.04	
1.56	1.36	
2.00	1.38	0.17
2.90	1.40	
4.01	1.39	0.56
4.90	1.40	0.60
5.20[b]	1.40[b]	
5.57	1.11	
6.01	0.946	0.62
6.20[b]	0.958[b]	
6.80	0.963	0.66
7.00[b]	0.966[b]	

7.29	0.749	
7.80[b]	0.868[b]	
8.60[b]	0.598[b]	
9.20[b]	0.523[b]	
11.1	0.394	0.67

[a] pH = 2.3; I = 0.01 M.

[b] Equilibration time = 35 days; all others were equilibrated for 10 days.

FIGURE 27. Solubility of methyl cinnamate as a function of cyclodextrin concentration at 25.0°. (The data are given in Table XVI.)

$10^3 S_+ / \Sigma$
16
12
8
4
0
0
1
2
3
4
5
6
7
8
9
10
$10^2 L_t / \underline{M}$

$$SL_2 + R \xrightarrow{k_{12}} P$$

where R represents the reagent OH^-.

The relationships between the observed rate constants, L_t, and the system parameters are given in Equations (18) and (19) (see Appendix for details). As was the case for the spectral and potentiometric studies, it is not practical to

$$L_t = [L] + \frac{S_t(K_{11}[L] + 2K_{11}K_{12}[L]^2)}{1 + K_{11}[L] + K_{11}K_{12}[L]^2} \qquad (18)$$

$$\frac{k_s - k_s'}{k_s} = \frac{q_{11}K_{11}[L] + q_{12}K_{11}K_{12}[L]^2}{1 + K_{11}[L] + K_{11}K_{12}[L]^2} \qquad (19)$$

where k_s' is the apparent second order rate constant in the presence of cyclodextrin

$$q_{11} = 1 - k_{11}/k_s$$

$$q_{12} = 1 - k_{12}/k_s$$

obtain an expression for k_s' as a function of L_t. Thus realistic values of [L] were chosen for which L_t and k_s' were calculated. Table XXVII gives the kinetic data obtained for this system and Figure 28 shows a plot of k_s' *vs.* L_t. The smooth line in Figure 28 was calculated with Equations (18) and (19) by fixing the values of K_{11} and K_{12} at 1200 $\underline{M}^{-1}$ and 50 $\underline{M}^{-1}$, respectively (from the solubility study), and varying q_{11} and q_{12} until a best fit was

TABLE XXVII. Kinetic data for the alkaline hydrolysis of methyl cinnamate in the presence of cyclodextrin at 25 ± 0.1°.[a]

10^2 L_t/M	pH[b]	10^5 k_{obs}/sec^{-1}	10^2 k_{OH}/$M^{-1}sec^{-1}$
0.000	10.20	1.32	8.33
0.0479	10.21	1.01	6.23
0.102	10.20	0.819	5.17
0.308	10.18	0.442	2.79
0.997	10.14	0.259	1.88
2.08	10.13	0.235	1.74
2.99	10.08	0.195	1.62
5.04	10.02	0.152	1.42
6.99	9.95	0.123	1.38
9.99	9.87	0.0626	0.844

[a] I = 0.01 M.

[b] A carbonate buffer, pH 10.20, was used; the pH of each sample was measured after completion of the study. It was assumed that the pH did not change during the study.

FIGURE 28. Rate of alkaline hydrolysis of methyl cinnamate as a function of cyclodextrin concentration at 25.0°. (The data are given in Table XXII.) The smooth curve was calculated with Eqns. (18) and (19).

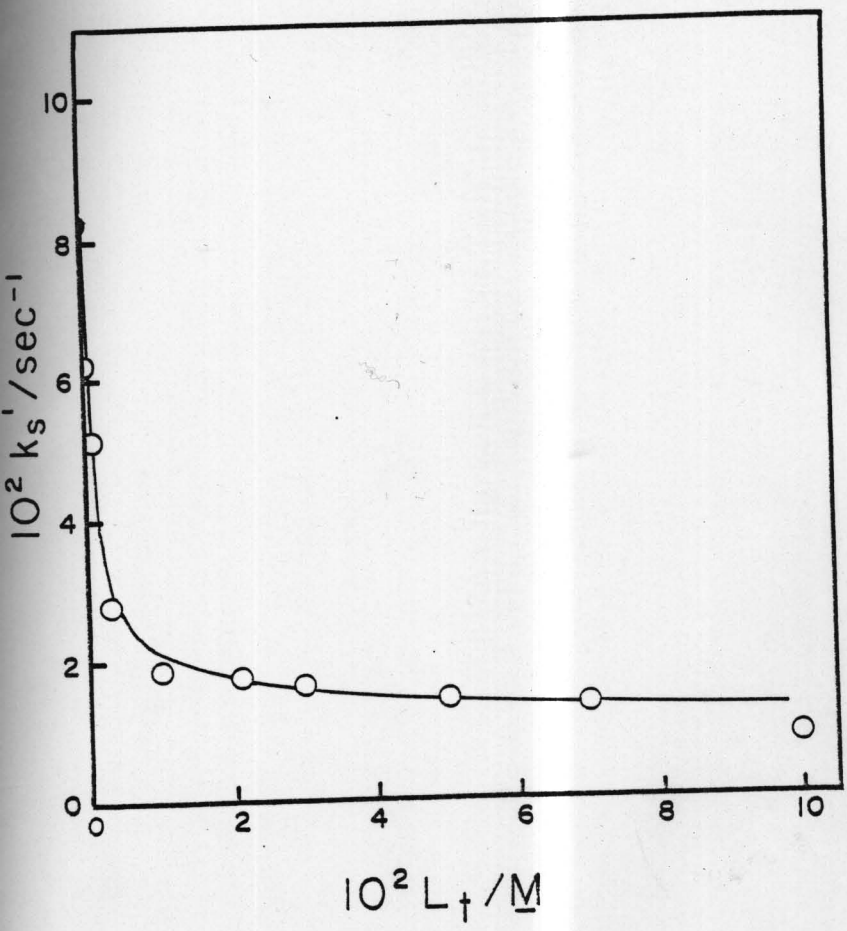
$10^2 k_s'/sec^{-1}$
0
2
4
6
8
10
$10^2 L_t/\underline{M}$

achieved. The values of q_{11} and q_{12} found were 0.75 and 0.86, respectively.

CHAPTER FOUR: DISCUSSION

A. Complex Stoichiometry and Stability

Several kinds of evidence show that the cinnamic acid: cyclodextrin system cannot be described solely in terms of 1:1 complexes: (1) the isosbestic points observed at low ligand concentrations are lost at higher concentrations; (2) the shape of the plot of ΔA *vs.* $\log L_t$ (Fig. 8) requires some process in addition to 1:1 complexation; (3) apparent 1:1 stability constants, evaluated assuming only 1:1 stoichiometry and using data at low ligand concentration, are 1300 M^{-1} from the solubility method and 2900 M^{-1} from the spectral method, the disagreement being inconsistent with the assumption; (4) the increase in total dissolved substrate after the initial plateau portion of the solubility diagram cannot occur if only 1:1 complexation occurs; (5) the solid phase composition in the solubility study requires an L:S ratio greater than 1:1; (6) the potentiometric curve cannot be fitted with the assumption of 1:1 stoichiometry.

Few modern workers appear to use the solubility method to study molecular complexes, and the technique has been criticized on the basis that it does not permit the estimation of stability constants unless the stoichiometry of the interaction is known. Of course, this is correct, but the

limitation applies equally to every other experimental technique. In the present investigation the solubility method was the single most useful tool, because it not only showed that more than one type of complex must be present, it indicated the probable stoichiometric ratios. But the strongest evidence for the interpretation of the cinnamic acid:cyclodextrin system in terms of SL and SL_2 complexes is in the quantitative agreement among the three experimental techniques when analyzed according to this model. Such comparative study by independent techniques is one desirable feature of investigations into complex stoichiometries and stabilities; another is extension of the measurements over as wide a range of ligand concentrations as is feasible, preferably over the full binding isotherm.

Lest the small values of K_{12} relative to K_{11} (Table XVIII) be thought to render incursion of SL_2 formation negligible except at high ligand concentration, note that the fractional distribution of species S, SL, and SL_2 depends on the product $K_{11}K_{12}$. These distributions can be calculated with (e.g., for SL_2) Equation (20) and Equation (13).

$$\text{fraction } SL_2 = \frac{[SL_2]}{S_t} = \frac{K_{11}K_{12}[L]^2}{1 + K_{11}[L] + K_{11}K_{12}[L]^2} \qquad (20)$$

Figure 29 is a fractional distribution diagram for the cinnamic acid:cyclodextrin system at 25° with $S_t = 8.5 \times 10^{-5}$ M,

FIGURE 29. Fractional distribution diagram for the cinnamic acid:cyclodextrin system at 25°; the total cinnamic acid concentration is 8.5×10^{-5} M. Curves from left to right: S, SL, SL_2.

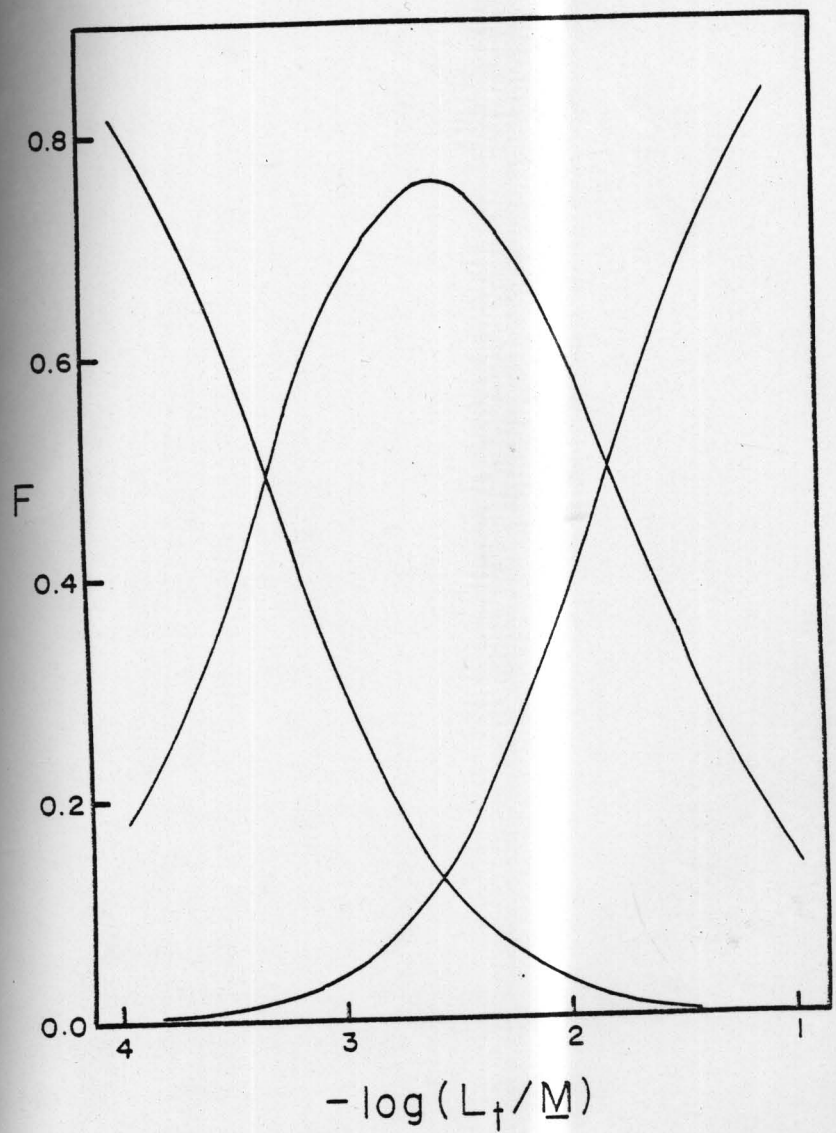
0.8
0.6
F
0.4
0.2
0.0
4
3
2
1
$-\log(L_t/\underline{M})$

corresponding to the conditions for the spectral study. At the relatively low total cyclodextrin concentration of 0.01 M, about 37% of the cinnamic acid is present as the ternary SL_2 complex. Diagrams of this type should be valuable in selecting experimental conditions for studying complex properties.

The evidence for a ternary SL_2 complex in the cinnamate ion:cyclodextrin system is less compelling, consisting of the need to include the term K_{12b} in Equation (14) in order to achieve a satisfactory fit to the potentiometric data.

The benzalacetone:cyclodextrin and methyl cinnamate: cyclodextrin systems contain complexes with stoichiometries of higher order than unity in L, as noted by the mole fractions of L greater than 0.5 in the precipitates from the solubility study. Based on the results from the cinnamic acid:cyclodextrin study, the analysis was carried out assuming a 1:1 + 1:2 system, and reasonable fits were made to the spectral (benzalacetone) and kinetic (methyl cinnamate) data. Quantitatively accounting for the entire solubility diagram based on the 1:1 + 1:2 model is more difficult. Obviously, the analysis used to explain the cinnamic acid:cyclodextrin system does not apply here, since the first plateau is followed by a decrease in S_t, an apparent leveling off, and another decrease in S_t. The quantitative nature of the second decrease in S_t is not exactly known,

since at the high concentrations of ligand employed, spectral perturbations due to complexation are present. These perturbations may be significant, but they do not account entirely for the observed decrease in S_t.

In attempting to explain the solubility diagram, one possibility is that the solubility limit of SL_2 is reached before that of SL. Qualitatively, we would then expect the diagram shown in Figure 30a, where $a' = b'$. X_L would be expected to increase from 0 to 0.67 along the plateau. This model obviously cannot account for the experimental data and thus will not be considered further.

The other possibility is that the solubility limits of SL and SL_2 are reached at the same point. Initially, this may seem too great a coincidence, but consider what is implied by this behavior in the context of the experimental method. When we say that SL and SL_2 reach their solubility limits simultaneously, we mean that they reach their solubility limits at the same L_t. But at any given L_t, in the presence of solid S, the value of [L] is fixed. Thus we mean that SL and SL_2 reach their solubility limits at the same [L]. The required condition for this is given by Equation (21). It may seem improbable that the condition should

$$\frac{s_{11}}{s_{12}} = \frac{K_{11}s_0}{K_{12}s_{11}} \qquad (21)$$

often, if ever, be met. But experimentally, even if we assume that there is no error in fixing L_t at any desired value, it is likely that in a set of replicate ampuls all having an identical L_t value, there will be a range of [L] values rather than the expected single value, this range being a consequence of experimental uncertainty, primarily in the extent of equilibration, but also including variation in solvent volume, temperature, total substrate added, etc. The result is that if SL and SL_2 both reach their solubility limits within this range of [L] associated with a single L_t, they will appear to have reached these limits simultaneously. Quantitatively, this condition requires that both Equations (22) and (23) be satisfied at the same value of L_t, which can occur at a fixed [L] if Equation (21) is satisfied, but can also occur if [L] varies enough to bracket small deviations from condition (21).

$$s_{11} = K_{11}s_0[L] \tag{22}$$

$$s_{12} = K_{11}K_{12}s_0[L]^2 \tag{23}$$

We can qualitatively picture the solubility diagrams for benzalacetone:cyclodextrin and methyl cinnamate:cyclodextrin as shown in Figure 30b. Segment a-b has already been accounted for in an earlier discussion. Now if we

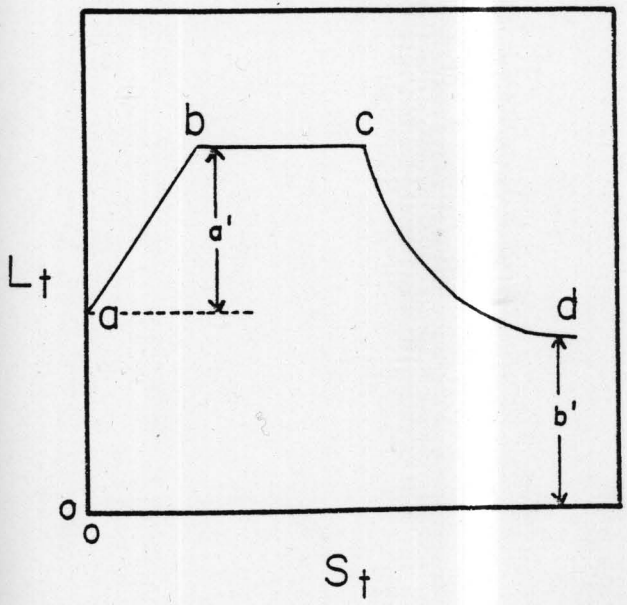

FIGURE 30a. Expected solubility diagram for a 1:1 + 1:2 complexation system where SL_2 reaches its solubility limit before SL.

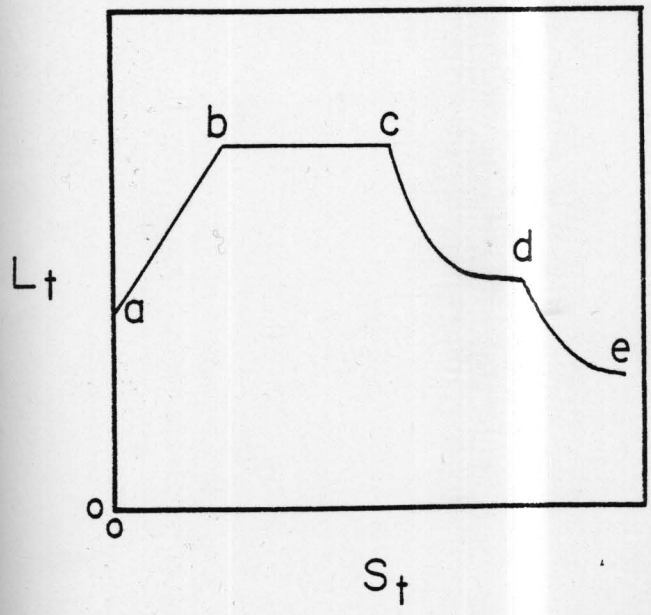

FIGURE 30b. Observed solubility diagram for methyl cinnamate and benzalacetone.

consider the situation where [SL] and [SL_2] reach their solubility limits at the same L_t, we have for segment b-c

$$S_t = s_0 + s_{11} + s_{12} \tag{24}$$

Hence, along the plateau, three solid phases are present. If we assume that beyond point c, all solid S is depleted, we have

$$[L] = \frac{[SL]}{K_{11}[S]} = \frac{s_{11}}{K_{11}[S]} \tag{25}$$

and

$$[L] = \frac{[SL_2]}{K_{12}[SL]} = \frac{s_{12}}{K_{12}s_{11}} \tag{26}$$

According to Equation (26), as more ligand is added, past point c, [L] is held fixed by the presence of solid SL and solid SL_2; in fact [L] is held at exactly the same level it had since point b, since Equation (26) is satisfied from point b to point c. Since [L] is fixed by Equation (26), [S] is fixed by Equations (25) and (26):

$$[S] = \frac{K_{12}s_{11}^{\ 2}}{K_{11}s_{12}} \tag{27}$$

But this is exactly the value it had before. Hence S cannot

decrease. In fact, for any number of complexes in the system, when two solid phases are present, the system is invariant. The above interpretation, thus, does not seem to apply to the systems under discussion, as solid phase analysis shows. It is possible that solid S is depleted before we reach point c, and any ligand added subsequently converts SL to SL_2, thus making the solid phase at point c purely SL_2. When all of the SL is depleted, there is only one solid phase present (SL_2), and S_t can now decrease as L_t increases. However, if this is the case, we would expect X_L to have a value of 0.67 at point c, and again this is inconsistent with the data (cf. Figs. 25 and 27, and Tables XXIV and XXVI). Also, this would not account for the apparent shoulder at point d. S_t would simply decrease to the value of s_{12}.

Another approach to the problem is to postulate the formation of a solid solution of SL and SL_2. This does not seem unlikely if SL and SL_2 are inclusion complexes. Saenger has reported x-ray evidence for solid complexes with channel-like structures (83,133). The solid phase would be a new structure in which discrete molecules of SL and SL_2 no longer exist, but rather a single structure (phase) is present. Then upon depletion of solid S, only one phase is present and we now have one more degree of freedom, i.e., S_t can now vary with L_t. This could account for the solid

phase analytical data. However, it doesn't appear that this can explain the discontinuity at point d.

The solid phase analysis gives evidence of a complex with a higher stoichiometry than unity in L, but a complete quantitative analysis of the solubility data cannot be given at this time for these two substrates. However, since the stability constant estimates are based solely on data in the initial rising portion, these sections of the solubility diagrams can be fully accounted for.

B. Thermodynamic Analysis of the Cinnamic Acid:Cyclodextrin System

In this section, as well as the next, it will be convenient to adopt the symbolism used in the development of the potentiometric method. Thus HA represents cinnamic acid and A^- is cinnamate ion.

The values of free energy and entropy changes depend on the concentration units used in evaluating them, and Gurney (134) has pointed out that these quantities can be corrected for the entropy of mixing if the concentrations are expressed on the mole fraction scale. The resulting values are called unitary quantities. Table XVIII gives unitary entropy changes (the last column) for the process studied

here.[6]

Evidently the favorable free energy changes are manifested, for the HAL, HAL_2, and AL_2^- complexes, as favorable $\Delta H°$ and unfavorable $\Delta S°$ values, whereas for the AL^- complex the entropy change is favorable and the enthalpy change is very small. Another observation is that, for each substrate, $\Delta H°$ is more favorable and $\Delta S°$ is less favorable for the 1:2 complexes than for the 1:1 complex. (Note that $\Delta H°$ and $\Delta S°$ for the 1:2 complexes refer to the stepwise process, Equation (3), not to the overall process, $S + 2L \rightleftarrows SL_2$.)

The conventional interpretation of favorable enthalpy changes and of entropy decreases invokes the role of water "structure," or ordering, in the complexation process. The negative $\Delta S°$ may signify an increase in solvent ordering in the product state (complex) compared with the individual solvated species. Non-polar solutes, upon association, show entropy increases, but moderately polar solutes lead to entropy decreases. Jencks (136) has pointed out that a favorable $\Delta H°$ may result from solute-solute interactions or from increased solvent-solvent interactions that are made possible by the greater solvent order. Cyclodextrins are rather special solutes, because the cavity contains highly

---

[6]For other discussions of unitary quantities see references (129) and (135). Professor P. Mukerjee is credited for first calling unitary quantities to the attention of our laboratory

ordered solvent molecules which must be displaced upon inclusion of a substrate. Bender has suggested that these water molecules cannot form the normal complement of hydrogen bonds because of steric restrictions, and that their release to bulk solvent is manifested as a favorable enthalpy change for complex formation (45). Restriction of rotational motion of an included substrate molecule sould lead to an entropy decrease.

Such rationalizations do not provide much predictive power. For the AL^- complex an entropy increase is seen, and the enthalpy change is very small. If the carboxylate group enters the cavity, the net result may be a considerable decrease in solvent order, by release of water from the cavity and from the carboxylate group. Presumably, the counter-ion remains outside the cyclodextrin. Komiyama and Bender (102) interpreted similar $\Delta H°$ and $\Delta S°$ values in the complexation of 1-adamantanecarboxylate with cyclodextrin as evidence for apolar binding of the non-polar substrate to the top of the cavity. This, however, does not seem applicable to the cinnamate ion system.

The $\Delta H°$ and $\Delta S°$ values for HAL_2 and AL_2^- are similar, considering the uncertainties. In each case, the process may be much the same: a ligand (L) cavity is evacuated, the ligand slides over the portion of substrate protruding in an SL complex, S readjusts its position within the L_2

aggregate, and solvent re-ordering occurs.

The solubility data provide for a different kind of thermodynamic analysis. Table XXVIII gives unitary free energy changes for processes described earlier. Steps (1)-(4) are for the formation of complex HAL; these processes when added give net process (5). Reaction (5) is solvent-independent (if solid L is understood to represent the hydrated ligand); it is expected that the same value would be obtained for $\Delta G°$ for reaction (5) if corresponding experimental values were available for steps (1)-(4) in another solvent such as a mixed aqueous-organic solvent. Thus $\Delta G°$ for process (5) can be compared with $\Delta G°$ for process (4) (Table XXVIII), indicating that the complex formation is thermodynamically more favorable in water than in the solid state. Tables XXVIII and XXIX show a similar relationship for the HAL_2 and AL^- complexes, respectively. It is an interesting result that formation of these complexes in the solid phase is thermodynamically favorable.

These processes can be represented as a cycle, e.g., for the complex SL:

$$\begin{array}{ccccc} S(aq) & + & L(aq) & \rightleftarrows & SL(aq) \\ \uparrow\downarrow & & \uparrow\downarrow & & \uparrow\downarrow \\ S(s) & + & L(s) & \rightleftarrows & SL(s) \end{array}$$

TABLE XXVIII. Thermodynamic Analysis of the Cinnamic Acid:Cyclodextrin System

	Process[a]	$\Delta G°$(unitary)[b]/cal-mol^{-1}
(1)	$S(s) \rightleftarrows S(aq)$	+5850 ± 10
(2)	$L(s) \rightleftarrows L(aq)$	+3610 ± 50
(3)	$SL(aq) \rightleftarrows SL(s)$	-4800 ± 70
(4)	$S(aq) + L(aq) \rightleftarrows SL(aq)$	-6950 ± 15
(5)	$S(s) + L(s) \rightleftarrows SL(s)$	-2320 ± 90
(6)	$SL(s) \rightleftarrows SL(aq)$	+4800 ± 70
(7)	$L(s) \rightleftarrows L(aq)$	+3610 ± 50
(8)	$SL_2(aq) \rightleftarrows SL_2(s)$	-5460 ± 100 (-6280 ± 260)
(9)	$SL(aq) + L(aq) \rightleftarrows SL_2(aq)$	-4810 ± 50
(10)	$SL(s) + L(s) \rightleftarrows SL_2(s)$	-1860 ± 140 (-2680 ± 280)

[a](s) represents solid phase; (aq) represents aqueous solution.

[b]Uncertainties represent standard deviation estimates calculated from experimental estimates of uncertainties in solubilities and stability constants.

TABLE XXIX. Thermodynamic Analysisof the 1:1 Cinnamate Ion:Cyclodextrin Complex

Process	$\Delta G°(\text{unitary})^b$/cal-mol^{-1}
(1) $M^+S^-(s) \rightleftarrows M^+S^-(aq)$	+2790 ± 120
(2) $L(s) \rightleftarrows L(aq)$	+3610 ± 50
(3) $M^+SL^-(aq) \rightleftarrows M^+SL^-(s)$	[-2790 + 120 to -4800 ± 70][a]
(4) $M^+S^-(aq) + L(aq) \rightleftarrows M^+SL^-(aq)$	-5160 ± 20
(5) $M^+S^-(s) + L(s) \rightleftarrows M^+SL^-(s)$	[-1550 ± 200 to -2430 ± 150]

[a] Estimated limits. These values are discussed in the following section.

[b] Uncertainties represent standard deviation estimates calculated from experimental estimates of uncertainties in solubilities and stability constants.

Just as other solvents should lead to the same free energy change for the solid phase process, so also the solid phases in this cycle could be replaced by liquid phases, and rather than use solubilities in the model, partition coefficients would be employed. This cycle suggests why, for series of closely related compounds, limited correlations between complex stability constants and substrate solubility or partition coefficient may be observed.

C. Complex Properties and Structures

We consider first the cinnamic acid:cyclodextrin system. We conclude from this study that HAL and HAL_2 are inclusion complexes. This conclusion follows from the abnormally large equilibrium constants for their formation. (The overall constant for the process $HA + 2L \rightleftarrows HAL_2$ is equal to $K_{11}K_{12}$.) When two species interact non-covalently in solution in a simple "stacking" manner, the stability constant for the process is proportional to the area of contact between the molecules (112). For a molecule the size of cinnamic acid, the maximum value to be expected is of the order 10^2 $\underline{M}^{-1}$. Since K_{11} for the cinnamic acid:cyclodextrin system is much in excess of this, some extraordinary stabilizing phenomenon, presumably inclusion, must be occurring. The ternary complex HAL_2 is formed from L and the inclusion complex HAL, so it too must be an inclusion complex.

Several properties of the complexes, other than the standard thermodynamic quantities, have been measured in the course of this study. These properties may be helpful in determining complex structures. The complex molar absorptivities for HAL, HAL_2, AL^-, and AL_2^- have been obtained, but these are known only at a single wavelength. The general spectral shifts in the presence of cyclodextrin are not dramatic, and do not at this point seem helpful.

The pK_a values reported earlier are $pK_a = 4.35$ for uncomplexed cinnamic acid, $pK_{a11} = 5.66$ and $pK_{a12} = 6.27$ for the 1:1 and 1:2 complexes, respectively. It is a general result that complexing between carboxylic acids and cyclodextrin leads to a decrease in acid strength of the substrate; this is equivalent to saying that the unionized carboxylic acid complexes more strongly than does the carboxylate ion (80). Since the two above statements are equivalent, a rationalization of one of them equally accounts for the other. Consider the acidity of HAL, that is, the acidity of complexed cinnamic acid, relative to that of cinnamic acid in water. Spectroscopic data (45) indicate that the cyclodextrin cavity is apolar. If the carboxyl group of the cinnamic acid is included within the ligand cavity, then, from a dielectric viewpoint, it experiences an environment that is comparable (except for "end" effects and restricted molecular motion) to that provided by a solvent

such as dioxane or a ketone. In such a medium, having an effective dielectric constant smaller than that of water, the extent of ionization of the carboxylic acid will be less than in water. Therefore we anticipate that $K_{a11} < K_a$ for carboxylic acids, from which it follows that $K_{11a} > K_{11b}$, as is observed for these substrates.[7] The same argument applies to the ternary complex HAL_2.

The solubility of HAL was determined to be 1.7×10^{-2} M. If the substrate HA is included within the ligand cavity, it is reasonable that the species HAL would have a solubility intermediate to those of the hydrophobic HA ($s_o = 3.01 \times 10^{-3}$ M) and the hydrophilic ligand ($S_L = 0.125$ M). (This expectation might be extended to other neutral, relatively hydrophobic substrates.) The solubility of HAL_2 is 5.5×10^{-3} M (or 1.4×10^{-3} M), considerably smaller than those of L or HAL, and comparable to that of HA. If HA is included in a channel formed by an end-to-end association of two cyclodextrins, the solubility of HAL_2 will be determined in

---

[7] The same argument applied to phenols may seem to lead to the same prediction. However, phenols are known to behave differently from carboxylic acids in nonaqueous media. E.g., in pyridine, the acid strengths of phenols are enhanced relative to those of carboxylic acids, with the result that, e.g., p-nitrophenol is a stronger acid than is benzoic acid in this solvent (137). Similar behavior is observed in acetone (138). Thusit is possible, even likely, that phenol acidity will be increased in the cyclodextrin cavity, with the consequence that $K_{11b} > K_{11a}$, as is seen (45,80).

part by solvent interactions with a dimer-like species L_2; this species is twice as large as L or HAL, and provides no additional sites for solvent interaction, hence, its solubility probably will be smaller.

The solubility of the 1:1 cinnamate ion:cyclodextrin complex was not determined; if this is an inclusion complex with the carboxylate group buried in the cavity, its solubility might be as low as that of HAL. If on the other hand, the carboxylate function is exposed, the complex may be as soluble as the substrate; sodium cinnamate was found to have a solubility of 0.505 M. These limits were used in Table XXIX to estimate the free energy for reaction (3).

Carbon-13 nuclear magnetic resonance studies of the sodium cinnamate:cyclodextrin system under conditions such that (as calculated with our present results) the fractional distribution of species was A^-, 0.33; AL^-, 0.55; AL_2^-, 0.12, showed chemical shift displacements of each of the side-chain carbons, but no significant changes for the phenyl carbons (139). Adopting the symbolism of Gelb *et al.* (104), we specify the side chain carbons as α, β, γ, the carboxylate carbon being the γ carbon. For sodium cinnamate, chemical shift displacements of -0.4 (α), +0.9 (β), and -1.3 (γ) ppm were observed (139). Gelb *et al.* (104) interpreted similar effects with p-methylcinnamate ion in terms of an inclusion complex having the carboxylate group included in

the cyclodextrin cavity.

The picture that results from these several kinds of evidence and lines of reasoning is of binary (1:1) inclusion complexes, probably with the side-chain included in the cavity. The ternary (1:2) complexes may have the substrate included in a cavity formed by two ligand molecules associated end-to-end. Although cyclodextrin does not form a dimer (106), in the presence of cinnamic acid or cinnamate ion (and possibly related compounds) the SL_2 complex is formed. In a sense, cyclodextrin dimerization is promoted by the substrate molecule, the complex structure possibly being much like a dowel joint. Such SL_2 complexes are formed by cinnamic acid, cinnamate ion, p-methylcinnamate ion (104), and 4-biphenylcarboxylate ion (105) whereas benzoate ion (82) and p-nitrophenolate ion apparently form only 1:1 complexes and it is questionable whether or not benzoic acid and p-nitrophenol form 1:2 complexes. Possibly a factor in determining whether ornot a substrate is capable of forming a 1:2 complex is the length of the molecule.

It is desirable to be able to predict values of stability constants. Toward this end, the following argument may have some importance. Let h———H represent cyclodextrin (the different symbols representing the non-symmetry of the molecule) and let g———G represent a non-symmetrical substrate (or guest). Then all of the possible 1:1

complexes can be represented as shown below.

Complex	Complex symbol	Stability constant
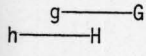	gH	K_{gH}
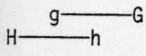	gh	K_{gh}
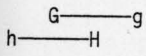	GH	K_{GH}
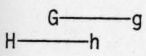	Gh	K_{Gh}

We assume that within each orientation above, the energy distribution of the positional isomers is narrow, so that only a single, e.g. Gh, complex need be considered. From the above structural representations, it is in principle possible to form both 2:1 and 1:2 inclusion complexes. For the 2:1 complexes we would have

Complex	Complex symbol	Stability constant
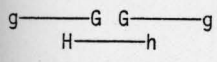	HGGh	K_{HGGh}
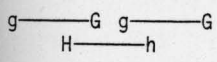	HGgh	K_{HGgh}
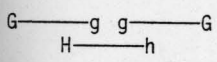	Hggh	K_{Hggh}
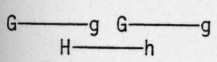	HgGh	K_{HgGh}

Note that there are only four possibilities if the complexes are formed by inserting the ends of two S molecules into the L cavity. Now consider the possible 1:2 complexes. We have

Complex	Complex symbol	Stability constant
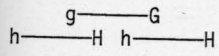	gHhG	K_{gHhG}
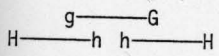	ghhG	K_{ghhG}
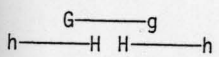	GHHg	K_{GHHg}
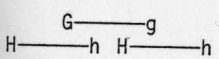	GhHg	K_{GhHg}

Again there are only four possibilities. The formation of the four S_2L complexes implies that S is capable of entering both ends of the L cavity. No evidence has been reported for existence of this type of S_2L complex. If no S_2L complexes exist, then it is reasonable to assume that (for substrates similar to the ones studied) S can only enter one end of the cavity. As a consequence of this, there are only two possible 1:1 complexes and only one 1:2 complex. The following discussion is based on the above conclusion and its consequences.

Let the H end of the ligand be the end of the cavity that can be entered by the substrate. Then the two possible 1:1 complexes are gH and GH, and the only possible 1:2

complex is gHHG. If there are two isomeric 1:1 complexes, then the experimentally determined K_{11} is the sum of the stability constants for both isomeric 1:1 complexes. Hence, in our case

$$K_{11} = K_{gH} + K_{GH} \tag{28}$$

We earlier defined the complex formation as a stepwise equilibrium (see Eqns. (1)-(4)). Consider now how gHHG can be formed:

$$\begin{array}{ccccccc} & & L & & L & & \\ & & + & & + & & \\ S + L & \overset{K_{gH}}{\rightleftharpoons} & gH & \rightleftharpoons & GH & \overset{K_{GH}}{\rightleftharpoons} & S + L \\ & & \uparrow\downarrow K' & & K'' \downarrow\uparrow & & \\ & & & gHHG & & & \end{array}$$

Therefore, we can write

$$gH + L \rightleftarrows gHHG \tag{29}$$

$$K'_{gHHG} = \frac{[gHHG]}{[gH][L]} \tag{30}$$

as well as

$$GH + L \rightleftarrows gHHG \tag{31}$$

$$K''_{gHHG} = \frac{[gHHG]}{[GH][L]} \tag{32}$$

Hence,

$$\frac{[gHHG]}{[L]} = K'_{gHHG}[gH] = K''_{gHHG}[GH] \tag{33}$$

and

$$\frac{[gH]}{[GH]} = \frac{K''_{gHHG}}{K'_{gHHG}} \tag{34}$$

We can write the stability constants for the formation of the 1:1 complexes gH and GH as

$$K_{gH} = \frac{[gH]}{[S][L]} \tag{35}$$

$$K_{GH} = \frac{[GH]}{[S][L]} \tag{36}$$

So

$$\frac{[gH]}{[GH]} = \frac{K_{gH}}{K_{GH}} \tag{37}$$

From Equations (34) and (37), we get

$$K_{gH}K'_{gHHG} = K_{GH}K''_{gHHG} \tag{38}$$

If one of the 1:1 complexes, e.g. gH, is greatly favored over the other (GH) so that $K_{gH} >> K_{GH}$, it follows that $K'' >> K'$, since the formation of gHHG via the K" route is essentially the same process as the formation of gH.

To determine what the experimental K_{12} is equal to in these terms, consider the hypothetical system in which a product P is formed from a reactant A and two different species (B and C) in mutual equilibrium, i.e.,

$$A + B \rightleftarrows P \qquad K_B = \frac{[P]}{[A][B]} \tag{39}$$

$$A + C \rightleftarrows P \qquad K_C = \frac{[P]}{[A][C]} \tag{40}$$

The net observable process is

$$A + (B \text{ or } C) \rightleftarrows P \tag{41}$$

hence the observable equilibrium constant is

$$K_{obs} = \frac{[P]}{[A]([B] + [C])} = \frac{K_B K_C}{K_B + K_C} \tag{42}$$

Returning to our system, if we equate B with gH and C with GH, then K_{obs} becomes the experimental K_{12} value and we have

$$K_{12} = \frac{K_{gH}K_{GH}}{K_{gH} + K_{GH}} = \frac{K_{gH}K_{GH}}{K_{11}} \qquad (43)$$

With Equations (28) and (43), we can calculate the values of K_{gH} and K_{GH}.

The equations just derived are general. If the argument is valid, it is expected that related substrates will have similar values for K_{gH} and K_{GH}. Thus, if K_{11} and K_{12} are obtained for a single substrate we should be able to predict the K_{11} and K_{12} for related substrates. The model does not account for substituent effects at either end of the substrate molecules, and the effect of this will be discussed later. The hypothesis described above was tested by studying the interaction of cinnamic acid and some related compounds with cyclodextrin. The calculated values of K_{gH} and K_{GH} along with corresponding standard free energies are given in Table XXX. It should be kept in mind that the assignments of K_{gH} and K_{GH} are purely arbitrary. If, as we proposed earlier, the 1:1 cinnamic acid:cyclodextrin has the cinnamic acid carboxyl group located inside the cyclodextrin cavity, then from Table XXX this complex has a stability constant of 2199 $\underline{M}^{-1}$, and has been designated K_{GH}. The 1:1 complex having the aromatic moiety located in the cavity then has a stability constant of 61.5 $\underline{M}^{-1}$ (K_{gH}). On this basis, it is expected that closely related compounds will have similar stability constants. The 3,5-dimethoxycinnamic

TABLE XXX. Calculated isomeric 1:1 stability constants and the corresponding standard free energy changes for cinnamic acid and some related compounds.

Substrate	$K_{GH}/\underline{M}^{-1}$	ΔG°_{GH}/cal/mole	$K_{gH}/\underline{M}^{-1}$	ΔG°_{gH}/cal/mole
Cinnamic acid	2199	-4560	61.5	-2340
Methyl cinnamate	1148	-4180	52.3	-2340
3,5-Dimethoxycinnamic acid	1970	-4490	0	--
Benzalacetone	86.9	-2640	18.1	-1710
Cinnamate ion	92.1	-2680	17.9	-1710

acid and methyl cinnamate appear to fit the model well as judged from ΔG°_{GH} and ΔG°_{gH} (Table XXX). The smaller values in Table XXX have been designated gH for consistency. The K_{gH} value of zero for 3,5-dimethoxycinnamic acid is expected because the aromatic moiety is too bulky to fit into the cyclodextrin cavity. The aromatic moiety is essentially the same for all substrates (except the 3,5-dimethoxycinnamic acid) and hence the same value of K_{gH} (or ΔG°_{gH}) is expected; the calculated values are in relatively good agreement as is seen in Table XXX.

The benzalacetone:cyclodextrin appears to be an exception. But, as mentioned earlier,the model does not account for major changes in substituent at either end of the molecule. If the cinnamic acid:cyclodextrin 1:1 complex with the carboxyl group located in the cavity is the stronger complex (described by K_{GH}), then changing this end of the molecule may have a more dramatic effect on the complexing ability than can be accounted for by the model. While the changes in the carboxyl end of the substrates may not seem dramatic, there is a large change in dipole moment as is seen in Table XXXI. Since cinnamic acid, methyl cinnamate, and benzalacetone all have practically the same length, the dipole moment is a good comparative measure of the magnitude of charge development.

TABLE XXXI. Dipole moments of cinnamic acid, methyl cinnamate, and benzalacetone.

Compound	μ (D)[a]
Trans-cinnamic acid	1.31
Methyl cinnamate	1.95
Benzalacetone	3.34

[a]From reference (140).

Figure 31 shows plots of log K *vs.* substrate μ for cyclodextrin complexes with cinnamic acid, methyl cinnamate, and benzalacetone. The very good correlation observed is consistent with the view of the cyclodextrin as having a cavity that is relatively non-polar. It is therefore expected that for a series of closely related compounds, the strength of the inclusion complex should be inversely proportional to substrate polarity. The relative slopes of the log K_{GH} *vs.* μ and log K_{gH} *vs.* μ plots (Fig. 31) lend strong support to our hypothesis in that a substituent change on the end of the molecule showing the stronger inclusion should have a larger effect on the stability of that 1:1 complex than on the 1:1 complex having the opposite end (where no substituent change has been made) included in the molecule. The K_{GH} values, representing the polar group being located in the cavity, were approximately 3 times more sensitive to changes in dipole moment than were the K_{gH} values (aromatic moiety included).

The cinnamate ion:cyclodextrin system is qualitatively consistent with this interpretation, since the anionic side chain is highly polar. The essentially identical K_{11} and K_{12} values for benzalacetone and cinnamate ion complexes may be a coincidence, or it may indicate that a methyl ketone is a good model for a carboxylate species in such systems.

FIGURE 31. Plots of log K_{11} *vs.* dipole moment (μ) for three structurally related substrate molecules. Open circles, K_{GH}; solid circles, K_{gH}.

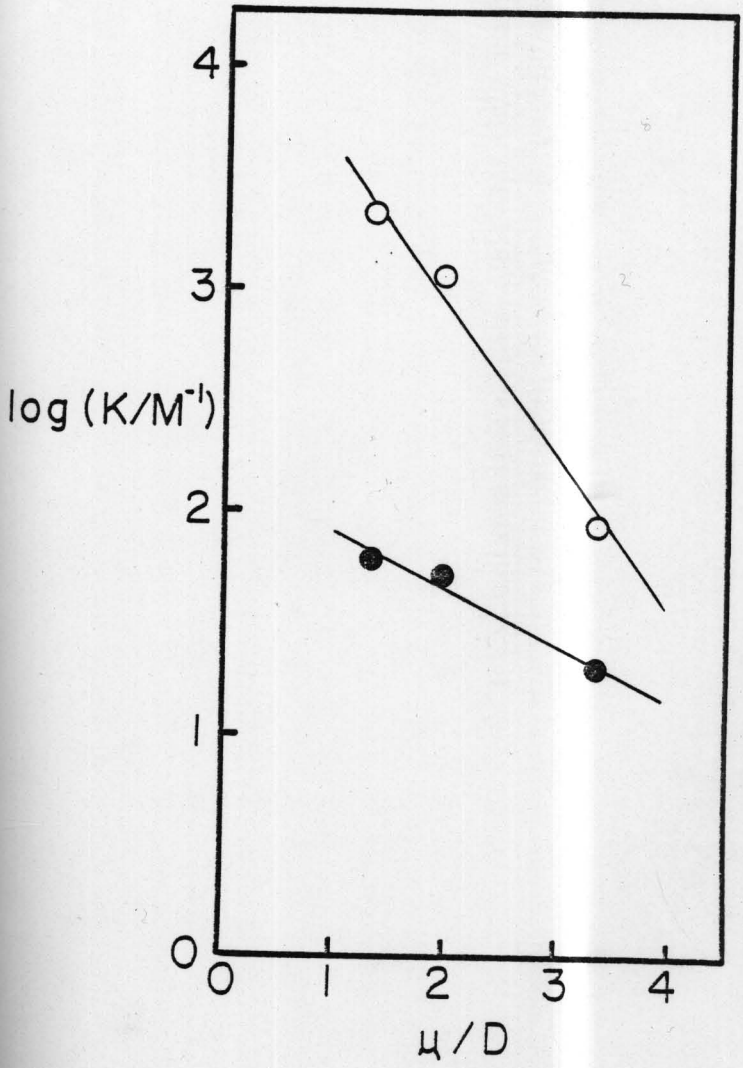
4
3
2
1
0
log (K/M⁻¹)
0
1
2
3
4
μ/D

REFERENCES

1. D. French, Adv. Carbohyd. Chem., 12, 189(1957).
2. A. Villiers, Compt. Rend., 112, 536(1891).
3. F. Schardinger, Wien. klin. Wochschr., 16, 468(1903).
4. H. Pringsheim and A. Langhans, Ber., 45, 2533(1912).
5. K. Freudenberg and R. Jacobi, Ann., 518, 102(1935).
6. D. French, M. L. Levine, J. H. Pazur and E. Norberg, J. Am. Chem. Soc., 71, 353(1949).
7. A. Hybl, R. E. Rundle and D. E. Williams, J. Am. Chem. Soc., 87, 2779(1965).
8. V. S. R. Rao and J. F. Foster, J. Phys. Chem., 67, 951 (1965).
9. B. Casu, M. Reggiani, G. G. Gallo and A. Vigivani, Tetrahedron, 24, 803(1968).
10. C. A. Glass, Can. J. Chem., 43, 2652(1965).
11. B. Casu, M. Reggiani, G. G. Gallo and A. Vigivani, Carbohyd. Res., 12, 157(1970).
12. K. Takeo and T. Kuge, Agr. Biol. Chem., 34, 1416(1970).
13. D. J. Wood, F. E. Hruska and W. Saenger, J. Am. Chem. Soc., 99, 1735(1977).
14. F. Cramer, G. Mackensen and K. Sensse, Chem. Ber., 102, 494(1969).
15. M. L. Bender and M. Komiyama, "Cyclodextrin Chemistry," Springer-Verlag, New York, 1978.

16. B. Casu, M. Reggiani, G. G. Gallo and A. Vigivani, Tetrahedron, 22, 3061(1966).

17. R. L. Van Etten, G. A. Clowes, J. F. Sebastian and M. L. Bender, J. Am. Chem. Soc., 89, 3253(1967).

18. T.-F. Chin, P.-H. Chung and J. L. Lach, J. Pharm. Sci., 57, 44(1968).

19. C. Van Hooidonk and C. C. Groos, Rec. Trav. Chim. Pay-Bas, 89, 845(1970).

20. F. Cramer, Rec. Trav. Chim., 25, 891(1956).

21. W. J. James, D. French and R. E. Rundle, Acta Crystallog., 12, 385(1959).

22. J. A. Thoma and L. Stewart in "Starch: Chemistry and Technology," R. L. Whistler and E. F. Paschall, eds., Academic Press, New York, 1965, pp. 209-249.

23. F. Cramer, W. Saenger and H.-Ch. Spatz, J. Am. Chem. Soc., 89, 14(1967).

24. J. F. Wojcik and R. P. Rohrbach, J. Phys. Chem., 79, 2251(1975).

25. P. V. Demarco and A. L. Thakkar, Chem. Comm., 1970, 2.

26. A. L. Thakkar and P. V. Demarco, J. Pharm. Sci., 60, 652(1971).

27. J. Cohen and J. L. Lach, J. Pharm. Sci., 52, 132(1963).

28. J. L. Lach and J. Cohen, J. Pharm. Sci., 52, 137(1963).

29. J. L. Lach and T.-F. Chin, J. Pharm. Sci., 53, 69 (1964).

30. W. A. Pauli and J. L. Lach, J. Pharm. Sci., 54, 1745 (1965).

31. Y. Hamada, N. Nambu and T. Nagai, Chem. Pharm. Bull., 23, 1205(1975).

32. K. Uekama and F. Hirayama, Chem. Pharm. Bull., 26, 1195(1978).

33. H. Schlenk, D. M. Sand and J. A. Tillotson, J. Am. Chem. Soc., 77, 3587(1955).

34. T.-F. Chin and J. L. Lach, J. Pharm. Sci., 57, 44 (1968).

35. J. L. Lach and T.-F. Chin, J. Pharm. Sci., 53, 924 (1964).

36. K. H. Fromming and I. Weyerman, Arzneim.-Forsch., 23, 424(1973).

37. J. H. Perrin, F. D. Field, D. A. Hansen, R. A. Mufson and G. Torosian, Res. Comm. Chem. Pathol. Pharmacol., 19, 373(1978).

38. K. Uekama, F. Hirayama, K. Esaki and M. Inoue, Chem. Pharm. Bull., 27, 76(1979).

39. D. D. MacNicol, Tetrahedron Lett., 1975, 3325.

40. F. Cramer and W. Dietsche, Chem. Ber., 92, 1739(1959).

41. F. Cramer and W. Dietsche, Chem. Ind., 1958, 892.

42. N. Hennrich and F. Cramer, J. Am. Chem. Soc., 87, 1121 (1965).

43. M. L. Bender, R. L. Van Etten, G. A. Clowes and J. F. Sebastian, J. Am. Chem. Soc., 88, 2318(1966).

44. M. L. Bender, R. L. Van Etten and G. A. Clowes, J. Am. Chem. Soc., 88, 2319(1966).

45. R. L. Van Etten, J. F. Sebastian, G. A. Clowes and M. L. Bender, J. Am. Chem. Soc., 89, 3242(1967).

46. H. J. Brass and M. L. Bender, J. Am. Chem. Soc., 95, 5391(1973).

47. C. van Hooidonk and J. C. A. E. Breebart-Hansen, Rec. Trav. Chim. Pays-Bas, 89, 289(1970).

48. D. E. Tutt and M. A. Schwartz, Chem. Comm., 1970, 113.

49. D. E. Tutt and M. A. Schwartz, J. Am. Chem. Soc., 93, 767(1971).

50. D. L. Vander Jagt, F. L. Killian and M. L. Bender, J. Am. Chem. Soc., 92, 1016(1970).

51. T. S. Straub and M. L. Bender, J. Am. Chem. Soc., 94, 8875(1972).

52. T. S. Straub and M. L. Bender, J. Am. Chem. Soc., 94, 8881(1973).

53. D. L. Griffiths and M. L. Bender, J. Am. Chem. Soc., 95, 1679(1973).

54. M. Komiyama and M. L. Bender, J. Am. Chem. Soc., 99, 8021(1977).

55. M. Komiyama and M. L. Bender, J. Am. Chem. Soc., 100, 4576(1978).

56. M. Komiyama and M. L. Bender, Bioorg. Chem., 6, 323 (1977).

57. F. Cramer and G. Mackensen, Chem. Ber., 103, 2138 (1970).

58. Y. Iwakura, K. Uno, F. Toda, S. Onozuka, K. Hattori and M. L. Bender, J. Am. Chem. Soc., 97, 4432(1975).

59. Y. Kitura and M. L. Bender, Bioorg. Chem., 4, 237 (1974).

60. W. B. Gruhn and M. L. Bender, Bioorg. Chem., 3, 324 (1974).

61. M. Komiyama and M. L. Bender, Proc. Nat. Acad. Sci., USA, 73, 2969(1976).

62. Y. Kurono, V. Stamoudis and M. L. Bender, Bioorg. Chem., 5, 393(1976).

63. H. Kitano and T. Okubo, J. Chem. Soc., Perkin II, 1977, 432.

64. R. Breslow and L. E. Overman, J. Am. Chem. Soc., 92, 1075(1976).

65. J. Emert and R. Breslow, J. Am. Chem. Soc., 97, 670 (1975).

66. I. Tabushi, K. Shimokawa, N. Shimizu, H. Shirakata and K. Fujita, J. Am. Chem. Soc., 98, 7855(1976).

67. I. Tabushi, K. Shimokawa and K. Fujita, Tetrahedron Lett., 1977, 1527.

68. I. Tabushi, N. Shimizu, T. Sugimoto, M. Shiozuka and K. Yamamura, J. Am. Chem. Soc., 99, 7100(1977).

69. R. Breslow, J. Doherty, G. Guillot and C. Lipsey, J. Am. Chem. Soc., 100, 3227(1978).

70. R. Breslow and P. Campbell, J. Am. Chem. Soc., 91, 3085(1969).

71. R. Breslow and P. Campbell, Bioorg. Chem., 1, 140 (1971).

72. I. Tabushi, K. Fujita and H. Kawakubo, J. Am. Chem. Soc., 99, 6456(1977).

73. I. Tabushi, K. Yamamura, K. Fujita and K. Kawakubo, J. Am. Chem. Soc., 101, 1019(1979).

74. K. Ikeda, K. Uekama and M. Otagiri, Chem. Pharm. Bull., 23, 201(1975).

75. M. Otagiri, K. Uekama and K. Ikeda, Chem. Pharm. Bull., 23, 188(1975).

76. K. Uekama, M. Otagiri, Y. Kanie, S. Tanaka and K. Ikeda, Chem. Pharm. Bull., 23, 1421(1975).

77. M. Otagiri, T. Miyaji, K. Uekama and K. Ikeda, Chem. Pharm. Bull., 24, 1146(1976).

78. K. Uekama, F. Hirayama, M. Otagiri, Y. Otagiri and K. Ikeda, Chem. Pharm. Bull., 26, 1162(1978).

79. K. Uekama, F. Hirayama, S. Nasu, N. Matsuo and T. Irie, Chem. Pharm. Bull., 26, 3477(1978).

80. K. A. Connors and J. M. Lipari, J. Pharm. Sci., 65, 379(1976).

81. T. Miyaji, Y. Kurono, K. Uekama and K. Ikeda, Chem. Pharm. Bull., 24, 1155(1976).

82. R. I. Gelb, L. M. Schwartz, R. F. Johnson and D. A. Laufer, J. Am. Chem. Soc., 101, 1869(1979).

83. P. C. Manor and W. Saenger, Nature, 237, 392(1972).

84. P. C. Manor and W. Saenger, J. Am. Chem. Soc., 96, 3630(1974).

85. W. Saenger, M. Noltemeyer, P. C. Manor, B. Hingerty and B. Klar, Bioorg. Chem., 5, 187(1976).

86. B. Hingerty and W. Saenger, Nature, 225, 396(1975).

87. R. K. McMullan, W. Saenger, J. Favos and D. Mootz, Carbohyd. Res., 31, 211(1973).

88. M. Noltmeyer and W. Saenger, Nature, 259, 629(1976).

89. W. Saenger and M. Noltmeyer, Chem. Ber., 109, 503 (1976).

90. W. Saenger and K. Beyer, Acta Crystallog., B32, 120 (1976).

91. K. Harata and H. Vedaira, Nature, 253, 190(1975).

92. P. R. Sundararajan and V. S. R. Rao, Carbohyd. Res., 13, 351(1970).

93. R. Bergeron and M. Meeley, Bioorg. Chem., 5, 197 (1976).

94. R. Bergeron and M. Rowan, Bioorg. Chem., 5, 425(1976).

95. D. W. Griffiths and M. L. Bender, Adv. Cat., 23, 209 (1973).

96. B. Siegel and R. Breslow, J. Am. Chem. Soc., 97, 6869 (1975).

97. Y. Matsui, H. Naruse, K. Mochida and Y. Date, Bull. Chem. Soc. Japan, 43, 1909(1970).

98. G. Nemethy and H. A. Scheraga, J. Phys. Chem., 36, 3401(1962).

99. E. A. Lewis and L. O. Hansen, J. Chem. Soc., Perkin II, 1973, 2081.

100. R. J. Bergeron, D. M. Pillor, G. G. Gibeily and W. P. Roberts, Bioorg. Chem., 7, 263(1978).

101. I. Tabushi, Y. Kiyosuke, T. Sugimoto and K. Yamamura, J. Am. Chem. Soc., 100, 916(1978).

102. M. Komiyama and M. L. Bender, J. Am. Chem. Soc., 100, 2259(1978).

103. H. Schlenk and D. M. Sand, J. Am. Chem. Soc., 83, 2312 (1961).

104. R. I. Gelb, L. M. Schwartz and D. A. Laufer, J. Am. Chem. Soc., 100, 5875(1978).

105. R. I. Gelb, L. M. Schwartz, C. T. Murray and D. A. Laufer, J. Am. Chem. Soc., 100, 3553(1978).

106. R. I. Gelb, L. M. Schwartz, R. F. Johnson and D. A. Laufer, J. Am. Chem. Soc., 101, 1864(1979).

107. K. A. Connors and J. A. Mollica, J. Am. Chem. Soc., 87, 123(1965).

108. J. A. Mollica and K. A. Connors, J. Am. Chem. Soc., 89, 308(1967).

109. P. A. Kramer and K. A. Connors, J. Am. Chem. Soc., 91, 2600(1969).

110. K. A. Connors, M. H. Infeld and B. J. Kline, J. Am. Chem. Soc., 91, 3597(1969).

111. H. Stelmach and K. A. Connors, J. Am. Chem. Soc., 92, 863(1970).

112. J. L. Cohen and K. A. Connors, J. Pharm. Sci., 59, 1271(1970).

113. K. A. Connors and S. Sun, J. Am. Chem. Soc., 93, 7239 (1971).

114. K. A. Connors and J. A. Mollica, J. Pharm. Sci., 55, 772(1966).

115. T. Higuchi and K. A. Connors, Advan. Anal. Chem. Instrum., 4, 117(1965).

116. H. Benesi and J. H. Hildebrand, J. Am. Chem. Soc., 70, 2832(1948).

117. M. L. Bender, G. R. Schonbaum and B. Zerner, J. Am. Chem. Soc., 84, 2540(1962).

118. M. L. Bender and B. Zerner, J. Am. Chem. Soc., 84, 2550(1962).

119. A. L. Wilds, L. W. Beck, W. J. Close, C. Djerassi, J. A. Johnson, Jr., T. L. Johnson and C. H. Shunk, J. Am. Chem. Soc., 69, 1985(1947).

120. F. T. Wall and P. E. Rouse, J. Am. Chem. Soc., 63, 3002(1941).

121. W. S. Wise and E. B. Nicholson, J. Chem. Soc., 1955, 2714.

122. J. A. Mollica, Ph.D. Thesis, University of Wisconsin, Madison, 1966.

123. A. Wong, unpublished results.

124. T. Higuchi and K. A. Connors, Advan. Anal. Chem. Inst., 4, 117(1965).

125. H. Benesi and J. H. Hildebrand, J. Am. Chem. Soc., 71, 2703(1949).

126. G. D. Johnson and R. E. Bowen, J. Am. Chem. Soc., 87, 1655(1965).

127. M. L. Boas, "Mathematical Methods in the Physical Sciences," John Wiley and Sons, Inc., New York, 1966, pp. 714-718.

128. F. Daniels, J. Mathews, J.Williams, P. Bender, G. W. Murphy and R. A. Alberty, "Experimental Physical Chemistry," McGraw-Hill, New York, 1949, pp. 351-371.

129. K. A. Connors, "Reaction Mechanisms in Organic Analytical Chemistry," Wiley-Interscience, New York, 1973, pp. 17-20.

130. B. Casu and L. Rava, Ric. Sci., 36, 733(1966).

131. R. J. Bergeron, M. Channing and K. A. McGovern, J. Am. Chem. Soc., 100, 2878(1978).

132. R. J. Bergeron, M. A. Channing, G. J. Gibeily and D. M. Pillor, J. Am. Chem. Soc., 99, 5146(1977).

133. M. Noltemeyer and W. Saenger, Nature, 259, 629(1976).

134. R. W. Gurney, "Ionic Processes in Solution," McGraw-Hill, New York, 1953 (Dover Publications, N.Y., reprint, 1962), Chapter 6.

135. C. Tanford, "The Hydrophobic Effect," Wiley-Interscience, New York, 1973, Chapter 2.

136. W. P. Jencks, "Catalysis in Chemistry and Enzymology," McGraw-Hill, New York, 1969, Chapter 7.

137. C. A. Streuli, Anal. Chem., 32, 407(1960).

138. J. S. Fritz and S. S. Yamamura, Anal. Chem., 29, 1079 (1957).

139. K. A. Connors and H. P. Corrick, Interest, 12, 11 (1973) (published 1977).

140. A. L. McClellan, "Tables of Experimental Dipole Moments," W. H. Freeman, San Francisco, 1963.

APPENDIX

A. Analysis of a 1:1 + 1:2 Complexation System by a Solubility Method

The solubility method for studying complexation is based on an increase in the apparent solubility of the substrate as a result of complex formation. The theory and practice of this method have been reviewed in detail (1). This theoretical development of the equations that govern the analysis of a 1:1 + 1:2 complexation system is divided into five parts, corresponding to the four distinct segments of the solution phase diagram shown in Figure 4, and the solid phase analysis.

The complex formation equilibria and stability constants are defined

$$S + L \rightleftarrows SL \qquad \text{(A-1)}$$

$$K_{11} = \frac{[SL]}{[S][L]} \qquad \text{(A-2)}$$

$$SL + L \rightleftarrows SL_2 \qquad \text{(A-3)}$$

$$K_{12} = \frac{[SL_2]}{[SL][L]} \qquad \text{(A-4)}$$

where S represents the substrate and L the ligand.

Assumptions in describing this system include constancy of activity coefficients, a negligible medium effect, and negligible volume changes.

1. Analysis of the Initial Rising Portion of the Solution Phase Diagram

Throughout the initial rising portion of the solution phase diagram, solid substrate is present, hence the concentration of S is held constant at the solubility limit, s_o. The mass balance on S gives

$$S_t = [S] + [SL] + [SL_2] \qquad (A-5)$$

which, with the above condition and Equations (A-2) and (A-4), becomes

$$S_t = S_o + K_{11}s_o[L] + K_{11}K_{12}s_o[L]^2 \qquad (A-6)$$

where [L] is the free ligand concentration. The mass balance on L gives

$$L_t = [L] + [SL] + 2[SL_2] \qquad (A-7)$$

which becomes

$$L_t = [L] + K_{11}s_o[L] + 2K_{11}K_{12}s_o[L]^2 \qquad \text{(A-8)}$$

Eliminating [L] between Equations (A-6) and (A-8) yields

$$S_t = s_o + \frac{L_t}{2} + \frac{ab}{c} - \frac{b}{c}(a^2 + 8K_{11}K_{12}s_oL_t)^{1/2} \qquad \text{(A-9)}$$

where

$$a = 1 + K_{11}s_o$$

$$b = \frac{a}{2K_{11}s_o} - 1$$

$$c = 4K_{12}$$

Equation (A-9), which is valid only for finite values of K_{11} and K_{12}, gives S_t, the total substrate as a direct function of L_t, the total ligand concentration, for the rising portion of the solubility diagram before the solubility limit of either complex has been reached. The slope is given by dS_t/dL_t (Eqn. (A-10)).

$$\frac{dS_t}{dL_t} = \frac{1}{2}\left[1 - \frac{8bK_{11}K_{12}s_o}{c(a^2 + 8K_{11}K_{12}s_oL_t)^{1/2}}\right] \qquad \text{(A-10)}$$

Since a and c must be positive quantities, the curvature in the slope depends on the sign of b. If b = 0, the slope is

constant with the value 0.5; this implies that $K_{11} = 1/s_o$. If b is negative, the slope will decrease as L_t increases, whereas if b is positive, the slope increases as L_t decreases. Whether these cases can be distinguished experimentally will be determined by the magnitudes of the parameters and the range of L_t over which the variable S_t can be observed. The value of the slope at $L_t = 0$ is obtained from Equation (A-11):

$$\left(\frac{dS_t}{dL_t}\right)_{L_t=0} = \frac{1}{2} - \frac{1}{2}\left[\frac{1 - K_{11}s_o}{1 + K_{11}s_o}\right] \qquad \text{(A-11)}$$

2. Analysis of the First Plateau

As L_t increases, S_t rises because of the formation of soluble SL and SL_2 complexes. Ultimately, the solubility limit of at least one of the complexes will be reached. Three cases can be considered here:

(i) the solubility limit of SL is reached before that of SL_2;

(ii) the solubility limit of SL_2 is reached before that of SL;

(iii) the solubilities of SL and SL_2 are reached at the same point.

Case (i): Define

$s_{11} \equiv$ solubility of SL

$s_{12} \equiv$ solubility of SL_2

Upon reaching the solubility limit of SL, Equation (A-5) becomes (solid S is still present)

$$S_t = s_o + s_{11} + [SL_2] \qquad \text{(A-12)}$$

Substituting the equilibrium expression for $[SL_2]$ gives

$$S_t = s_o + s_{11} + \frac{K_{12} s_{11}^2}{K_{11} s_o} \qquad \text{(A-13)}$$

Therefore S_t is invariant, i.e., as soon as SL reaches its solubility limit, S_t becomes invariant, even though SL_2 has not yet reached its solubility limit. Knowing the stability constants, s_o, and S_t, Equation (A-13) allows the calculation of the solubility of SL. Note that Equation (A-13) is quadratic in s_{11}; thus two values are possible and it may be difficult to determine which is correct.

Case (ii): Equation (A-5) now becomes

$$S_t = s_o + [SL] + s_{12} \qquad \text{(A-14)}$$

which, when combined with the equilibrium expression for SL, gives

$$S_t = s_0 + \left(\frac{s_{12}}{K_{12}}\right)^{1/2} + s_{12} \qquad \text{(A-15)}$$

Once again we find that S_t is invariant, even though in this case [SL] is below its solubility limit. Equation (A-15) is quadratic in s_{12} and, in a similar manner to case (i), it is possible to obtain two values for s_{12}, the correct one of which may be difficult to determine.

Case (iii): In the case where both SL and SL_2 reach their solubility limit at the same point, we have for the total solubility of substrate

$$S_t = s_o + s_{11} + s_{12} \qquad \text{(A-16)}$$

and again S_t is invariant.

Thus as soon as at least one complex reaches its solubility limit, the S_t value reaches a plateau, on which it remains until all of the solid S is depleted, at which point another discontinuity is observed. We next explore this region.

3. Analysis of the Second Rising Segment

In the analysis of this part of the solubility diagram, only the case where SL has reached its solubility

limit before SL_2 is considered, since this was found to be the case for cinnamic acid. Immediately beyond the point where solid S is depleted Equation (A-5) becomes (SL remains at its solubility limit)

$$S_t' = [S] + s_{11} + [SL_2] \qquad \text{(A-17)}$$

Substituting in the equilibrium expressions for $[SL_2]$ gives

$$S_t' = [S] + s_{11} + \frac{K_{12}s_{11}^2}{K_{11}[S]} \qquad \text{(A-18)}$$

Subtracting Equation (A-13) from Equation (A-18) gives

$$S_t' - S_t = ([S] - s_o)(1 - \frac{K_{12}s_{11}^2}{K_{11}s_o[S]}) \qquad \text{(A-19)}$$

Since [S] must be less than s_o, the quantity $([S] - s_o)$ is negative. Therefore if

$$\frac{K_{12}s_{11}^2}{K_{11}s_o[S]} > 1$$

$S_t' - S_t$ will be positive, which means that the total substrate concentration will increase above the initial plateau level when all solid S has been depleted. If this quantity equals unity, $S_t' = S_t$; this fixes a unique value for [S], i.e.,

$$[S] = \frac{K_{12}s_{11}^2}{K_{11}s_o} \qquad \text{(A-20)}$$

In any case, once solid S has been depleted, addition of ligand can only decrease [S], which increases $K_{12}s_{11}^2/K_{11}s_o[S]$, and thus $S_t' - S_t$ in a positive direction.

It is desirable to have an expression for the dependence of S_t' on L_t after solid S has been depleted. For the ligand, we have

$$L_t - \underline{SL} = [L] + [SL] + 2[SL_2] \qquad \text{(A-21)}$$

where $\underline{SL}$ represents solid SL, here defined in terms of a molar quantity. Replacing [SL] by s_{11}, substituting the equilibrium expressions for $[SL_2]$, and solving for [L] gives

$$[L] = \frac{L_t - \underline{SL} - s_{11}}{1 + 2K_{12}s_{11}} \qquad \text{(A-22)}$$

which, when substituted into Equation (A-7) results in

$$S_t' = s_{11} + \frac{K_{12}s_{11}L_t}{1 + 2K_{12}s_{11}} - \frac{K_{12}s_{11}\underline{SL}}{1 + 2K_{12}s_{11}} - \frac{K_{12}s_{11}^2}{1 + 2K_{12}s_{11}} + \frac{s_{11}(1 + 2K_{12}s_{11})}{K_{11}(L_t - \underline{SL} - s_{11})} \qquad \text{(A-23)}$$

If L_t is sufficiently large, the last term in Equation

(A-23) becomes negligible and S_t' is a linear function of L_t with slope

$$\frac{dS_t'}{dL_t} = \frac{K_{12}s_{11}}{1 + 2K_{12}s_{11}} \qquad \text{(A-24)}$$

When the solubility of the second complex, in this case SL_2, is reached, another discontinuity is observed in the solubility diagram.

4. Analysis of the Second Plateau

When the solubility limit of SL_2 is reached, Equation (A-17) becomes

$$S_t = [S] + s_{11} + s_{12} \qquad \text{(A-25)}$$

which combined with the equilibrium expression for [S] gives

$$S_t = \frac{K_{12}s_{11}^2}{K_{11}s_{12}} + s_{11} + s_{12} \qquad \text{(A-26)}$$

Thus, S_t is again invariant, and another plateau is observed. From Equations (A-13) and (A-26) it is seen that whenever any two of the species are held at fixed concentrations by their solubility limits, the third species is held fixed by the equilibria, and the total substrate is fixed.

If L_t could be made large enough, it is probable that

eventually all SL would be depleted by conversion to SL_2, and S_t would decrease to the solubility of SL_2.

5. Analysis of the Solid Phase

We consider first the composition of the solid phase in the initial plateau region of the solution phase diagram. From Equation (A-13), we have

$$S_t = s_o + s_{11} + \frac{K_{12}s_{11}^2}{K_{11}s_o} \qquad \text{(A-13)}$$

Since the total substrate in the system is a constant, and since S_t (the concentration of substrate in solution) is a constant, the amount of substrate in the solid phase is also a constant. We can find how much this is by finding its value at any point along the first plateau. Let v represent the system volume (there is an ambiguity here which is discussed later). Then if m_S^t is the total number of moles of S in the system, m_S^t/v is the total formal concentration of S in the system. S_t is the total concentration of dissolved S in the system, so the moles of S in solution is vS_t. The moles of solid S is

$$\begin{matrix}\text{moles S in} \\ \text{solid phase}\end{matrix} = m_S^t - vS_t = m_s^{\text{solid}} \qquad \text{(A-27)}$$

For the ligand in this region, we have

$$L_t = [L] + [SL] + 2[SL_2] + \frac{m_L^{solid}}{v} \qquad \text{(A-28)}$$

where m_L^{solid} is the number of moles of L in the solid phase. Substituting equilibrium expressions into Equation (A-28) gives

$$L_t = \frac{ds_{11}}{K_{11}s_o} + \frac{m_L^{solid}}{v} \qquad \text{(A-29)}$$

where $d = 1 + K_{11}s_o + 2K_{12}s_{11}$

Hence

$$m_L^{solid} = vL_t - \frac{vds_{11}}{K_{11}s_o} \qquad \text{(A-30)}$$

We define

$$X_L = \frac{m_L^{solid}}{m_L^{solid} + m_S^{solid}} \qquad \text{(A-31)}$$

so X_L is the mole fraction of L in the solid phase. From Equation (A-31), we obtain

$$X_L = \frac{v(L_tK_{11}s_o - ds_{11})}{v(L_tK_{11}s_o - ds_{11}) + K_{11}s_o(m_S^t - vS_t)} \qquad \text{(A-32)}$$

Thus the mole fraction of L in the solid phase increases in

a non-linear manner as L_t increases along the first plateau.

An expression for the mole fraction of L in the solid phase as a function of L_t in the second plateau region can be derived in a similar manner. The result is

$$X_L = \frac{v(L_t - s_{11} - s_{12}(2 + \frac{1}{K_{12}s_{11}}))}{v(L_t - s_{11} - s_{12}(2 + \frac{1}{K_{12}s_{11}})) + m_S^t - vS_t} \quad \text{(A-33)}$$

The ambiguity in the volumes used in the preceding equations may introduce some error in applying these equations, especially if there is a large amount of precipitate. In the preceding discussion a single volume was used in two different ways. The vS_t in Equations (A-27) and (A-33) refer to moles of substrate in solution. Hence v is the solution phase volume. The v used in terms involving the ligand refer to the volume of the entire system. If we let v_S be the solution volume and v_t be the system volume, then Equation (A-27) becomes

$$X_L = \frac{v_t(L_tK_{11}s_o - ds_{11})}{v_t(L_tK_{11}s_o - ds_{11}) + K_{11}s_o(m_S^t - v_SS_t)} \quad \text{(A-34)}$$

and Equation (A-33) becomes

$$X_L = \frac{v_t(L_t - s_{11} - s_{12}(2 + \frac{1}{K_{12}s_{11}}))}{v_t(L_t - s_{11} - s_{12}(2 + \frac{1}{K_{12}s_{11}})) + m_S^t - v_SS_t} \quad \text{(A-35)}$$

In the cinnamic acid:cyclodextrin study, the solid

phase curve (Fig. 4) was calculated assuming $v_t = v_S =$ 0.005 l. Errors introduced by the volume ambiguity were assumed to be negligible. This assumption did not appear to cause a serious problem because the solid phase volumes were small. However, when SL_2 began to precipitate, the volume of the solid phase became significant. Since it is difficult to determine the solid phase volume it is not practical to calculate a theoretical solid phase curve for comparison with experimental data in the second plateau region.

B. Analysis of a 1:1 + 1:2 Complexation System by a Spectral Method

The spectral method may be used to study complexation provided the molar absorptivities of the complexes and substrate differ at the analytical wavelength. Assuming adherence to Beer's law for all species, the absorbance for unit path length in a substrate solution containing ligand is

$$A = a_S[S] + a_{11}[SL] + a_{12}[SL_2] + a_L[L] \qquad \text{(A-36)}$$

and that in a solution without ligand is

$$A_0 = a_S S_t \qquad \text{(A-37)}$$

where a_i is the molar absorptivity of species i. The total substrate concentration S_t is held constant. If we incorporate the same total concentration L_t of ligand in each sample and its corresponding reference solution, and if we make the assumption $L_t = [L]$, then the measured absorbance is corrected for the free ligand contribution, so Equation (A-36) becomes

$$A = a_S[S] + a_{11}[SL] + a_{12}[SL_2] \qquad \text{(A-38)}$$

Combining Equation (A-38) with the mass balance on S (Equation (A-5)), we get

$$A = A_0 - [SL](a_S - a_{11}) - [SL_2](a_S - a_{12}) \qquad \text{(A-39)}$$

Let $\Delta A = A_0 - A$. Then

$$\Delta A = [SL]\Delta a_{11} + [SL_2]\Delta a_{12} \qquad \text{(A-40)}$$

where $\Delta a_{11} = a_S - a_{11}$ and $\Delta a_{12} = a_S - a_{12}$. From Equation (A-5) and the equilibrium expressions for [SL] and $[SL_2]$ we obtain

$$[S] = \frac{S_t}{1 + K_{11}[L] + K_{11}K_{12}[L]^2} \qquad \text{(A-41)}$$

Combining Equations (A-40) and (A-41) (with [SL] and $[SL_2]$ in Eqn. (A-40) being replaced by their equilibrium expressions), we get

$$\Delta A = \frac{S_t K_{11}[L](\Delta a_{11} + K_{12}\Delta a_{12}[L])}{1 + K_{11}[L] + K_{11}K_{12}[L]^2} \qquad \text{(A-42)}$$

which gives ΔA as a function of free ligand concentration. From the mass balance on L (Eqn. (A-7)), we get

$$L_t = [L] + \frac{S_t\ K_{11}[L](1 + 2K_{12}[L])}{1 + K_{11}[L] + K_{11}K_{12}[L]^2} \qquad \text{(A-43)}$$

which gives L_t as a function of free ligand concentration. It is not practical to derive an expression for ΔA as an explicit function of L_t, but a numerical curve-fitting procedure is straight-forward. An arbitrary but realistic value of [L] is selected, and with Equations (A-42) and (A-43) the corresponding quantities ΔA and L_t are calculated. These are compared with experimental values and the parameters are adjusted until satisfactory agreement with experimental results is achieved.

C. Analysis of a 1:1 + 1:2 Complexation System by a Potentiometric Method

The potentiometric method for studying cyclodextrin complexes of weak acids and bases was first introduced in

1976 and applied to some 1:1 complexing systems (2). It is based on changes in the apparent pK_a of the substrate due to complex formation. In the potentiometric analysis of a 1:1 + 1:2 complexation system, it is assumed that both the conjugate acid and conjugate base forms of the substrate form 1:1 and 1:2 complexes. For convenience, the symbolism used in the derivation of equations for this method will differ from that used for the other methods.

Let HA and A^- represent a weak acid and its conjugate base, respectively, as substrates, and L, the ligand. Then there are three acid-base equilibria:

$$HA \rightleftarrows H^+ + A^- \qquad \text{(A-44)}$$

$$HAL \rightleftarrows H^+ + AL^- \qquad \text{(A-45)}$$

$$HAL_2 \rightleftarrows H^+ + AL_2^- \qquad \text{(A-46)}$$

with acid-base dissociation constants given by

$$K_a = \frac{[H^+][A^-]}{[HA]} \qquad \text{(A-47)}$$

$$K_{a11} = \frac{[H^+][AL^-]}{[HAL]} \qquad \text{(A-48)}$$

$$K_{a12} = \frac{[H^+][AL_2^-]}{[HAL_2]} \qquad \text{(A-49)}$$

and four complexation equilibria

$$HA + L \rightleftarrows HAL \qquad \text{(A-50)}$$

$$A^- + L \rightleftarrows AL^- \qquad \text{(A-51)}$$

$$HAL + L \rightleftarrows HAL_2 \qquad \text{(A-52)}$$

$$AL^- + L \rightleftarrows AL_2^- \qquad \text{(A-53)}$$

with corresponding stability constants given below:

$$K_{11a} = \frac{[HAL]}{[HA][L]} \qquad \text{(A-54)}$$

$$K_{11b} = \frac{[AL^-]}{[A^-][L]} \qquad \text{(A-55)}$$

$$K_{12a} = \frac{[HAL_2]}{[HAL][L]} \qquad \text{(A-56)}$$

$$K_{12b} = \frac{[AL_2^-]}{[AL^-][L]} \qquad \text{(A-57)}$$

Not all of the constants defined above are independent. From the definitions we obtain

$$K_a K_{11b} = K_{a11} K_{11a} \qquad \text{(A-58)}$$

$$K_{a12}K_{12a} = K_{a11}K_{12b} \qquad \text{(A-59)}$$

The apparent acid dissociation constant in the presence of ligand, K_a', is defined by

$$K_a' = \frac{[H^+][A^-]_{total}}{[HA]_{total}} = \frac{[H^+]([A^-] + [AL^-] + [AL_2^-])}{[HA] + [HAL] + [HAL_2]} \qquad \text{(A-60)}$$

Substitution from Equations (A-54)-(A-57) leads to

$$K_a' = K_a\left[\frac{1 + K_{11b}[L] + K_{11b}K_{12b}[L]^2}{1 + K_{11a}[L] + K_{11a}K_{12a}[L]^2}\right] \qquad \text{(A-61)}$$

If we define $\Delta pK_a' = pK_a' - pK_a$, then

$$\Delta pK_a' = \log\left[\frac{1 + K_{11a}[L] + K_{11a}K_{12a}[L]^2}{1 + K_{11b}[L] + K_{11b}K_{12b}[L]^2}\right] \qquad \text{(A-62)}$$

At large [L], Equation (A-62) approaches

$$(\Delta pK_a')_{L\to\infty} = \log\frac{K_{11a}K_{12a}}{K_{11b}K_{12b}} \qquad \text{(A-63)}$$

From Equation (A-62), if $\Delta pK_a' \neq 0$, then

$$\frac{1 + K_{11a}[L] + K_{11a}K_{12a}[L]^2}{1 + K_{11b}[L] + K_{11b}K_{12b}[L]^2} \neq 1$$

If [L] is very small so that the $[L]^2$ terms become negligible, this means that for a finite $\Delta pK_a'$ to be observed

$K_{11a} \neq K_{11b}$. At very high [L], if $\Delta pK_a' \neq 0$, then $K_{11a}K_{12a}/K_{11b}K_{12b} \neq 0$, and thus $K_{11a}K_{12a} \neq K_{11b}K_{12b}$.

As in the spectral study, it is not feasible to find $\Delta pK_a'$ as an explicit function of L_t, but L_t can be related to [L] to give a practical method for evaluating the stability constants. The mass balances on ligand and substrate are written

$$L_t = [L] + [HAL] + [AL^-] + 2[HAL_2] + 2[AL_2^-] \quad \text{(A-64)}$$

$$A_t = [HA] + [A^-] + [HAL] + [AL^-] + [HAL_2] + [AL_2^-] \quad \text{(A-65)}$$

Substitution with equilibrium expressions yields

$$L_t = [L] + [HA](K_{11a}[L] + CK_{11b}[L] + 2K_{11a}K_{12a}[L]^2 + 2CK_{11b}K_{12b}[L]^2) \quad \text{(A-66)}$$

and

$$A_t = [HA](1 + C + K_{11a}[L] + CK_{11b}[L] + K_{11a}K_{12a}[L]^2 + CK_{11b}K_{12b}[L]^2) \quad \text{(A-67)}$$

where $$C = \frac{1 + K_{11a}[L] + K_{11a}K_{12a}[L]^2}{1 + K_{11b}[L] + K_{11b}K_{12b}[L]^2}$$

For conveninece, let

$$K_{11}' = K_{11a} + K_{11b}C \qquad \text{(A-68)}$$

$$K_{12}' = K_{11a}K_{12a} + K_{11b}K_{12b}C \qquad \text{(A-69)}$$

Then Equation (A-70) is obtained.

$$L_t = [L]\left[\frac{1 + K_{11}'A_t + 2K_{12}'A_t[L]}{1 + C + K_{11}'[L] + K_{12}'[L]^2}\right] \qquad \text{(A-70)}$$

As in the spectral method, the procedure for evaluating stability constants is to assign an arbitrary but realistic value to [L] and, with Equations (A-62) and (A-70) and estimates of the stability constants, to calculate $\Delta pK_a'$ and L_t for comparison with experimental results. The pK_a values of the 1:1 and 1:2 complexes can be obtained with knowledge of the stability constants and Equations (A-58) and (A-59).

D. Analysis of a 1:1 + 1:2 Complexation System by a Kinetic Method

The kinetic method for studying complexation is based on a reduction in rate of reaction of substrate when ligand

is present, with the assumption that the rate decrease is caused by complexation. This method is generally used to obtain information about the structure of the complex. The usual S-L symbolism is used in this discussion. The complexation equilibria are given in Equations (A-1) and (A-3), and the kinetic scheme can be represented

$$S + R \xrightarrow{k_S} P \qquad \text{(A-71)}$$

$$SL + R \xrightarrow{k_{11}} P \qquad \text{(A-72)}$$

$$SL_2 + R \xrightarrow{k_{12}} P \qquad \text{(A-73)}$$

If a reagent R is involved in the reaction, then k_S is the second-order rate constant (often determined under pseudo first-order conditions with the reagent in excess). It is assumed that R does not form complexes with S or L. The theoretical rate equation is

$$v = k_S[S][R] + k_{11}[SL][R] + k_{12}[SL_2][R] \qquad \text{(A-74)}$$

and the experimental rate equation is

$$v = k_{obs}S_t \qquad \text{(A-75)}$$

where k_{obs} is the observed pseudo first-order rate constant. Setting Equations (A-74) and (A-75) equal and dividing through by [R] and S_t, we obtain

$$k_S' = k_S f_S + k_{11} f_{11} + k_{12} f_{12} \qquad \text{(A-76)}$$

where k_S' is the apparent second-order rate constant, f_S is the fraction of S that is uncomplexed, f_{11} is the fraction present as SL, and f_{12} is the fraction present as SL_2. Combining the definitions of these fractions with the stability constants gives

$$f_S = \frac{[S]}{S_t} = \frac{1}{1 + K_{11}[L] + K_{11}K_{12}[L]^2} \qquad \text{(A-77)}$$

$$f_{SL} = \frac{[SL]}{S_t} = \frac{K_{11}[L]}{1 + K_{11}[L] + K_{11}K_{12}[L]^2} \qquad \text{(A-78)}$$

$$f_{SL_2} = \frac{[SL_2]}{S_t} = \frac{K_{11}K_{12}[L]^2}{1 + K_{11}[L] + K_{11}K_{12}[L]^2} \qquad \text{(A-79)}$$

Defining $q_{11} = 1 - (K_{11}/K_S)$ and $q_{12} = 1 - (K_{12}/K_S)$, Equation (A-79) becomes

$$k_S - k_S' = q_{11} k_S f_{11} + q_{12} k_S f_{12} \qquad \text{(A-80)}$$

Combining this with Equations (A-2) and (A-4) gives

$$\frac{k_S - k_S'}{k_S} = \frac{q_{11}K_{11}[L] + q_{12}K_{11}K_{12}[L]^2}{1 + K_{11}[L] + K_{11}K_{12}[L]^2} \qquad \text{(A-81)}$$

This gives k_S' as a function of [L]. The relationship between [L] and L_t was derived earlier (Eqn. (A-43)). Together, Equations (A-81) and (A-43) give a complete description of the system, which can be analyzed in the way described for the spectral and potentiometric methods, using K_{11}, K_{12}, q_{11}, and q_{12} as adjustable parameters.

REFERENCES

1. T. Higuchi and K. A. Connors, Advan. Anal. Chem. Inst., 4, 117(1965).
2. K. A. Connors and J. M. Lipari, J. Pharm. Sci., 65, 379 (1976).